CHARACTERIZATION OF FSR1-INTERACTING COMPLEX AND ITS DOWNSTREAM PATHOGENIC SUBNETWORK MODULES IN *FUSARIUM VERTICILLIOIDES*

A Dissertation

by

HUAN ZHANG

Submitted to the Office of Graduate and Professional Studies of
Texas A&M University
in partial fulfillment of the requirements for the degree of

DOCTOR OF PHILOSOPHY

Chair of Committee,	Won-Bo Shim
Committee Members,	Ping He
	Mikhailo V. Kolomiets
	Clint Magill
Head of Department,	Leland S. Pierson III

August 2017

Major Subject: Plant Pathology

ABSTRACT

Fusarium verticillioides is an ascomycete fungus responsible for stalk and ear rots of maize. Previously, we identified a striatin-like protein Fsr1 that plays a key role in stalk rot pathogenesis. In mammals, striatin interacts with multiple proteins to form a STRIPAK (striatin-interacting phosphatase and kinase) complex that regulates a variety of developmental processes and cellular mechanisms. In this study, we identified the homolog of a key mammalian STRIPAK component STRIP1/2 in *F. verticillioides*, FvStp1, that interacts with Fsr1 in vivo. Gene deletion analysis showed that FvStp1 is critical for *F. verticillioides* stalk rot virulence. In addition, we identified three proteins, designated FvCyp1, FvScp1 and FvSel1, that interact with the Fsr1 CC domain by yeast-two-hybrid screen. Importantly, FvCyp1, FvScp1, and FvSel1 co-localize to endomembrane structures, each having preferred localization in the cell, and they are all required for *F. verticillioides* virulence in stalk rot. Moreover, these proteins are necessary for proper localization of Fsr1 to endoplasmic reticulum (ER) and nuclear envelope. To further characterize genetic networks downstream of Fsr1, we performed RNA-Seq with maize B73 stalks inoculated with wild type and fsr1 mutant. We used a computationally efficient branch-out technique, along with an adopted probabilistic pathway activity inference method, to identify functional subnetwork modules likely involved in *F. verticillioides* virulence. We identified two putative hub genes, *i.e.*, *FvSYN1* and *FvEBP1* identified from the potential virulence-associated subnetwork modules for functional validation and network robustness studies, such as gene knockout,

virulence assays and qPCR studies. Our results provide evidence that *FvSYN1* and *FvEBP1* are important virulence genes that can infulence the expression of closely correlated genes, providing evidence that these are important hub genes of their respective subnetworks. Further characterization of *FvSYN1* showed that FvSyn1 is important for regulating spore germination and hyphal morphology. Furthermore, FvSyn1 is localized to vacuoles, plasma membranes, and septa, and has been shown to play a role in the response to cell wall stressors. Motif-deletion studies showed that both N-terminal SynN domain and C-terminal SNARE domain of FvSyn1 are required for pathogenicity but dispensable for fumonisin production and sexual mating.

DEDICATION

This dissertation is dedicated to my parents, Xuezheng Zhang and Yurong Jiang,

and my husband, Zhenhua He,

for their love, support and sacrifices during the course of this work.

ACKNOWLEDGEMENTS

Firstly, I would like to express my sincere gratitude to my advisor Dr. Won-Bo Shim for his continuous support of my Ph.D. study, for his guidance and mentoring in scientific research as well as the nonscientific conversations and support in my life. I couldn't accomplish this work without him. I would also like to thank the rest of my committee members: Drs. Ping He, Mikhailo Kolomiets and Clint Magill for their advice, insightful discussions and comments which widens my research from various perspectives throughout the course of this journey.

My sincere thanks also go to my former and current members of Dr. Shim's lab, especially Martha Malapi and Carlos Ortiz, who guided me around the lab when I joined in the lab and Angelyn Hilton, Huijuan Yan and Jun Huang for their friendship and their sharing of knowledge with me.

I would like to thank the faculty, staff and students of the department of plant pathology and microbiology for making my time at Texas A&M University a great experience.

Finally, great thanks to my husband for his support and love, to my son for bringing me so much joy and motivation, and to my mother and father as well as in-laws for their encouragement and help.

CONTRIBUTORS AND FUNDING SOURCES

Contributors

This work was supervised by a dissertation committee consisting of Professor Won-Bo Shim [major advisor] of plant pathology and microbiology and Professors Mikhailo Kolomiets and Clint Magill of the Department of Plant pathology and microbiology and Professor Ping of the Department of Biochemistry and Biophysics.

For studies performed in Chapter II, previous laboratory members partially contributed to generating outcomes. Namely, I would like to thank Drs Mala Mukherjee and Wenying Yu for Y2H library generation and screening. Dr. Kung-Eun Kim contributed to preliminary mutational analyses of genes identified in Y2H screening. The computational subnetwork modules prediction in Chapter III and IV were conducted in collaboration with Drs Byung-Jun Yoon and Man Kim in the Department of Computer and Electrical Engineering. All other work conducted for the dissertation was completed by the candidate independently.

Funding Sources

This work was supported in part by the National Research Initiative Competitive Grants Program (No. 2007-35319-18334) and the Agriculture and Food Research Initiative (No. 2013-68004-20359) from the US Department of Agriculture.

NOMENCLATURE

FB_1	Fumonisin B_1
PCR	Polymerase chain reaction
HPLC	High Pressure Liquid Chromatography
Dpi	Days post inoculation
RT	Room temperature
NGS	Next Generation Sequencing
CWI	Cell wall integrity

TABLE OF CONTENTS

Page

LIST OF FIGURES

Page

Page

LIST OF TABLES

Page

CHAPTER I

INTRODUCTION*

MAIZE AND STALK ROT

Maize is one of the main agricultural crops in the world. More than 960 million metric tons of maize were harvested from more than 179 million hectares of farmland in 2016, and an excess of 35% of this is grown in the United States according to the United States Department of Agriculture - Foreign Agricultural Service (Foreign Agricultural Service, 2017). Notably, maize production is negatively impacted by a variety of diseases caused by microbial pathogens. Stalk rot is one of the most devastating diseases of maize worldwide in terms of yield (Sobek & Munkvold 1999; Stack 1999; Yang et al., 2002). Multiple pathogens are known to cause stalk rots, and they can occur singly or as a complex (Koehler 1960). Charcoal rot (by *Macrophomina phaseolina*), Fusarium stalk rot (by *Fusarium verticillioides*), Gibberella stalk rot (by *F. graminearum*) and Anthracnose stalk rot (by *Colletotrichum graminicola*) are the most common stalk rots in the United States (Kommedahl & Windels, 1981; White, 1999). It is reported that the first sign of stalk rot is permanent wilting symptoms. Rot usually starts from the lowest internodes, and develops quickly with rising temperature. The discoloration can be seen on the surface of the lower stalks. The roots also become rotted, and therefore plants can

* Part of this chapter is reprinted with permission from "Computational prediction of pathogenic net- work modules in *Fusarium verticillioides*" by Mansuck Kim, Huan Zhang, Charles Woloshuk, Won-Bo Shim, and Byung-Jun Yoon. 2015. *IEEE/ACM Transactions on Computational Biology and Bioinformatics*, DOI: 10.1109/TCBB.2015.2440232, 2015. Copyright © [2015] IEEE.

be pulled out easily due to deteriorated root system (Dodd et al., 1980). Stalk rot usually lead to significant yield loss, poor grain quality, and problems during harvest (Cook, 1978; Ledencan et al., 2003).

FUSARIUM STALK ROT

Fusarium verticillioides causes Fusarium stalk rot in maize. The fungus typically overwinters in crop residue by producing thickened hyphae and spores (Leslie et al., 1990). Seed-borne and seed-transmitted fungus usually cause seedling disease (McGe, 1988), while soil-borne and air-borne conidia can penetrate stalks at the base of leaf sheaths and progress to lower internode through natural entry points and wounds created by insects or mechanical damage on stalk and root tissue (Foley, 1962; Kingsland & Wernham, 1962; Koehler, 1960; Sobek and Munkvold, 1999). Besides these factors, environmental stresses, such as low soil moisture, decreased light density by cloudy weather and high plant density which influences plants to produce carbohydrates, have been reported to be associated with stalk rots occurrence (Dodd, 1980). The pathogen can also take advantage of and colonize vulnerable stalk tissues at the end of growing season to cause stalk rot when the developing ear competes with the stalk for carbohydrates (Dodd, 1980; Smith &White, 1989). Infected corns show wilt symptom, the inner stalks show a light pink to tan discoloration. The stalks may be easily crushed at lower internodes, and may lodge when pushed sideways or impacted by wind. Pathogen invasion before maize physical maturity usually causes reduced grain fill and premature death, resulting in yield reduction. Severe yield loss can occur in the years

with conditions conducive to disease, e.g. high temperature and draught (Dodd, 1980; White, 1999).

The stalk rot management strategies include crop rotation, breakdown residues, proper plant densities and the minimization of stress. In addition, a limited number of resistant hybrids with good stalk strength and good insect control are available to manage this disease (Munkvold, 1996). It has been reported that the use of Bt hybrids is one of the most effective ways to prevent injury caused by European corn borers on corns (Gatch et al., 2002).

FUMONISIN AND FUMONISIN BIOSYNTHESIS

F. verticillioides spores can be transmitted by air or rainfall to infect maize silk and tassels and cause ear rot (Kommedahl & Windels, 1981). Infected kernels usually exhibit starburst symptoms with white streaks radiating from the cap of the kernel (Wilson & Maronpot, 1971). Furthermore, the fungus produces a group of mycotoxins known as fumonisins, one of the most commonly occurring mycotoxins in the infected corn ears. Fumonisin B1 (FB1) is the predominant form of fumonisins which are very stable in nature and cannot be eliminated by conventional cooking method. Consumption of fumonisin-contaminated corn can cause equine leukoencephalomalacia (ELEM), porcine pulmonary edema, and liver cancer in rats (Abbas et al., 1988; Kriek et al., 1981, Ross et al., 1990; Wilson et al., 1992). Moreover, the fungus is capable of infecting immunocompromised patients, producing skin lesions and causing allergic reactions in humans (Guarro et al., 1995; Petmy et al., 2002; Shaoxi et al., 1996). Because of these

concerns, the US Food and Drug Administration has established several parameters to monitor fumonisin levels in feed and foodstuff (Park & Terry, 2002).

Fumonisins are 19-20 carbon backbone polyketide secondary metabolites. It can disrupt sphingolipid metabolism by inhibiting ceramide synthase activity (ApSimon, 2001). The genes involved in fumonisin biosynthesis are named *FUM* genes, which are located on chromosome 1 and clustered in an 80-kb region. The cluster is composed of 22 genes expanding 42 kb, 15 of which are co-regulated (Procter et al., 1999; Proctor et al., 2003). *FUM1*, a key component of this cluster, encodes a polyketide synthase for the formation of the 19-20 carbon fumonisin backbone (Proctor et al., 1999). *FUM21* contains a $Zn(II)_2Cys_6$ DNA-binding domain, located adjacent to *FUM1*. It is the only known regulatory gene present in the *FUM* cluster. *FUM21* deletion mutation negatively affected *FUM1* and *FUM8* expression and produced little to no fumonisin in cracked maize cultures (Brown et al., 2007). Moreover, environmental factors also play important roles in regulating fumonisin biosynthesis in *F. verticillioides*, including nitrogen, carbon, pH as well as the kernel developmental status and specific tissue types (Woloshuk & Shim, 2013). It has been reported that high concentrations of nitrogen repress FB1 biosynthesis (Shim & Woloshuk, 1999). Further examination revealed that acidic pH enhances FB1 biosynthesis in *F.verticillioides* (Flaherty et al., 2003; Shim & Woloshuk, 2001). Bluhm & Woloshuk (2005) showed that amylopectin containing medium supported higher production of FB1 than glucose or maltose containing medium. FB1 was production significantly increased in the R5-stage kernels while there was no FB1 production in the R2 stage. Additionally, FB1 biosynthesis has been shown to be

regulated by genes not linked to the *FUM* cluster, such as *FCC1*, *FCK1*, *ZFR1*, *PAC1* and *GBP1* (Sagaram et al., 2006). *FCC1* is a C-type cyclin gene, the gene deletion strain showed reduced FB1 production on maize cracked kernels. Further study showed that *FCC1* is a pH-regulated positive regulator, and it interacts with a cyclin-dependent kinase, Fck1 (Shim & Woloshuck, 2001). *FCK1* is also a pH regulated positive regulator, *FCK1* disruption strain showed the same phenotype with *FCC1* mutant (Bluhm & Woloshuck, 2006). These results indicate that Fcc1 and Fck1 proteins form a regulatory complex involved in FB1 biosynthesis. *ZFR1* is a transcriptional activator of *FUM1*, and it is *FCC1*-dependent positive regulator for FB1 biosynthesis. Deletion of the *ZFR1* gene resulted in a drastic decrease in fumonisin production, but did not affect the growth and development of *F. verticillioides* on maize kernels (Flaherty & Woloshuck, 2004). *PAC1* is a transcriptional activator, but *PAC1* disruption strain produced more fumonisin than the wild type on maize kernels and in acidic synthetic medium. It turns out *PAC1* represses *FUM* genes under alkaline conditions (Flaherty et al., 2003). *GBP1*, a heterotrimeric G protein β subunit, is a transcriptional repressor of *FUM1*. Gene deletion mutant showed increased FB1 production, and increased *FUM1* and *FUM8* expression compared with the wild-type progenitor (Sagaram et al., 2006).

FSR1 AND STRIPAK COMPLEX

While there are extensive studies on ear rot due to the significance of fumonisins in food and feeds, very limited study has been reported on *F. verticillioides* stalk rot virulence mechanism. Previously, our lab identified and characterized a striatin-like

protein, Fsr1, in *F. verticillioides* through a forward genetic screen while investigating maize stalk rot pathogenicity in *F. verticillioides*. The predicted Fsr1 protein contains multiple protein-binding domains, namely a caveolin-binding domain, a coiled-coil structure, and a calmodulin-binding motif and seven WD40 repeat domains. Gene deletion study showed that *FSR1* is important for corn stalk rot virulence and female fertility. Microscopic examination of inoculated stalks revealed the wild-type fungus vigorously colonizing vascular bundle and causing rot, whereas the mutant showing limited colonization and rot in stalks. Further analysis suggested that N-terminal coiled-coil domain is important for stalk rot pathogenicity while the C-terminal WD40 repeat domain is dispensable (Shim et al., 2006; Yamamura & Shim, 2008).

Fsr1 protein is a homolog of a member of the striatin family proteins, which are mainly expressed in the central and peripheral nervous systems (Castets et al., 2000). Three members of the striatin family, striatin, SG2NA and zinedin, have been identified in mammals and all contain four protein domains: caveolin-binding domain, coiled-coil structure, Ca^{2+}-calmodulin (CaM)-binding domain, and WD40 repeat domains (Beonist et al., 2006; Breitman et al., 2008; Goudreault et al., 2009). Striatin is the first member identified in this family and is localized in the central nervous system in rats performing important role in motor control (Castets et al., 1996). The downregulation of striatin in rats resulted in reduced locomotor activity and impaired dendrites growth (Bartoli et al., 1999). This role has also been supported by further functional characterization of striatin homologue in *Drosophila melanogaster* (Chen et al., 2002; Hwang et al., 2014). The functional domains and their domain-mediated protein interactions in striatin family

members provide some insight into the function and the molecular mechanisms of this protein. Striatins are suggested to function as scaffolding proteins that organize multiple complexes involved in a variety of signaling pathways. Via its caveolin-binding domain, striatin has been characterized as a membrane-bound protein by binding to cavelolins, which are small integral membrane proteins (Gaillard et al., 2001). All striatin family proteins bind to CaM in a Ca^{2+}-dependent manner through their calmodulin-binding domain, and they function as Ca^{2+} sensors and convey signals to other proteins (Benoist et al., 2006). The coiled-coil domain has been proposed to be important for striatin family protein to localize to dendritic spines (Gaillard et al., 2006). In addition, oligomerization of coiled-coil domain is essential for the binding to other striatin-family associated proteins (Chen et al., 2014). WD40 repeat domains are considered to be folded into propeller structure to create a platform that is critical for interaction with other proteins involving in diverse cellular processes (Castets et al., 2000; Smith et al., 1999).

Homologues of striatin in filamentous fungi is highly conserved and have similar domain structure as in the mammalian striatins, indicating some important common functionalities (Kück et al., 2016; Pöggeler & Kück, 2004; Shim et al., 2006). Striatin homolog in *Sordaria macrospora*, Pro11, is suggested to play an important role in fungal cell differentiation (fruiting body formation) and complementation with a mouse striatin cDNA restored the sterile phenotype of pro11 mutation, suggesting the homologous functions in both proteins (Pöggeler & Kück, 2004). Striatin homolog in *Neurospora crassa*, Ham-2, was demonstrated to be important for hyphal fusion (Xiang et al., 2002).

Notably, Fsr1 is important for virulence and female fertility in *F. verticilloides* and *F. graminearum* (Shim et al., 2006). Striatin has been identified to be a part of a larger multiple protein assembly in human, referred to as striatin-interacting phosphatase and kinase (STRIPAK) complex (Goudreault et al., 2009). STRIPAK complex is composed of scaffolding subunit of protein phosphate 2A (PP2Aa), PP2A catalytic subunit (PP2Ac), PP2A regulatory subunits (striatins), striatin-interacting protein STRIP1 and STRIP2, striatin associated protein Mob3, the cerebral cavernous malformation 3 (CCM3) and several members of the germinal center kinase III family of Ste20 kinases (Bloemendal et al., 2012; Goudreault et al., 2009). The studies of STRIPAK-like complex have been performed in *S. macrospora* and *N. crassa* recently. A study in *S. macrospora* suggested that this STRIPAK-like complex is important for controlling sexual development via protein-protein interaction (Bloemendal et al., 2012). It was shown that STRIPAK-like complex in *N. crassa* plays important roles in fruiting body formation and cell fusion (Dettmann et al., 2013).

Although the important role of Fsr1 in pathogenicity was characterized in *F. verticillioides*, little is known about how putative STRIPAK complex components are assembled together and what the roles are in *F. verticillioides*. Coiled-coil domain is known to interact with other proteins *in vivo* and we hypothesize that this interaction promotes the formation of STRIPAK-like complex in *F. verticillioides* and triggers further downstream signaling associated with stalk rot pathogenesis. Accordingly, our objectives are to identify Fsr1-interacting proteins and characterize their role in virulence.

COMPUTATIONAL ANALYSIS TO IDENTIFY VIRULENCE GENES

The Fsr1-mediated virulence in *F. verticillioides* provides a new avenue to explore a novel signaling mechanism that controls virulence mechanisms in maize stalk rot pathogens (Shim et al., 2006). In order to explore the broader impact of Fsr1 in cellular signaling associated with *F. verticillioides* virulence to better understand the mechanism of stalk rot pathogenesis, we decided to take advantage of next-generation sequencing (NGS) and explore the transcriptomic subnetwork modules underpinning *FSR1*-mediated fungal virulence. Majority, if not all, of fungal NGS data analyses that have been published to date are two-dimensional, i.e. comparison of transcript abundance in different culture or strain backgrounds, and failed to investigate interrelationship between multiple genes. Knowing that genes do not perform their biological functions in isolation (i.e., independent from other genes), systematic approaches that aim to investigate the interrelationship between genes have been receiving attention in recent years. However, few have taken a network-based approach for analyzing the interactions among genes that contribute to the pathogenicity of fungi. He et al. (2008) predicted pathogenic subnetworks of *Magnaporthe grisea* from a protein-protein interaction (PPI) network constructed using its orthologs in *Escherichia coli*, *Saccharomyces cerevisiae*, *Caenorhabditis elegans*, *Drosophila melanogaster*, and *Homo sapiens*. Liu et al. (2010) predicted network modules with a limited number of known pathogenic genes of *F. graminearum*, whose PPI network was predicted previously *in silico* (Zhao et al., 2009), and Lysenko et al. (2013) extended the study of

Liu et al. (2010) by predicting functional modules with known virulence genes by using gene co-expression, predicted PPI network, and sequence similarity.

However, while these studies used network topology for their analysis, these approaches also possess a number of limitations. For example, for building modules, previous methods strongly relied on prior knowledge of pathogenic genes in other species and they did not explicitly consider the coordinated activities of genes that belong to the same module. In recent years, methods attempting to collectively analyze genes that belong to the same pathway or a subnetwork module have become popular in other areas, especially, in the study of complex human diseases such as cancer. For example, a number of pathway based methods have been proposed to jointly analyze the expression levels of genes in a given pathway to predict the pathway activity level and to relate it with the phenotype (Bild et al., 2006; Su et al., 2009; Lee et al., 2008; Wang et al., 2005; Tian et al., 2005; Subramanian et al., 2005; Khunlertgit & Yoon, 2013).

Other methods have taken a network-based approach, which analyzes gene expression data and network data in an integrative manner to identify subnetwork modules that consist of interacting genes with coordinated activities (Chuang et al., 2007; Su et al., 2010; Khunlertgit & Yoon, 2014). Such network-based methods for analyzing gene expression data have received increasing attention during the last several years, as they can lead to the prediction of novel functional gene modules that are associated with specific biological functions of interest, unveil the underlying gene interactions, and give rise to detailed working hypotheses that can be experimentally validated. For instance, Chuang et al. (2007) proposed a network-based approach for jointly analyzing gene

expression data with protein-protein interaction (PPI) data to identify potential subnework modules that might be responsible for breast cancer metastasis, which could be used as prognostic markers for assessing the risk of metastasis. Bild et al. (2006) tried to find gene expression signatures that reflect the activation level of oncogenic pathways. In this work, we performed a systematic network-based comparative analysis of two distinct *F. verticillioides* RNA-Seq datasets, where one set was obtained from wild-type *F. verticillioides* and the other set from a loss-of-virulence mutant.to identify potential gene modules that are responsible for the stalk rot of *F. verticillioides*.

CHAPTER II

FSR1, A STRIATIN HOMOLOG, FORMS AN ENDOMEMBRANE-ASSOCIATED COMPLEX THAT REGULATES VIRULENCE IN THE MAIZEPATHOGEN *FUSARIUM VERTICILLIOIDES*[*]

SUMMARY

Fsr1, a homolog of mammalian striatin, containing multiple protein-binding domains and a coiled-coil (CC) domain is critical for *F. verticillioides* virulence. In mammals, striatin interacts with multiple proteins to form a STRIPAK (striatin-interacting phosphatase and kinase) complex that regulates a variety of developmental processes and cellular mechanisms. In this study, we identified the homolog of a key mammalian STRIPAK component STRIP1/2 in *F. verticillioides*, FvStp1, that interacts with Fsr1 *in vivo*. Gene deletion analysis indicates that FvStp1 is critical for *F. verticillioides* stalk rot virulence. In addition, we identified three proteins, designated FvCyp1, FvScp1 and FvSel1, that interact with the Fsr1 CC domain via a yeast-two-hybrid screen. Importantly, FvCyp1, FvScp1, and FvSel1 co-localize to endomembrane structures, each having preferred localization in the cell, and they are all required for *F. verticillioides* virulence in stalk rot. Moreover, these proteins are necessary for proper

[*] This chapter was reprinted with permission from "Fsr1, a striatin homolog, forms an endomembrane-associated complex that regulates virulence in the maize pathogen *Fusarium verticillioides*" by Huan Zhang, Mala Mukherjee, Jung-Eun Kim, Wenying Yu, and Won-Bo Shim. 2017. *Molecular plant pathology*, DOI: 10.1111/mpp.12562, Copyright © [2017] BSPP and John Wiley & Sons Ltd.

localization of Fsr1 to endoplasmic reticulum (ER) and nuclear envelope. Thus, we identified several novel components in the STRIPAK complex that regulates *F. verticillioides* virulence and propose that proper organization and localization of Fsr1 is critical for STRIPAK complex function.

INTRODUCTION

The striatin family is comprised of a small group of proteins found in eukaryotic organisms, namely from filamentous fungi to mammals, but not in plants (Bartoli et al., 1999; Benoist et al., 2006; Castets et al., 2000; Pöggeler & Kück, 2004). Three well-known family members in mammal are striatin, SG2NA, and zinedin, all of which harbor a number of protein-protein interaction domains, *i.e.* a caveolin-binding domain, a putative coiled-coil domain, a Ca^{2+}-calmodulin (CaM)-binding domain, and a WD40-repeat domain (Castets et al., 2000). These domains are suggested to play critical roles in cellular functions by mediating interactions with other regulatory proteins (Castets et al., 1996; Moreno et al., 2000). Mammalian striatin homologs are involved in Ca^{2+}-dependent signaling in cells of the central nervous system and in endocytosis (Castets et al., 1996; Moreno et al., 2000). In addition, published reports demonstrate that striatin forms a complex with kinases and phosphatases to regulate critical cellular mechanisms in other eukaryotic organisms (Beier et al., 2016; Bloemendal et al., 2012; Dettmann et al., 2013; Frey et al., 2015; Hwang & Pallas, 2014; Kean et al., 2011). Homologs of striatin in filamentous fungi are highly conserved and have similar domain architecture

as mammalian striatins, suggesting some common functionalities (Dettmann et al., 2013; Pöggeler & Kück, 2004; Shim et al., 2006; Wang et al., 2010). Fungal striatin homologs have been implicated in a variety of important biological functions, including cell cycle regulation, sexual development, hyphal fusion, conidiation, and virulence.

While striatin proteins have no intrinsic catalytic activity, it is recognized that they organize multiple signaling complexes, *i.e.* signalosomes, that spatially and temporally coordinate distinct and diverse cellular mechanisms (Benoist et al., 2006; Breitman et al., 2008; Goudreault et al., 2009; Qing et al., 2004). One of the first striatin-interacting proteins discovered was phocein, an intracellular 26-kDa protein (Baillat et al., 2001). A splicing variant of rat striatin-3 (rSTRN3g) associates with estrogen receptor-a (ERa) in a ligand-dependent manner (Tan et al., 2008). Subsequently, with additional insights obtained on striatin-interacting proteins Goudreault et al. (2009) defined a novel large multi-protein assembly referred to as the striatin-interacting phosphatase and kinase (STRIPAK) complex that includes protein phosphatase 2A catalytic (PP2Ac) and scaffolding A (PP2Aa) subunits. Striatin is proposed as a regulatory subunit of the PP2A complex, most likely belonging to the B''' family of PP2A regulatory (PP2Ar) subunits (Eichhorn et al., 2009; Goudreault et al., 2009; Moreno et al., 2000; Shin et al., 2013). The complex also contains the novel proteins STRIP1 and STRIP2 (formerly FAM40A and FAM40B), the cerebral cavernous malformation 3 (CCM3) protein, and members of the germinal center kinase III family of Ste20 kinases. And recent studies have shown that striatin indeed forms complexes with phosphatases and kinases and that these STRIPAK complexes have critical roles in

devastating human disorders and diseases, including diabetes, autism, parkinsons, and cancer (Hwang & Pallas, 2014).

STRIPAK complex is highly conserved in eukaryotes, and recent studies in filamentous ascomycetes, e.g. *Sordaria macrospora* and *Neurospora crassa*, provide evidence that this complex plays important but also diverse roles in fungi. In *S. macrospora*, deletion mutations in STRIPAK complex components, Δpro11, Δpro22, Δpro45, ΔSmmob3, and PP2Ac1 exhibited defects in fruiting body formation, vegetative growth, and hyphal fusion (Beier et al., 2016; Bernhards & Pöggeler, 2011; Bloemendal et al., 2012; Nordzieke et al., 2015). Mutations in *N. crassa* STRIPAK components Δham-2, Δham-3, and Δpp2A led to similar defects observed in *S. macrospora* (Dettmann et al., 2013; Fu et al., 2011). Likewise, striatin homolog StrA in *Aspergillus nidulans* was shown to be important for fruiting body formation (Wang et al., 2010). In budding yeast, Far complex subunits show partial sequence similarity with mammalian STRIPAK complex, and these are involved in the control of post-mating cell fusion (Goudreault et al., 2009; Kemp & Sprague, 2003). STRIPAK-like complex in *Schizosaccharomyces pombe* was also shown to be important for the control of septation and cytokinesis (Singh et al., 2011).

Our earlier studies have shown that striatin plays an important role in plant pathogenic fungus *Fusarium verticillioides* (teleomorph: *Gibberella moniliformis* Wineland). We originally identified the gene encoding striatin homolog, *FSR1,* through a forward genetic screen when investigating maize stalk rot pathogenicity in *F. verticillioides* (Shim et al., 2006). The knockout mutant (Δfsr1) revealed two important

deficiencies: virulence and female fertility. When inoculated through artificial wounding, Δfsr1 colonized and advanced through maize vascular bundle but failed to develop stalk rot symptoms (unpublished data). Further characterization of Fsr1 has determined that the coiled-coil domain in the N-terminus is essential for virulence whereas the WD40 repeat in the C-terminus is dispensable (Yamamura & Shim, 2008). The coiled-coil domain is known to mediate protein-protein interaction in eukaryotes, and we hypothesize that this interaction triggers further downstream cellular signaling directly associated with stalk rot pathogenesis. Homologs of striatin in filamentous fungi, *e.g.* Fsr1 in *F. verticillioides*, Str1 in *A. nidulans*, Str1 in *Colletotrichum graminicola*, Pro11 in *Sodaria macroapora*, and Ham-3 in *Neurospora crassa*, are highly conserved, suggesting some common functionalities (Dettmann et al., 2013; Pöggeler & Kück, 2004; Shim et al., 2006; Wang et al., 2010; Wang et al., 2016) . However we also predict that striatin/STRIPAK interacts with a unique set of proteins in different fungi and in turn regulates species-specific functions through modulating protein localization, vesicular trafficking, and phosphorylation (Benoist et al., 2006; Goudreault et al., 2009; Kean et al., 2011). In *F. verticillioides*, we have yet to characterize striatin-interacting proteins that can help us explain how Fsr1 regulates virulence. Therefore, our first aim was to test whether Fsr1 forms a complex with one of the key STRIPAK proteins, STRIP1/2 homolog, and to study its function. Subsequently, we sought to identify *F. verticillioides* proteins that interact with Fsr1 *in vivo*, and characterize their role in stalk rot virulence through gene mutation and cellular localization studies.

RESULTS

Functional characterization of *F. verticillioides* STRIP1/2 homolog FvSTP1

One of the key components of eukaryotic STRIPAK complex is STRIP1/2 (striatin interacting proteins 1 and 2), which was first reported in mammalian systems by Goudreault and colleagues (2009). We identified a *F. verticillioides* homologous locus FVEG_08004 (designated *FvSTP1*), with 2,268-bp encoding a 705-aa predicted proteins with two functional motifs, pfam07923 and pfam11882 (Figure A-1) using the BLASTP algorithm. We generated a gene knockout mutant by homologous recombination to study its function (Figure 2.1A). Hygromycin B phosphotransferase (*HPH*) was used as the selective marker, and homologous recombination was confirmed by PCR (data not shown) and Southern blot (Figure 2.1B). Notably, Δfvstp1 strain exhibited almost identical phenotypes with *FSR1* gene knockout mutant Δfsr1, *i.e.*, reduced colony growth and less aerial mycelia, when grown on PDA, V8 agar and defined medium agar (Figure 2.1C). Therefore we used the relative growth difference data (63.6 ± 3.1%) to normalize stalk rot and seedling rot assay results to accurately measure virulence.

In order to test whether the mutant phenotype is due to a single gene mutation, we generated a complementation strain Fvstp1C by co-transforming Δfvstp1 protoplasts with the wild-type *FvSTP1* gene (with its native promoter and terminator) along with the geneticin-resistance gene, southern analyses was also performed to confirm gene complementation (Figure 2.1B). We also amplified and transformed *N. crassa ham-2* gene, a STRIP1/2 homolog, into Δfvstp1 protoplasts along with the geneticin-resistance

gene to generate a second complementation strain Fvstp1-NC. PCR was performed to confirm this gene complementation (Figure A-2). On PDA, V8 agar and defined medium agar, *FvSTP1* and its *N. crass* homolog were able to restore the growth rate in Δfvstp1 mutant (Figure 2.1C).

To test virulence, we inoculated internodes of B73 maize stalks (V10 ~ VT developmental stage) with spore suspension of wild-type, Δfvstp1, Fvstp1C, Fvstp1-NC, Δfsr1 (negative control) strains and water (negative control). When stalks were split open longitudinally after a 10-day incubation, the Δfvstp1 mutant showed significantly decreased levels of rot when compared with the wild-type progenitor. Both Δfvstp1 and Δfsr1 mutants showed greater than 90% reduction in virulence when analysed by average stalk rot area (Figure 2.1D). Gene complementation partially restored stalk rot virulence in *FvSTP1C* strain, up to approximately 75% level when compared to the wild-type progenitor. We also tested virulence on B73 maize seedlings, which showed outcomes that are very comparable to stalk rot assays (Figure 2.1E). These results suggested that *FvSTP1* plays an important role in virulence on maize stalk rot.

Figure 2.1 Functional characterization of *F. verticillioides* STRIP1/2 homolog FvSTP1. (A) Schematic representation of the homologous gene recombination strategy resulting in knockout mutant strain. Hygromycin phosphotransferase (*HPH*) was used as the selective marker. Arrows indicate primers used for PCR. *HYG*, hygromycin phosphotransferase gene, *HY*, *HYG* 5' partial amplicon, *YG*, *HYG* 3' partial amplification. (B) Southern analyses of wild-type (WT), knockout mutant *(*Δ*FvSTP1*), complementation (*FvSTP1C*) and ectopic strains. 3'-flanking region was used as a probe for Southern hybridization. Genomic DNA samples were digested with *Eco*RV. Anticipated band sizes before and after recombination are indicated above and under the scheme picture. (C) Vegetative growth of WT, Δ*FvSTP1*, complementation strains (*FvSTP1C* and *FvSTP1-NC*), and Δ*FSR1* were examined on V8, 0.2XPDA, and Myro agar plates. Strains were point inoculated with an agar block (0.5 cm in diameter) and incubated for 6 days at 25 °C under 14 h light/10 h dark cycle. (D) Eight-week-old B73 maize stalks were inoculated with 10^8/ml spore suspensions of fungal strains at the internodal region and incubated in a growth chamber for 10 days at 25°C. Subsequently, maize stalks were split longitudinally to quantify the extent of the rot by Image J software. Three independent biological repetitions were performed. (E) Germinating B73 seedlings were inoculated with 10^8 /ml spore suspension of fungal strains on mesocotyls. Lesion areas were quantified by Image J after 2-week incubation. Asterisk above the column indicates statistically significant difference ($P<0.05$) analyzed by t-Test.

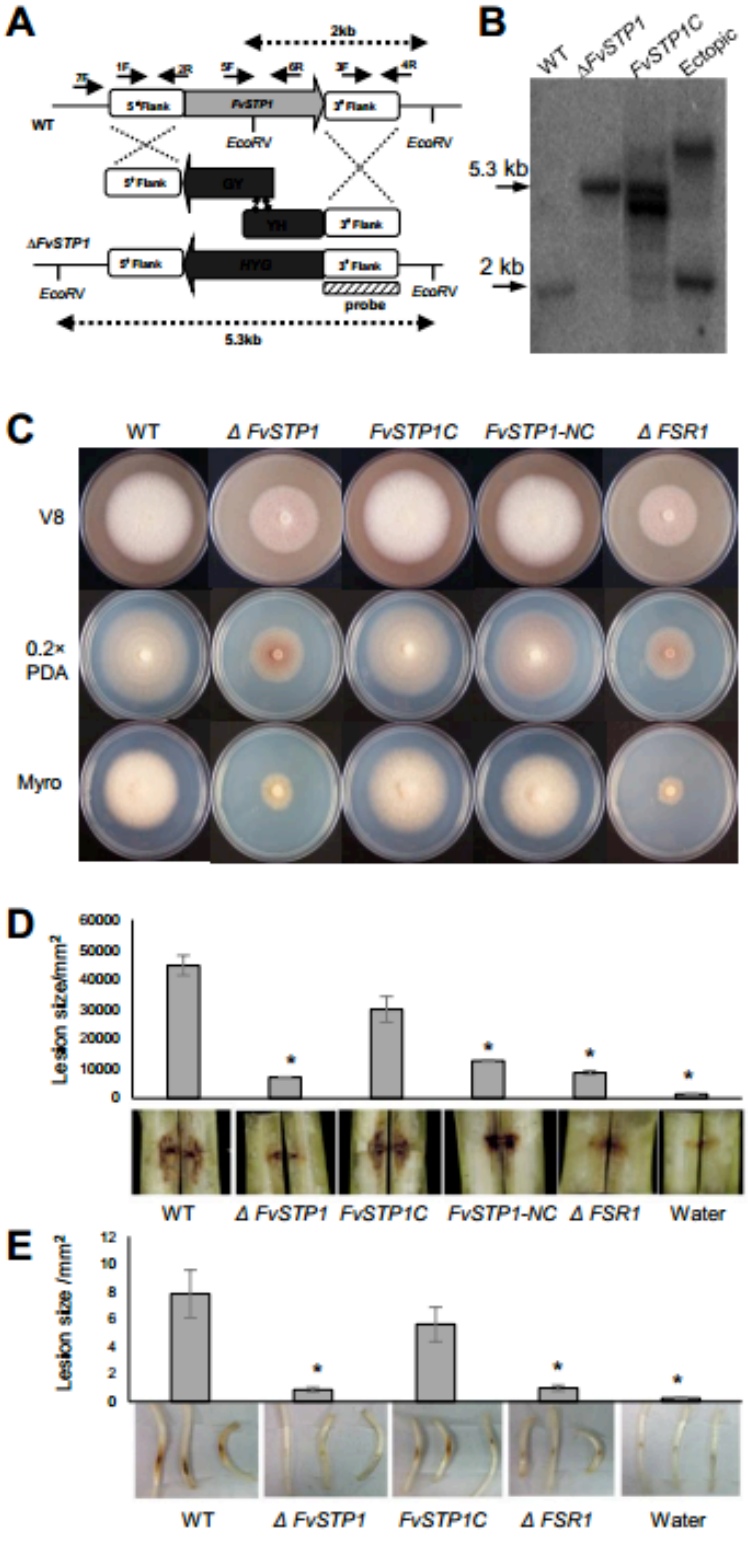
A
2kb
WT
FvSTP1
EcoRV
EcoRV
GY
YH
ΔFvSTP1
HYG
EcoRV
probe
EcoRV
5.3kb
B
WT
ΔFvSTP1
FvSTP1C
Ectopic
5.3 kb
2 kb
C
WT
Δ FvSTP1
FvSTP1C
FvSTP1-NC
Δ FSR1
V8
0.2× PDA
Myro
D
Lesion size/mm²
60000
50000
40000
30000
20000
10000
0
WT
Δ FvSTP1
FvSTP1C
FvSTP1-NC
Δ FSR1
Water
E
Lesion size /mm²
12
10
8
6
4
2
0
WT
Δ FvSTP1
FvSTP1C
Δ FSR1
Water

Fsr1-FvStp1 interaction in vivo confirmed by yeast two-hybrid and split luciferase assays

To test physical interaction between Fsr1 and FvStp1, we performed two independent assays: yeast two-hybrid assay and split luciferase complementation assay. For yeast two-hybrid assay, interaction between Fsr1 and FvStp1 was tested in *S. cerevisiae* strain AH109. When yeast colonies were grown on SD-Ade-His-Leu-Trp medium amended with X-alpha-Gal, we observed strong positive reaction (Figure 2.2A). To further verify physical interaction between Fsr1 and FvStp1 by split luciferase assay, we cloned *FSR1* and *FvSTP1* into pFNLucG and pFCLucH vectors, respectively (Kim et al., 2012), which were subsequently co-transformed into *F. verticillioides* protoplasts. Fungal transformants, co-expressing *FSR1*-nLuc and cLuc-*FvSTP1*, showed strong luciferase activity, approximately 20-fold higher than negative controls (Figure 2.2B). Four negative controls were used in this assay: one with two empty vectors (pFNLucG and pFCLucH), one is pFNLucG-*FSR1*+pFCLucH, and one is pFNLucG + pFCLucH-*FvSTP1* and one with no vectors. For positive control, we cloned *F. verticillioides FCC1* (cyclin C) and *FCK1* (cyclin-dependent kinase) genes, which were demonstrated to exhibit a strong *in vivo* interaction (Bluhm & Woloshuk, 2006), into pFNLucG and pFCLucH constructs. These two assays clearly demonstrated that Fsr1 physically interacts with FvStp1 in *F. verticillioides*.

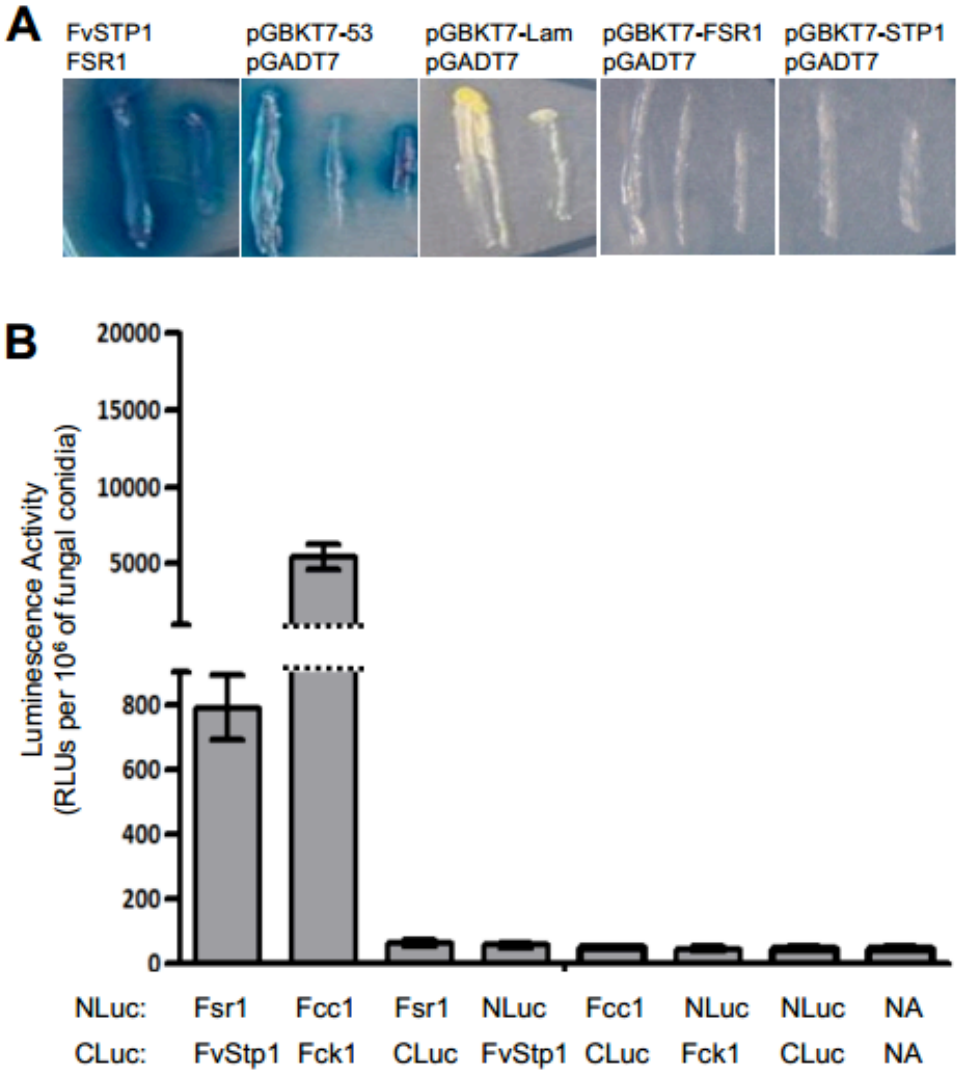

Figure 2.2 Verification of interaction between Fsr1 and FvStp1 interaction *in vivo*.
(A) The pair of plasmids pGADT7-FSR1 and pGBKT7-FvSTP1 was used to test interaction by monitoring blue colonies that developed on SD-Ade-His-Leu-Trp medium amended with X-alpha-Gal. The pair of plasmids pGBKT7-53 and pGADT7 was used as a positive control. The plasmid pairs pGBKT7-Lam/pGADT7, pGBKT7-FSR1/pGADT7, and pGBKT7-STP1/pGADT7 were used as negative controls. (B) Further verification of *in vivo* interactions between Fsr1 and FvStp1 was tested by split luciferase complementation assay. Fcc1/ Fck1 was used as positive control, and six negative controls were tested (including no vector [NA]). Luminescence activity was obtained from three replicates of fungal inoculations and is presented as the number of RLUs (relative light units) per 10^6 fungal conidia. Asterisk above the column means statistically significant ($P<0.05$) analyzed by t-Test.

Components of putative *F. verticillioides* STRIPAK complex

Earlier studies in eukaryotic systems lead us to hypothesize that Fsr1 regulates signaling in *F. verticillioides* by acting as a scaffolding protein and by interacting with kinases, phosphatases, and/or transcription factors. Based on the knowledge reported for other eukaryotic organisms, e.g. *Homo sapiens*, *Drosophila melanogaster*, *S. macrospora*, and *N. crassa* (Hwang & Pallas, 2014; Kück et al., 2016), we screened for putative STRIPAK components from *F. verticillioides* genome in addition to striatin (Fsr1) and STRIP1/2 (FvStp1). As predicted in other organisms, protein phosphatase subunits are key components of STRIPAK. The homologs of germinal center kinase were identified in *S. macrospora* (SmKIN3/24), *N. crassa* (Sid-1) as well as *F. verticillioides* genomes (Beier et al., 2016; Frey et al., 2015; Heilig et al., 2013; Maerz et al., 2009). Functional role of this kinase is not determined to date. Notably, Ccm3, a key component of mammalian STRIPAK known to interact with Stk24/Sok1, which is associated with vascular disease cerebral cavernous malformation was not identified in fungal genomes (Table 2.1). The study of STRIPAK components in mammalian systems and filamentous fungi led us to hypothesize that, while there are common core components, species-specific striatin-interacting proteins can perform unique roles in different organisms.

Table 2.1 STRIPAK components in *H. sapiens* (Hs), *S. macrospora* (Sm), *N. crassa* (Nc) and *F. verticiioides* (Fv).

Hs subunits[1]	Description	Sm subunits	Nc subunits	Fv subunits	Proposed function in filamentous fungi	References
STRN1/3/4	Striatin family (Striatin/ SG2NA/ Zinedin), PP2A regulatory subunit	Pro11	Ham-3	FVEG_09767 (*FSR1*)	Vegetative growth (Sm, Nc, Fv), cell/hyphal fusion and sexual development (Sm, Nc), Hyphal growth rate/density, female fertility, virulence (Fv)	2, 3, 4, 5, 6
PP2AAa/b	Protein phosphatase 2A structural subunit	PP2AA	PP2A-A	FVEG_07097	Hyphal growth, circadian clock (Nc)	7, 8
PP2ACa/b	Protein phosphatase 2A catalytic subunit	PP2Ac1	PP2A	FVEG_06252 FVEG_06432 FVEG_09543 (*CPP1*)	Vegetative growth, hyphal fusion and sexual development (Sm), Vegetative growth, conidia production and fumonision production (Fv)	9, 10
STRIP1/2	Striatin interacting protein 1/2 (FAM40A, FAM40B)	Pro22	Ham-2	FVEG_08004 (*FvSTP1*)	Vegetative growth (Sm, Nc, Fv), hyphal fusion (Sm, Nc) and sexual development (Sm, Nc), female fertility, virulence (Fv)	3, 11, 12, 13
MOB3	Monopolar spindle-one-binder family 3, Phocein	SmMob3	Mob-3	FVEG_06088	Vegetative growth, hyphal fusion and fruiting body development (Sm), vegetative cell fusion, fruiting body development (Nc)	4, 14
SLMAP	Sarcolemmal membrane-associated protein	Pro45	Ham-4	FVEG_03887	sexual propagation and cell-to-cell fusion (Sm), Vegetative growth, hyphal fusion and formation of protoperithecia (Nc),	3, 15
MST3/4	Germinal center kinase III family (Stk24/Sok1)	SmKin3/2 4	Sid-1	FVEG_05910 FVEG_07917 FVEG_08235	Abnormal septum distribution and development (Sm), septum initiation and formation (Nc)	16, 17
CCM3	Cerebral cavernous malformation 3	Not Found	Not Found	Not Found	Not characterized to date	-

References: 1) Hwang and Pallas (2013), 2) Pöggeler and Kück (2004), 3) Simonin *et al* (2010), 4) Bernhards and Pöggeler (2011), 5) Shim *et al* (2006), 6) Yamamura and Shim (2008), 7) Yatzkan *et al* (1998), 8) Yang *et al* (2004), 9) Beier *et al* (2016), 10) Choi and Shim (2008), 11) Bloemendal *et al* (2012), 12) Xiang *et al* (2002) 13) This study, 14) Maerz *et al* (2009), 15) Nordzieke *et al* (2015), 16) Heilig *et al* (2013), and 17) Frey *et al* (2015)

Identification of new Fsr1-interacting proteins in *F. verticillioides*

Our previous study showed that coiled-coiled domain in the N-terminus region of Fsr1 plays an important role in *F. verticillioides* virulence (Yamamura & Shim, 2008). Some of the key fungal STRIPAK subunits (Table 2.1), namely Phocein/Mob3, are known to associate with striatin primarily with the C-terminal region (Bloemendal et al., 2012). Meanwhile, studies have also shown that coiled-coil domain serves an important role in protein recruitment and structural assembly that can influence overall STRIPAK function in mammalian systems (Chen et al., 2014; Gordon et al., 2011). One of our key aims was to identify *F. verticillioides* proteins that primarily interacts with the Fsr1 coiled-coil motif and to test whether these proteins are involved in regulating stalk rot virulence. To do so, we first used the yeast two-hybrid system to screen *F. verticillioides* prey cDNA library with two bait constructs; one was *FSR1* cDNA corresponding to the uninterrupted N-terminal region (F1) and the other was *FSR1* cDNA devoid of the coiled-coil (F3). Prey library was prepared with *F. verticillioides* cDNAs generated from the fungus inoculated in corn stalk medium. We obtained a total of 74 and 71 positive colonies when constructs F1 and F3 were used as baits, respectively (Table A-1). We primarily aimed at proteins that are predicted to localize to fungal endomembrane, *i.e.* in proximity to striatin homologs in fungal cells (Dettmann et al., 2013; Nordzieke et al., 2015; Wang et al., 2010).

From the screening (Figure 2.3A), we selected three genes that showed interaction with F1 construct (FVEG_00403 [*FvCYP1*, cyclophilin], FVEG_04097 [*FvSCP1*, SCP-like extracellular protein], and FVEG_12134 [*FvSEL1*, Sel1-repeat

protein]) and two genes with F3 construct (FVEG_01920 [*FvHEX1*, Hex1-like protein] and FVEG_11334 [*FvPEX14*, peroxisomal membrane anchor protein 14]). The fact that FvHex1 and FvPex14 exhibit Y2H interaction with both F1 and F3 constructs suggested these two proteins do not require coiled-coil domain for physical interaction with Fsr1. Additional description of these putative proteins is provided in Table A-2 and Figure A-3.

To further verify protein-protein interaction, FvCyp1, FvScp1, FvSel1 along with FvStp1 were subjected to bait-prey switch yeast two-hybrid tests, and all showed positive results (Figure 2.3B). Further confirmation of physical interaction *in vivo* between Fsr1 N-terminus and FvCyp1, FvScp1 and FvSel1 came from split luciferase assay. Based on luminescence data, we concluded that Fsr1 interacts with FvCyp1, FvScp1and FvSel1in *F. verticillioides*. Notably FvSel1 exhibited the highest level of interaction. Meanwhile, the average luminescence intensity between Fsr1 and FvScp1 was only slightly higher than negative controls but was statistically significant ($P<0.05$) (Figure 2.3C). Based on these results, we selected FvScp1, FvSel1 and FvCyp1 as Fsr1 N-terminus interacting proteins for further characterization of their role in *F. verticillioides* virulence.

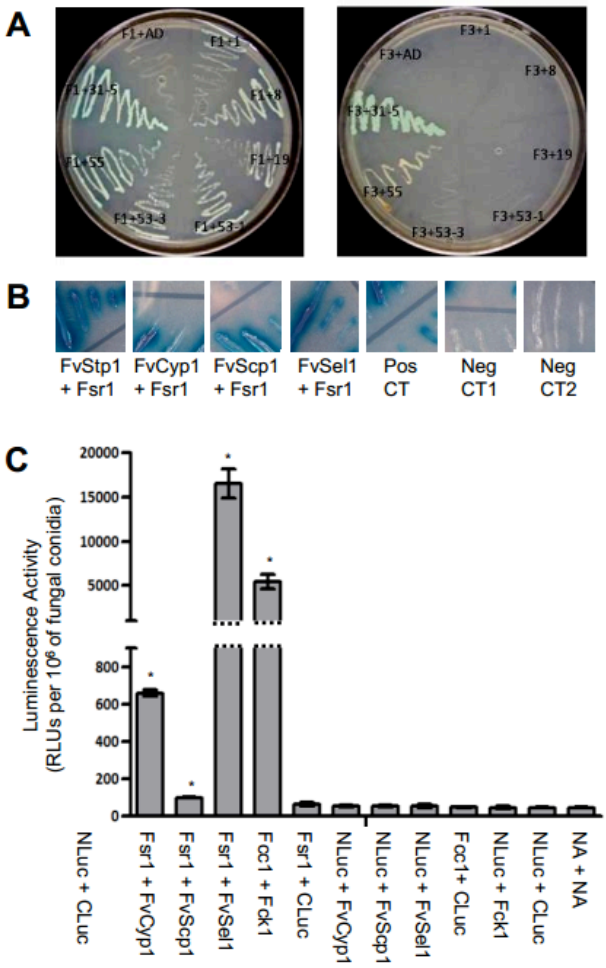

Figure 2.3 Identification of new Fsr1-interacting proteins in *F. verticillioides*.
(A) Bait F1 (N-terminal Fsr1 with coiled coil motif) and Bait F3 (N-terminal Fsr1 without coiled coil motif) were used for yeast-two hybrid screening. Yeast strains bearing both the bait and prey plasmids were streaked on SD-Ade-His-Leu-Trp media amended with X-alpha-Gal. Prey strains, 1: HSP98, 8: SCP like extracellular protein, 19: Sel1 repeat protein, 53-1: Cyclophilin, 53-3: Cyclophilin, 55: Hex1, 31-5: Pex14. (B) Bait-prey switch Y2H experiments were performed to verify performed interactions between Fsr1 and FvStp1 (positive control), FvCyp1, FvScp1, and FvSel1. The pair of plasmids pGBKT7-53 and pGADT7 was used as a positive control. The plasmid pairs pGBKT7-Lam/pGADT7 (Neg CT1) and pGBKT7-FSR1/pGADT7 (Neg CT2) were used as negative controls. (C) Further verification of *in vivo* interactions was tested by split luciferase complementation assay. Fcc1/Fck1 was used as positive control, and eight negative controls were tested (including no vector [NA]). Luminescence activity was obtained from three replicates of fungal inoculations and is presented as the number of RLUs (relative light units) per 10^6 of fungal conidia. Asterisk above the column means statistically significant ($P<0.05$) analyzed by t-Test.

Functional characterization of FvCYP1, FvSCP1, FvSEL1, FvHEX1, and FvPEX14

To investigate the role of *FvCYP1*, *FvSCP1*, *FvSEL1*, *FvHEX1*, and *FvPEX14* in *F. verticillioides* virulence, we generated gene knockout mutants following the established split-marker protocol (Figure A-4). We also generated gene complementation strains using the corresponding wild-type gene for each mutant. When we compared the vegetative growth of these mutants on synthetic media, the phenotypes of these mutants were very similar to the wild-type progenitor, although ΔFvCyp1 and ΔFvSel1 exhibited slightly slower growth (Figure 2.4A). However, when these strains were grown in synthetic liquid media, we did not see significant difference in fungal mass production (data not shown). ΔFvCyp1 strains produced less compact aerial mycelia when grown on synthetic media. Notably, the vegetative growth of ΔFvHex1 and ΔFvPex14 strains on V8 and PDA media were not significantly different from that of the wild-type progenitor (Figure A-5).

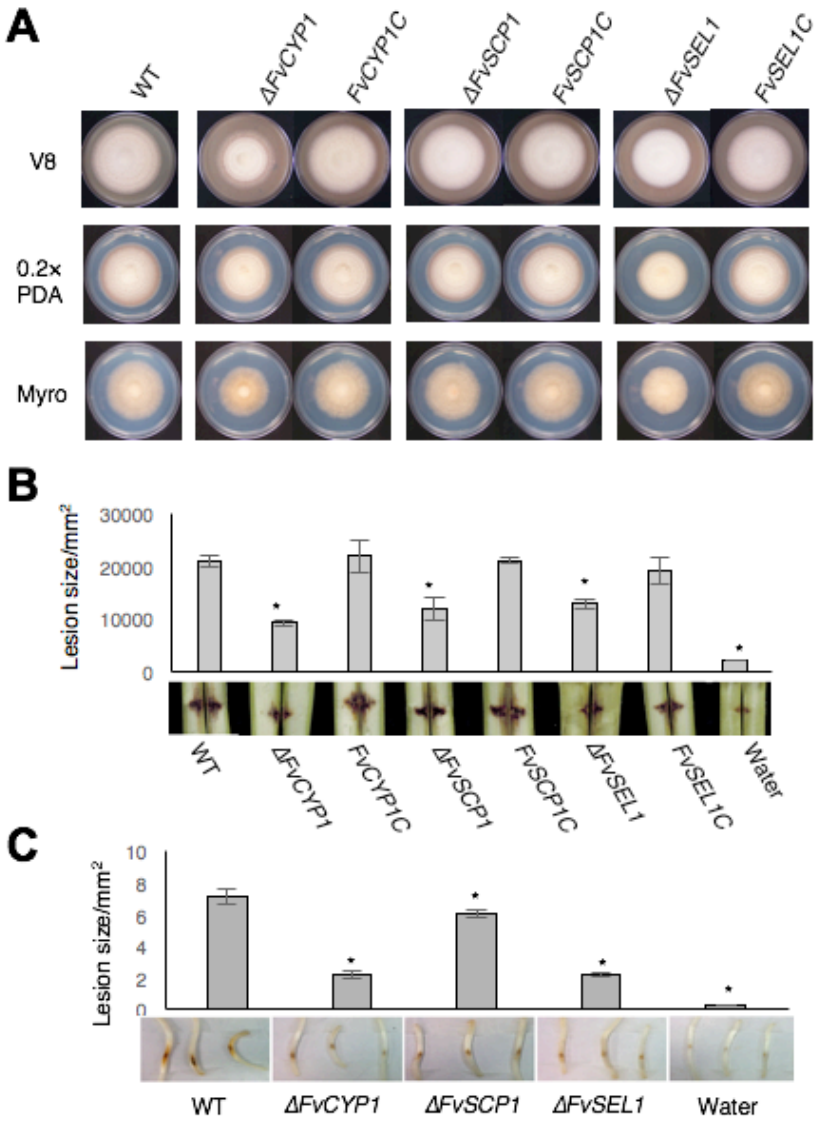

Figure 2.4 Functional characterization of FvCyp1, FvScp1, FvSel1.
(A) Vegetative growth of WT, mutants and complementation strains were examined on V8, 0.2XPDA, and Myro agar plates. (B) Stalk rot pathogenicity assay was performed as described earlier. (C) Seedling rot pathogenicity assay was performed as described earlier.

Subsequently, we performed stalk rot assays with these mutants following the procedure described earlier (Shim et al., 2006). Conidial suspensions ($1x10^8$/ml) of wild-type, mutants, complementation strains, and water (negative control) were inoculated into maize stalks between internodal regions. After a 10-day incubation, stalk rot symptoms generated by ΔFvCyp1, ΔFvScp1, and ΔFvSel1 strains were less severe when compared with wild-type and complementation strains (Figure 2.4B). In contrast, ΔFvHex1 and ΔFvPex14 showed no significant difference with *F. verticillioides* wild-type strain when we tested stalk rot (Figure A-5). When we quantified the lesion area distribution from longitudinally split stalks, the differences were significant, with ΔFvCyp1 mutant showing the biggest difference when compared to the wild-type strain (Figure 2.4B). To further assess the loss of virulence in these mutants, we performed maize seedling rot assay as previously described by Christensen and colleagues (2014). Once again, ΔFvCyp1, ΔFvScp1, and ΔFvSel1 showed significantly reduced symptoms (Figure 2.4C). These results strongly suggest that proteins that interact with Fsr1 N-terminus play important roles in *F. verticillioides* virulence.

Cellular localization of Fsr1-interacting proteins in *F. verticillioides*

After demonstrating physical interaction between Fsr1 and FvCyp1, FvScp1, and FvSel1 *in vivo*, we next investigated the cellular localization of these proteins in *F. verticillioides*. In our earlier study, we used *A. nidulans* to visualize the subcellular localization of StrA, a homolog of Fsr1, in a living cell and determined that StrA::eGFP colocalizes to FM4-64 stained endomembrane structures, likely endoplasmic reticulum

(ER) and nuclear envelope (Wang et al., 2010). FvCyp1, FvScp1, and FvSel1 are all predicted as membrane-associated proteins (The UniProt Consortium, 2017), and therefore we hypothesized that these interacting proteins co-localize to endomembrane structures in *F. verticillioides*. We transformed each *F. verticillioides* mutant with a construct that has GFP-tagged target gene fused to *Magnaporthe oryzae* ribosomal protein 27 (RP27) promoter (Ribot et al., 2013; Zheng et al., 2007). FvCyp1-GFP exhibited a pattern at or near ER in mycelia (Figure 2.5), and this association with ER was further tested by staining with ER-Tracker™ red dye. We also observed that FvCyp1 was also distributed irregularly in the cytoplasm, perhaps with other endomembrane structures in the cell. FvScp1-GFP and FvSel1-GFP exhibited a slightly different localization pattern than FvCyp1: they were more concentrated near the nucleus, which was confirmed by staining with DAPI (Figure 2.5). However, FvSel1 localization also differs from FvScp1 since it showed irregular dispersion in the cytoplasm with tubular and punctate structures. These data suggest that while FvCyp1, FvScp1, and FvSel1 co-localize to endomembrane structures, most likely the nuclear membrane and ER, in *F. verticillioides*, they each hold unique localization sites in the cell when studied in more detail.

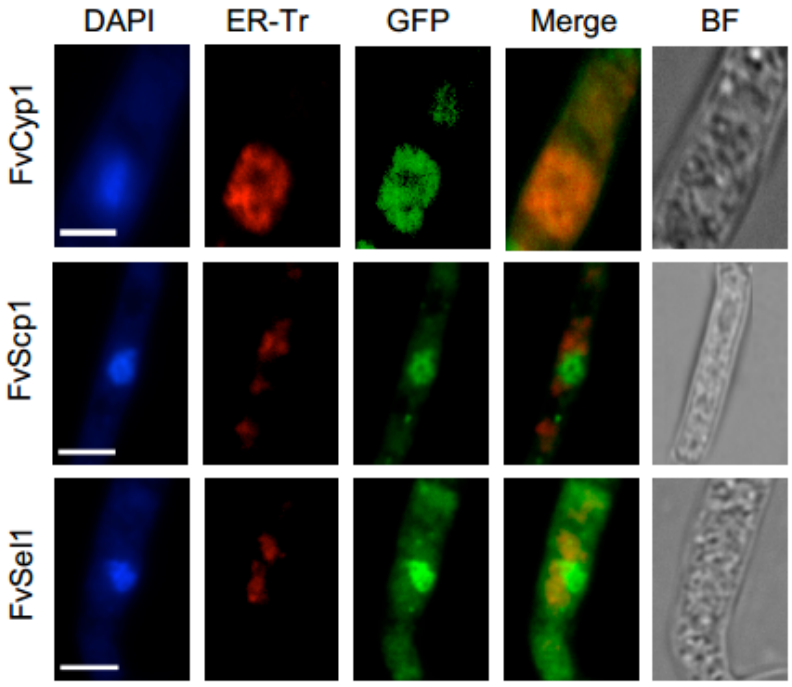

Figure 2.5 Cellular localization of FvCyp1, FvScp1, FvSel1 proteins in *F. verticillioides*. FvCyp1-GFP exhibited a pattern at or near ER in mycelia confirmed by ER-tracker red (ER-Tr). FvScp1-GFP and FvSel1-GFP exhibited a similar localization pattern near nucleus, which was confirmed by staining with DAPI. FM4-64 was used to stain the vacuole, septum, and vesicles. Scale bar = 5 μm.

Fsr1 localization is altered in *F. verticillioides* ΔFvCyp1, ΔFvScp1, ΔFvSel1 mutants

After observing the impact of ΔFvcyp1, ΔFvscp1, ΔFvsel1 mutations in *F. verticillioides*, we hypothesized that deletion of these genes, and thus the absence of these proteins, would negatively impact the cellular localization of Fsr1. Based on the fact that striatin serves as a critical component of STRIPAK complex, incorrect localization of Fsr1 could lead to critical defects in STRIPAK-mediated downstream cellular signaling. To test this hypothesis, we introduced *FSR1*::*GFP* construct into Δfsr1, ΔFvcyp1, ΔFvscp1and ΔFvsel1 mutants and followed its localization *in vivo*. When *FSR1*::*GFP* was complemented into Δfsr1, GFP was largely associated with late endosome structures in mycelia, as detected by FM4-64 staining. Surprisingly, Fsr1::GFP exhibited strong localization to vacuoles in ΔFvcyp1, ΔFvscp1, and ΔFvsel1 mutants (Figure 2.6). Our study suggests that FvCyp1, FvScp1, and FvSel1 are necessary for proper localization of Fsr1 to ER in *F. verticillioides* and perhaps for functional organization of STRIPAK complex. Vacuoles are commonly known to play key roles in protein degradation, autophagy and cell death, and a storage compartment for secondary metabolites (Xiao et al., 2009). We are not certain whether the localization shift seen in these mutants is due to damaged Fsr1 or due to the initiation of autophagy process. Further study is warranted to answer these questions.

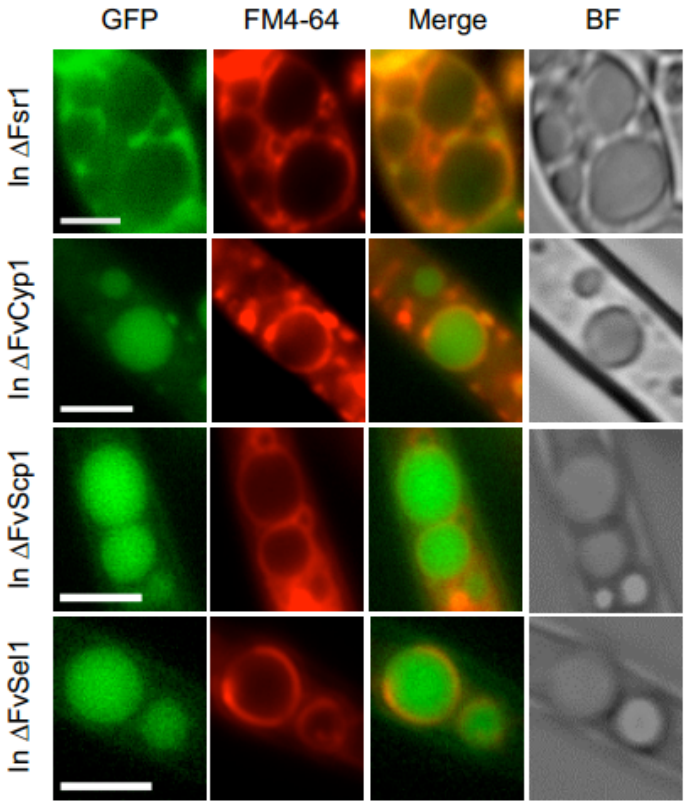

Figure 2.6 Fsr1 localization is altered in *F. verticillioides* ΔFvcyp1, ΔFvscp1, and ΔFvsel1 mutants.
ΔFsr1::Fsr1-GFP was associated with vacuolar membranes or late endosomes in mycelia, while Fsr1-GFP exhibited a localization pattern inside vacuole/endomembrane in ΔFvcyp1, ΔFvscp1 and ΔFvsel1 mutants as confirmed by staining with FM4-64. Scale bar = 5 μm.

DISCUSSION

Studies performed in eukaryotes, including filamentous fungi, strongly suggest that striatin homologs as well as STRIPAK components share highly conserved domain architectures. While structural conservation suggests common functionalities, we are also learning that STRIPAK components in different organisms perform unique cellular functions by interacting with different subsets of kinases, phosphatases, or transcription factors (Bloemendal et al., 2012, Dettmann et al., 2013, Qing et al., 2004, Shin et al., 2013). In the plant pathogenic fungus *F. verticillioides*, we demonstrated a role of striatin homolog Fsr1 in stalk rot virulence (Shim et al., 2006), and that the Fsr1 N-terminal serves an essential role in regulating virulence (Yamamura & Shim, 2008). In this study we characterized FvStp1, the homolog of human Strip1/2 protein, to confirm that Fsr1 indeed interacts with one of the main components of STRIPAK complex and that *F. verticillioides* FvStp1 is also necessary for virulence. Furthermore, with the understanding that the coiled-coil domain is critical for virulence, we sought out *F. verticillioides* proteins that interact with Fsr1 *in vivo* to investigate their role in stalk rot virulence.

Recent studies are providing a better understanding on how striatins work with other interacting protein to regulate cellular functions in fungi. In *S. macrospora*, STRIP1/2 homolog Pro22, which directly interacts with striatin homolog Pro11, plays a role in regulating septation, specifically during sexual development (Bloemendal et al., 2012). *N. crassa* ham-2 has also been characterized, which demonstrated its important

role in vegetative growth and hyphal fusion (Xiang et al., 2002). It was hypothesized that *ham-2* functions in MAP kinase pathway to regulate chemotropic polarized conidia growth and conidial germlings (Roca *et al.*, 2005). In budding yeast, a STRIP1/2 homolog Far11, a component of Far complex, is necessary for maintaining the G1 phase cell cycle arrest required for sexual polarized growth (Kemp & Sprague, 2003). This evidence supports the idea that not only STRIP1/2 homolog exists but also performs distinct features in maize pathogen *F. verticilliodes*. Our yeast two hybrid and split luciferase data revealed that FvStp1 interacts with Fsr1 *in vivo*, and subsequent molecular characterization demonstrated that FvStp1 is important for *F. verticillioides* virulence on maize stalk. Characterization of additional STRIPAK complex components (Table 2.1) can provide an improved understanding of how STRIPAK regulates important cellular functions, as demonstrated in *S. macrospora* and *N. crassa* (Beier et al., 2016; Bloemendal et al., 2012; Dettmann et al., 2013). STRIPAK complex is reported to be associated with multiple signaling pathways, *e.g.* RhoA pathway, rapamycin (TORC) 2 pathway, and cell wall integrity (CWI) MAP kinase pathway (Pracheil et al., 2012; Rispail & Di Pietro, 2009; Stockton et al., 2010; Zheng et al., 2010). Based on published reports, we hypothesized that Fsr1 functions together with putative phosphatases and kinases to regulate virulence. However, three *F. verticillioides* PP2A catalytic subunits (Table 2.1) did not show detectable level of interaction with Fsr1 in *F. verticillioides* when tested by split luciferase assay. Identifying novel Fsr1-interacting kinases and phosphatases will advance our understanding of STRIPAK-

mediated signaling mechanisms. However, this remains a challenging task due to the transient nature of these protein-protein interactions in fungal cells.

One of the key motivations for this study was to identify proteins that interact with the N-terminus of Fsr1, namely with the coiled-coil domain, and test whether these proteins play important roles in *F. verticillioides* virulence. Through our yeast two-hybrid screen of cDNA library generated from *F. verticillioides*-infected maize stalk, we discovered three new STRIPAK interacting proteins, FvCyp1, FvScp1, and FvSel1. Notably, FvCyp1 has a well conserved cyclophilin-like domain (CLD) of approximately 109 amino acids. Cyclophilin proteins are found across all organisms, with 16 cyclophilin proteins in humans (Waldmeier et al., 2003; Galat, 2003), 29 in *Arabidopsis thaliana* (He et al., 2004) and 8 in *Saccharomyces cerevisiae* (Arevalo-Rodriguez et al., 2004). All cyclophilins share a common CLD domain and are known to have peptidyl-prolyl *cis-trans* isomerase activity. Due to its conserved nature and distribution throughout the cell, it is believed that cyclophilins perform a variety of fundamental cellular functions. Our FvCyp1 knockout mutant displayed significantly reduced virulence, similar to the Fsr1 mutant level, when tested on stalks and seedling, suggesting a role in fungal virulence. In plant pathogenic fungi *Magnaporthe grisea* and *Botrytis cinearea,* cyclophilin was shown to act as a virulence determinant during plant infection (Viaud et al., 2003). Cyclophilin proteins are also known to act as modulators of protein function in eukaryotes. For instance, mammalian cyclophilin A forms a complex with cyclosporin A and calcineurin to prevent the regulation of cytokine gene transcription (Fox et al., 2001). A mammalian Cyp40 has been shown to inhibit the

activity of the transcription factor c-Myb (Leverson & Ness, 1998). In the budding yeast, cyclophilin Cpr1 is a part of the Set3 complex that maintains histone-deacetylase activities and is important for enabling the transcriptional events necessary during the switch from mitotic to meiotic cell division in budding yeast (Arevalo-Rodriguez et al., 2000; Arevalo-Rodriguez & Heitman, 2005; Pijnappel et al., 2001).

Two other proteins found in our yeast two-hybrid screen, FvScp1 and FvSel1, also provide us with new insight for striatin functions. FvScp1 is a sperm-coating protein (SCP)-like extracellular protein, also called SCP/Tpx-1/Ag5/PR-1/Sc7 (SCP/TAPS), and all SCP/TAPS molecules share a common primary structure which can act as a Ca^{2+}-chelator in various signaling processes (Cantacessi et al., 2009). SCP family members have been identified in various eukaryotes and belong to the cysteine-rich secretory protein (CRISP) superfamily (Chalmers et al., 2008). The broader SCP family includes plant pathogenesis-related protein 1 (PR-1), CRISPs, mammalian cysteine-rich secretory proteins and allergen 5 from vespid venom. FvSel1 was named after Sel1, a protein first identified in *C. elegans* that subsequently gave name to Sel1-like repeat (SLR) solenoid protein family (Grant & Greenwald, 1996). SLR proteins are commonly found in bacteria and eukaryotes with an average frequency of 4.8 Sel1-repeats per protein and are frequently involved in signal transduction pathways. FvSel1 has six Sel1 repeats, similar to Hrd3 protein in *S. cerevisiae*, however the lengths of the repeated sequences and the number of repetitions can vary in different prokaryotes and eukaryotes (Mittl & Schneider-Brachert, 2007). Homologues of Sel1 protein have been identified in several higher eukaryotes including humans, *Drosophila melanogaster*, and

Arabidopsis thaliana (Mittl & Schneider-Brachert, 2007; Zhang et al., 2015). In *S. cerevisiae* there are at least three SLR proteins identified (Hrd1, Hrd3 and Chs4) with functional annotations. SLR proteins have been reported to be involved in the ER-associated protein degradation (ERAD) in *S. cerevisiae* and *A. thaliana* under stress-inducing conditions (Gardner et al., 2000; Kamauchi et al., 2005). Significantly, recent studies have shown that *A. thaliana* Sel1 is involved in RNA editing and splicing of plastid genes (Pyo et al., 2013; Zhang et al., 2015).

While our study is the first to report *in vivo* interactions between STRIPAK and cyclophilin, SCP and SLR proteins in fungi, we still do not clearly understand how these proteins impact virulence activities. Based on literature it is reasonable to hypothesize that these proteins are involved in regulating STRIPAK complex assembly and therefore affecting fungal development and virulence. However, questions still remain as how these STRIPAK-interacting proteins modulate cellular function in *F. verticillioides* as well as other fungal pathogens. Since striatin has been recognized as endomembrane associated protein in eukaryotic cell, including in fungi (Castets et al., 2000; Okamoto *et al.*, 1998; Pöggeler & Kück, 2004; Wang et al., 2010), we investigated the cellular localization these Fsr1-interacting proteins in *F. verticillioides*. We showed that FvCyp1 localizes to ER membrane and perhaps serves a role in recruiting Fsr1 to ER membrane. It is important to note that ER is a Ca^{2+} storage site in fungal cells (Bowman et al., 2009), and this result supports the idea that Fsr1 interacts with FvCyp1 to regulate Ca^{2+}/calmodulin signaling pathways. Animal and human striatin homologs bind to calmodulin in a Ca^{2+}-dependent manner and are thought to be involved in the neuron-

specific Ca^{2+} signaling events (Moreno et al., 2000). Localization of FvScp1 and FvSel1 was slightly different than FvCyp1 in that both were concentrated near the nuclear envelope rather than the ER. However, when we consider that ER is adjacent to and encompasses the cell nucleus, we can conclude that these three proteins share localization with Fsr1 in *F. verticillioides*.

One of the surprising discoveries in this study was the altered cellular localization of Fsr1 in FvCyp1, FvScp1 and FvSel1 mutants. In the wild-type *F. verticillioides*, Fsr1 is localized to endomembrane near ER (Figure 6), which was in agreement with the study performed in *Aspergillus nidulans* (Wang et al., 2010). But in FvCyp1, FvScp1 and FvSel1 knockout mutants, Fsr1 failed to maintain its original localization and was seen inside vacuoles (Figure 6). While we were not completely surprised by the fact the Fsr1 localization was altered in these mutants, we were perplexed to see very similar outcomes in all three mutants. One possible explanation is that Fsr1 proteins fail to translocate to endomembrane for further processing without functional FvCyp1, FvScp1 and FvSel1 proteins, and that Fsr1 was shunted to vacuole for degradation. Vacuoles typically store water, ions, secondary metabolites and nutrients but they also act as a key repository for waste products, excess solutes and toxic substances (Hatsugai et al., 2004; Martinoia et al., 2007). Vacuoles are also known to play key roles in cell death and autophagy (Xiang et al., 2013; Xiao et al., 2009). We can hypothesize that the degradation of Fsr1 into vacuoles results in disruption of the STRIPAK complex and thus the loss virulence. However, the reason for incorrect

localization is still not completely understood, and this mechanism remains to be further investigated.

MATERIAL AND METHODS

Fungal strains and culture media

F. verticillioides strain 7600 (Fungal Genetics Stock Center, University of Missouri-Kansas City, Kansas City, MO, U.S.A) and all mutants generated in this study (Table A-3) were cultured at 25°C on V8 juice agar (200 ml of V8 juice, 3 g of $CaCO_3$ and 20 g of agar powder per liter). Colony morphology was visually assayed after 6 days of growth on V8 agar, potato dextrose agar (PDA; Difco) and defined medium agar (1 g of $NH_4H_2PO_4$, 3 g of KH_2PO_4, 2 g of $MgSO_4 \cdot 7H_2O$, 5 g of NaCl, 40 g of sucrose and 20 g of agar powder per liter). For genomic DNA extraction, strains were grown in YEPD liquid medium (3 g yeast extract, 10 g peptone and 20 g dextrose per liter) at 25 °C and shaking at 150 rpm.

Nucleic acid manipulation, polymerase chain reaction (PCR), and transformation

Standard molecular manipulations, including PCR and Southern hybridization, were performed as described previously (Sagaram & Shim, 2007). Fungal genomic DNA was extracted using the OminiPrep genomic DNA extraction kit (G Biosciences, Maryland heights, MO, USA). The constructs for transforming *F. verticillioides* were generated with a split-marker approach described earlier (Sagaram et al., 2007). Briefly,

DNA fragments of 5' and 3' flanking regions of each gene were PCR amplified from wild-type genomic DNA. Partial Hygromycin B phosphotransferase (*HPH*) gene (*HP-* and *-PH*) fragments were amplified from pBS15 plasmid. 5' and 3' flanking region fragments were then fused with *PH-* and *-HP* fragments by single-joint PCR, respectively. The single-joint PCR products were transformed into wild-type fungal protoplast. For complementation, respective wild-type genes driven by its native promoter was co-transformed with a geneticin-resistant gene (*GEN*) into mutant protoplasts. All primers used in this study were listed in Table A-4. *F. verticillioides* protoplast were generated and transformed following standard protocol (Sagaram & Shim, 2007) with minor modifications. Murinase (2 mg/ml) was replaced with Driselase (5 mg/ml) (Sigma, St Louis, MO, USA) in the protoplast digestion solution. Transformants were regenerated and selected on regeneration medium containing 100 μg/ml of hygromycin B (Calbiochem, La Jolla, CA, USA) and/or 150 μg/ml G418 sulfate (Cellgro, Manassas, VA, USA) as needed. Respective drug-resistant colonies were screened by PCR and further verified by Southern analysis.

Yeast two-hybrid experiments

Yeast two two-hybrid screening was performed using Matchmaker™ Library Construction and Screening system (Clontech) following the manufacturer's suggested protocol (Vidalain et. al. 2004). Total RNA was isolated from the wild-type fungus grown in autoclaved corn stalk medium (2 g pulverized B73 maize stalk in 100 mL deionized water) for 5 days. Subsequently, an *F. verticillioides* cDNA prey library was

generated by BD-SMART^{TM} kit using oligo-dT primer. Two bait vectors were constructed for the experiment: one with uninterrupted *FvFSR1* N-terminus cDNA (F1) and the other with coiled-coil motif omitted from the *FvFSR1* N-terminus cDNA (F3). Both constructs were prepared from *F. verticillioides* genomic DNA, and all amplifications were carried out using Expand Long Template Polymerase (Roche). All primers and amplication schemes were provided in Table A-3.

The two bait vectors F1 and F3 were independently transformed into *S. cerevisiae* strain AH109 to generate the yeast bait strains BF12 and BF31, respectively, and were tested for autoactivation and toxicity. For the BF12 strain, *HIS3* background was controlled by using $3AT_{10}$ (10mM 3-Aminotriazole) in the medium. The *F. verticillioides* cDNA library was independently transformed into bait strains BF12 and BF31, and blue colonies that developed on SD-Ade-His-Leu-Trp medium amended with X-alpha-Gal were isolated and purified. Yeast plasmids were isolated from each positive colony and the prey inserts were PCR amplified using primer pair 5'LD and 3'LD. The AD inserts were sequenced using T7 sequencing primer. After obtaining the sequence of putative Fsr1-interacting proteins, we performed bait-prey switch experiment. The coding sequence of each gene was amplified from the cDNA of *F. verticillioides* with the primers listed in Table A-3 and cloned into pGBKT7 as the bait vectors. F1 and F3 were cloned into pGADT7 as the prey vectors. The pairs of yeast two-hybrid plasmids were co-transformed into *S. cerevisiae* strain AH109 following the standard protocol.

Split luciferase complementation assay

Plasmids used for split luciferase assay were generated by following the method described by Kim et al. (2012). Briefly, the plasmids pUC19-nLUC and pUC19-cLUC carried N-terminal (nLuc) and C-terminal (cLuc) fragment of the luciferase, respectively. 35S promoter region was replaced in both plasmids with a fungal *crp* promoter. Fungal selectable *GEN* or *HYG* was introduced into these plasmids. The genes encoding the putative interactive proteins were amplified. Both PCR products were introduced into the *Sal*I site of pFNLucG or the *Kpn*I site of pFCLucH via In-Fusion^{erR} HD Cloning Kit (Clontech, Mountain View, CA, USA). These two constructs were co-transformed into *F. verticillioides* protoplast. Fungal colonies were selected from regeneration medium with hygromycin and geneticin and screened by PCR (data not shown). Fungal transformants carrying the constructed plasmids were used for further interaction studies. The strains carrying both empty vectors pFCLucH and pFNLucG were used as negative control. The strains carrying *FCC1* and *FCK1* were used as positive control. *FCC1* and *FCK1* are two strongly interacting proteins in *F. verticilioides*, as has been previously verified with Y2H (Bluhm & Woloshuk, 2006). All primers used are listed in Table A-3.

The split luciferase complementation assays were performed as described previously (Kim et al., 2012) with minor modifications. Briefly, 96-well plates filled with 170 µl defined medium agar were inoculated with 10 µl fungal conidia (10^8 per ml) harvested from V8 agar medium, and incubated at 25 °C for 2 days before assaying. When10 µl 15 mg/ml lucferin was added onto the colonies, light output was measured within 5 min after exposure to luciferin. Luciferase activity was measured using GloMax

96 Microplate Luminometer (Promega). Luminescence activity was obtained from three replicates and is presented as the number of RLUs (relative light units) per 10^6 of fungal conidia.

Maize infection assays

Stalk infection was performed on maize plants as previously described (Shim et al., 2006). B73 maize seeds (kindly provided by Dr. Michael Kolomiets, Department of Plant Pathology and Microbiology, TAMU) were planted in greenhouse and stalks (between V10 and VT stage) were inoculated with spores ($1x10^8$/ml) of fungal strains or water (negative control) between nodal regions. Three inoculations were performed in the same plant on continuous nodal regions. Plants were maintained in a growth chamber with 70% humidity for 10 days at 28°C with 14 h light/10 h dark cycle, watered once. Stalks were split longitudinally in half with a scalpel to assess disease severity. At least three biological and three technical replicates were performed for each fungal strain.

Maize seedling rot pathogenicity assay was performed on 2-week old maize inbred lines B73 seedlings as previously described (Christensen et al., 2014) with minor modifications. Briefly, $1x10^8$/ml spore suspensions in YEPD broth along with YEPD control were inoculated on maize B73 mesocotyls. Plant mesocotyls were first slightly wounded by a syringe needle about 3cm above the soil. A 5ul-spore suspension was applied to the wound site. The seedlings were immediately covered with a plastic cover to create a high moisture environment suitable for infection and colonization. The

seedlings were collected and analyzed after a 2-week growth period in the dark room. At least three biological and three technical replicates were performed for each fungal strain.

Construction of GFP fusion vectors and complementation

For *in vivo* localization, we generated GFP strains by introducing FvCyp1::GFP, FvScp1::GFP, FvSel1::GFP fusion constructs under their endogenous promoter. However we were not successful in obtaining strains with good fluorescent signals. As an alternative we redesigned our constructs under the control of the RP27 promoter, which has been successfully used in previous *M. oryzae*, *F. graminearum* and *F. verticillioides* protein localization studies (Bourett et al., 2002; Hou et al., 2015; Ribot et al., 2013). GFP was amplified from gGFP using the primers GFP-F1/GFP-R1, with five glycine–alanine repeat (GA-5) sequences attached at the N-terminus as a linker for GFP tagging at gene C-terminus. Primers GFP-F2/GFP-R2 with five glycine–alanine repeat (GA-5) sequences attached at the C-terminus as a linker were used to amplify GFP fragment for GFP tagging gene's N-terminus. Primers RP27-F and RP27-R were used to amplify RP27 promoter form PET11 plasmid. The primers CYP-F/CYP-R, SCP-F/SCP-R and SEL-F/SEL-R were used to amplify gene fragments separately. For RP27::GFP::FvCyp1, the RP27::GFP fusion construct was generated first, then fused with FvCyp1 by joint PCR. For RP27::FvScp1::GFP, RP27::FvSel1::GFP, each gene was first fused with GFP, then the joint fragment was fused with RP27 by joint PCR.

For Fsr1 altered localization study in Δfsr1, ΔFvcyp1, ΔFvscp1 and ΔFvsel1 mutants, the construct Rp27::GFP::Fsr1was generated by fusion PCR as described

earlier. FSR1 was amplified by using primers FSR1-F/FSR1-R and fused with Rp27::GFP construct. The generated construct together with geneticin-resistant cassette were co-transformed into Δfsr1, ΔFvcyp1, ΔFvscp1 and ΔFvsel1 mutant protoplasts. Transformants were screened by PCR. All primers used are listed in Table A-3.

Cytological Assay

To visualize GFP strains, GFP strains were grown on MM media for 6 days at room temperature (Momany et al., 1999). An Olympus BX51 microscope (Olympus America, Melville, NY, USA) was used for observation with assistance from Dr. Brian Shaw (Department of Plant Pathology and Microbiology, TAMU). A detailed description of the features used for imaging from this microscope has been published previously (Sagaram et al., 2007). DAPI staining at a concentration of 10 ng/ml was used to stain hyphae for nuclei visualization. To visualize the cell endomembrane, hyphae were treated with 25 μM FM4-64 solution for 30 min before being observed under the microscope. To visualize ER, hyphae were treated with ER-Tracker™ red dye (E34250, Invitrogen) at a final concentration of 1 μM for 20 min at 37 ℃ before observation. Images were prepared for publication with Adobe Photoshop CS5.1 following a previously described protocol (Schultzhaus et al., 2015).

CHAPTER III

CHARACTERIZING CO-EXPRESSION NETWORKS UNDERPINNING MAIZE STALK ROT VIRULENCE IN *FUSARIUM VERTICILLIOIDES* THROUGH FUNCTIONAL SUBNETWORK MODULE ANALYSES

SUMMARY

Fusarium verticillioides is an important stalk rot pathogen of maize. While a select number of genes associated with stalk rot virulence have been characterized, our knowledge of the genetic network underpinning this mechanism is very limited. Previously, we identified a striatin-like protein Fsr1 that plays a key role in stalk rot pathogenesis. To further characterize genetic networks downstream of Fsr1, we performed next-generation sequencing (NGS) with maize B73 stalks inoculated with *F. verticillioides* wild type and *fsr1* mutant. These datasets were first used to assess relative abundance in reads but we further inferred the co-expression networks for wild type as well as the *fsr1* mutant utilizing the preprocessed gene expression data through partial correlation. We used a computationally efficient branch-out technique, along with an adopted probabilistic pathway activity inference method, to identify functional subnetwork modules likely involved in *F. verticillioides* virulence. Through our analyses, potential virulence-associated subnetwork modules were identified, each consisting multiple correlated genes with coordinated expression patterns, but whose collective

activation level is significantly different in the wild type versus the mutant. We also identified two putative hub genes, *FvSYN1* and *FvEBP1,* from predicted subnetworks for functional validation and network robustness studies through gene knockout, virulence assays and qPCR studies. Our results provide evidence that *FvSYN1* and *FvEBP1* are important virulence genes that regulate the expression of closely correlated genes, providing evidence that these are important hub genes of their respective subnetworks. Lastly, we used key *F. verticillioides* virulence genes to computationally predict a subnetwork of maize genes that potentially responding to fungal virulence genes by applying cointegration-correlation-expression strategy. Our proposed network-based analysis of NGS help unveil novel genetic subnetwork modules and hub genes critical for improving our understanding of host-pathogen interactions.

INTRODUCTION

Maize stalk rot is a complex disease, primarily caused by a series of fungal pathogens. Charcoal rot (by *Macrophomina phaseolina*), Fusarium stalk rot (by *Fusarium verticillioides*), Gibberella stalk rot (by *F. graminearum*) and Anthracnose stalk rot (by *Colletotrichum graminicola*) are the major stalk rots that devastate maize-growing regions in the US (Stack, 1999; White, 1999). Losses due to stalk rot come in several different forms including stalk breakage, lodging, premature death of the plant, and the interruption of the normal grain filling process. Pathogens typically overwinter in the crop residue from the previous year and produce spores in the next growing season

that will serve as the primary inoculum source. It is generally perceived that when crops experience abiotic stress, particularly at the end of the growing season, pathogens take advantage and colonize vulnerable stalk tissues (Dodd, 1980; Michaelson, 1957; White, 1999). But overall, we still lack a clear understanding of how these stalk rot fungi colonize and progress through pathogenesis.

To better understand the mechanism of pathogenesis, we generated a loss-of-virulence *F. verticillioides* mutant and characterized the gene, *FSR1*, that is responsible for this deficiency (Shim et al., 2006). Microscopic examination of inoculated stalks revealed the wild-type fungus vigorously colonizing vascular bundle and causing rot, whereas the mutant showing limited colonization and rot in stalks. *FSR1* encodes a protein that share high similarity with striatin, a group of proteins found in eukaryotes that forms complex with kinases and phosphatases to regulate diverse cellular functions (Bartoli et al., 1999; Castets et al., 2000; Moreno et al., 2000). Recent studies have demonstrated important cellular and physiological roles of striatin protein in *Sordaria macrospora*, *Neurospora crassa*, *Aspergillus nidulans*, and *Colletrotrichum graminicola* (Dettmann et al., 2013; Pöggeler & Kück, 2004; Wang et al., 2010; Wang et al., 2016). Our laboratory also revealed the importance of the coiled-coil motif in *F. verticillioides* virulence and demonstrated how Fsr1 forms complex with other proteins to regulate stalk rot virulence (Yamamura & Shim, 2008; Zhang et al., 2017). These discoveries collectively support our hypothesis that Fsr1/striatin-mediated signal transduction plays a critical role in regulating stalk rot pathogenesis.

However, one of the intriguing questions we are aiming to answer is the broader impact of Fsr1 in cellular signaling associated with *F. verticillioides* virulence. To unravel the complex web of genetic interactions in *F. verticillioides* and maize, we decided to take advantage of next-generation sequencing (NGS) and explore the transcriptomic subtnetwork modules underpinning *FSR1*-mediated fungal virulence by computational network-based analysis. Our goal was to develop probabilistic and systematic models to investigate the interrelationship between genes rather than quantitative comparison of transcript abundance as a measure of significance. Our NGS study was designed to capture dynamic changes in gene expression during maize stalk colonization by *F. verticillioides* wild type and *fsr1* mutant. To capture dynamic changes in transcriptome, samples were harvested from three distinct phases of stalk pathogenesis: establishment of fungal infection, colonization and movement in vascular bundle, and host destruction and collapse (Kim et al., 2015a). A total of six independent biological replications were prepared for each sample, since increasing the number of replicates was important for us to implement our computational analysis for identifying subnetwork modules that show strong differential expression.

As described in our previous work (Kim et al., 2015a), our strategy is to first construct the co-expression network of *F. verticillioides* using partial correlation, and search through these networks to detect subnetwork modules that are differentially expressed in the two *F. verticillioides* strains. Subsequently, we use the probabilistic pathway activity inference scheme (Su et al., 2009) to predict the activity level of potential subnetworks, followed by applying a computationally efficient branch-out

technique to find the subnetworks that display the largest differential expression. Through this computational pipeline, we can identify potential pathogenic modules, which consist of genes that show coordinated behavior in *F. verticillioides* but also behaving differently in the wild type and the mutant. We can also screen for potential gene modules that contain orthologs of well-known virulence genes in other phytopathogenic fungi.

Biological functions, including virulence, are executed through elaborate collaboration of various biomolecules, and there has been increasing interest in the computational identification of functional modules from large-scale experimental data. In this study, we performed a comparative analysis of two distinct *F. verticillioides* RNA-Seq datasets, where one set was obtained from wild-type *F. verticillioides* and the other set from a loss-of-virulence mutant. For a systematic analysis of the infection transcriptome, we first predicted the co-expression network of the fungus. Subsequently, we identified functional subnetwork modules in the co-expression network consisting of interacting genes that display strongly coordinated behavior in the respective datasets. A probabilistic pathway activity inference method was adopted to identify three subnetwork modules likely to be involved in *F. verticillioides* virulence. Each subnetwork consisted of multiple genes with coordinated expression patterns, but more importantly we targeted subnetworks whose collective activation level is significantly different in the wild type versus the mutant. We then applied a series of mathematical criteria to predict the hub gene in each network and functionally tested their role in *F. verticillioides* virulence and the maintenance of network robustness.

RESULTS AND DISCUSSION

NGS data preparation and relative expression analysis

We performed NGS using Illumina HiSeq 2000 and generated 36 independent libraries (*i.e.*, six libraries per each time point - 3 dpi [infection], 6 dpi [colonization], and 9 dpi [rot] - for wild type and the *fsr1* mutant). In this analysis and prediction, we used 24 sample libraries from the last two time points (6 dpi and 9 dpi) to focus on gene regulation mechanism in the latter stages of maize-fungal interaction. Acquisition of read counts of all *F. verticillioides* genes was completed by mapping NGS reads to *F. verticillioides* strain 7600 reference genome (Ma et al., 2010) using Bowtie2 (Ballouz et al., 2015; Langmead & Salzberg, 2012) and Samtools (Li et al., 2009). Through filtering process, we eliminated genes with insignificant expression and therefore 9446 genes were selected for downstream analysis. We normalized the read counts of these genes by their corresponding gene length and also based on relative expression quantification against β-tubulin genes (FVEG_04081 and FVEG_05512). The general information of our NGS datasets is shown in Figure 3.1A. From these genes, we selected 324 most significantly differentially expressed genes from our datasets and investigated their individual relative expression levels at three different time points. As shown in a heat map with three distinct time points (Figure 3.1D), 155 genes (red) are expressed significantly higher in the wild type and 169 genes (blue) are expressed significantly higher in *fsr1* mutant (Fig 3.1D). As explained earlier, the relative abundance was acquired by the two-step normalization by each gene length as well as β -tubulin genes,

and was compared by *t*-test statistics score measurement. However, this common NGS analysis focuses on relative expression of individual genes but does not allow us to predict gene-gene associations and system-level changes across correlated genes during pathogenesis.

Identification of *F. verticillioides* subnetwork modules

We developed a computational workflow that allows us to build co-expression networks from *F. verticillioides* NGS datasets (Kim et al., 2015). We first inferred the co-expression networks for wild type as well as the *fsr1* mutant utilizing the preprocessed gene expression data through partial correlation (Hero & Rajaratnam, 2012). In this co-expression network, we applied five distinct thresholds (0.965, 0.97, 0.975, 0.98, and 0.985), thereby constructing five different co-expression networks. The number of genes and edges between genes are shown in Figure 3.1B. When these co-expression networks are illustrated with all member genes and possible edges, we can generate a complex web of scale-free networks (Figure 3.1C). However, the aim of our proposed network-based NGS data analysis is to search through these co-expression networks to identify subnetwork modules that are differentially activated between the *F. verticillioides* wild type and mutant, that can considerably differ in terms of virulence potentials (Figure 3.2).

A General statistics of NGS datasets

	Wild type		Mutant	
	6 dpi	9 dpi	6 dpi	9 dpi
Type of run	Single			
Read length	100 (bp)			
Mean # of reads aligned	100934		218264	
Median depth of coverage	14.18	16.64	4.48	9.77

B Co-Expression network of wild type and mutant *F. verticillioides*

Threshold	Wild type		Mutant	
partial correlation cut-off	# of genes	# of edges	# of genes	# of edges
0.985	6,161	198,310	6,057	184,278
0.98	7,017	371,064	6,908	356,837
0.975	7,637	583,097	7,518	565,812
0.97	8,063	826,857	7,922	805,236
0.965	8,381	1,096,076	8,249	1,072,693

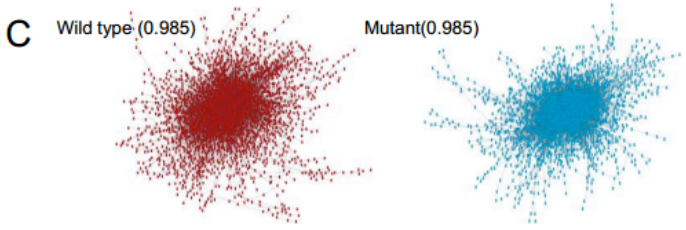

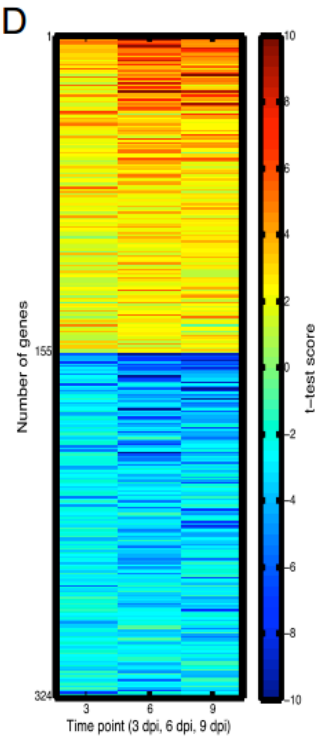

Figure 3.1 NGS statistics of significantly differentially expressed genes.
(A) General statistics of next-generation sequencing (NGS) datatsets. Reads from wild type and mutant (6 dpi and 9dpi) were ampped to *F. verticillioides* reference genome. (B) Co-expression network of wild type and mutant *F. verticillioides*. We applied five distinct threshold levels to generate five different co-expression networks. The table show number of genes and all possible edge combinations in each co-expressino network. (C) Schematic depiction of wild type and mutant co-expression networks at threshold level 0.985. (D) The heat map provides a schematic overview of 324 most significantly differentially expressed genes with three distinct time points. A total of 155 genes are expressed significantly higher in the wild type (red) while a total of 169 genes are expressed significantly higher in the mutant (blue). The relative abundance was acquired by the two-step normalization which considers each gene length as well as relative expression against beta-tubulin genes, and was compared by *t*-test statistics score measurement.

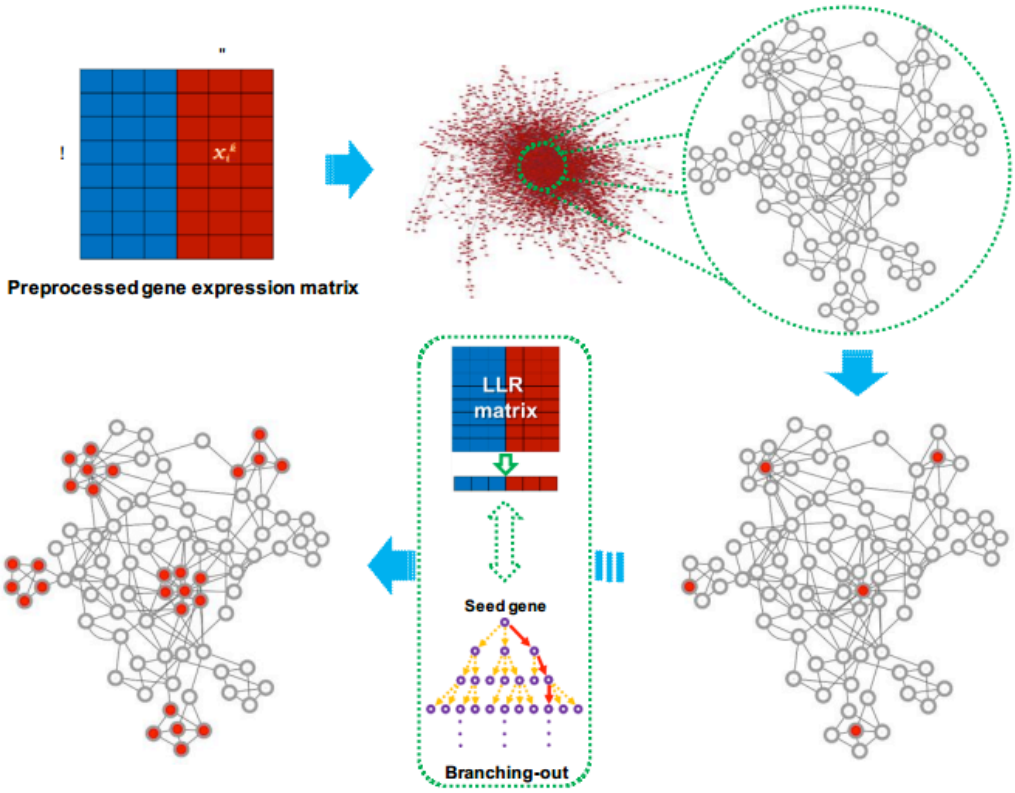

Figure 3.2 Schematic overview of our network-based NGS data analysis.
Our aim is to search through large co-expression networks to identify subnetwork modules that are differentially activated between two different conditions (*e.g.* wild type versus mutant). Initial selection of seed genes (*i.e.* top 1% differentially expressed genes) is followed by a series of computational procedures described previously (Kim et al., 2015a). Through this process, we can identify subnetwork modules that show significant difference in virulence potentials.

By following this proposed strategy, we selected three potential subnetwork modules differentially activated during *F. verticillioides* pathogenesis. In this effort, we performed additional analyses with six different characteristics for selecting hubs and their modules followed by our network-based comparative analysis approach (Kim et al., 2015a) (Figure 3.3). In the subnetwork module fine-tuning process, three modules in Figure 3.4 showed the minimum discriminative power increase for the entire module adjustment as 22%, 27%, and 22% while over 90% of modules displayed smaller than 20% increase. Note that our approach probabilistically focuses on generating subnetwork modules whose member genes have high likelihood of showing associated expression patterns to each other across all replicates using the log-likelihood-ratio (LLR) matrix that demonstrates how likely each gene would express in *F. verticillioides* wild type or the mutant. As a result, our network-based computational analysis approach found potential subnetwork modules that show harmonious coordination of member genes as well as strong differential activity between the two strains.

Figure 3.3 Computational prediction procedure for identifying key potential pathogenicity genes.
(A) Raw NGS datasets are preprocessed, *i.e.* alignment, filtering, and normalization, before they are applied for inferring *F. verticillioides* co-expression networks by means of partial correlation. In addition, these datasets were also converted into a log-likelihood ratio (LLR) matrix for downstream analysis. Next, subnetwork modules are extended from seed genes, significantly differentially expressed between the two different conditions (*F. verticillioides* wild type vs. mutant), as long as they keep sufficient strength of differential activity between the two strains. (B) Each potential hub (virulence-associated) gene is predicted in its detected subnetwork module based on several criteria: i) highly impactful in a probabilistic manner, ii) relatively differentially correlated between two strains (wild vs. mutant), iii) relatively more connected in the given module, iv) relatively significantly differentially expressed, v) orthologous to known pathogenicity-associated genes of other fungal species, vi) annotated to significant GO terms with other member genes. Through this proposed analysis approach, we identified potential functional genes showing significant differential activity between the two conditions as well as strong association with virulence.

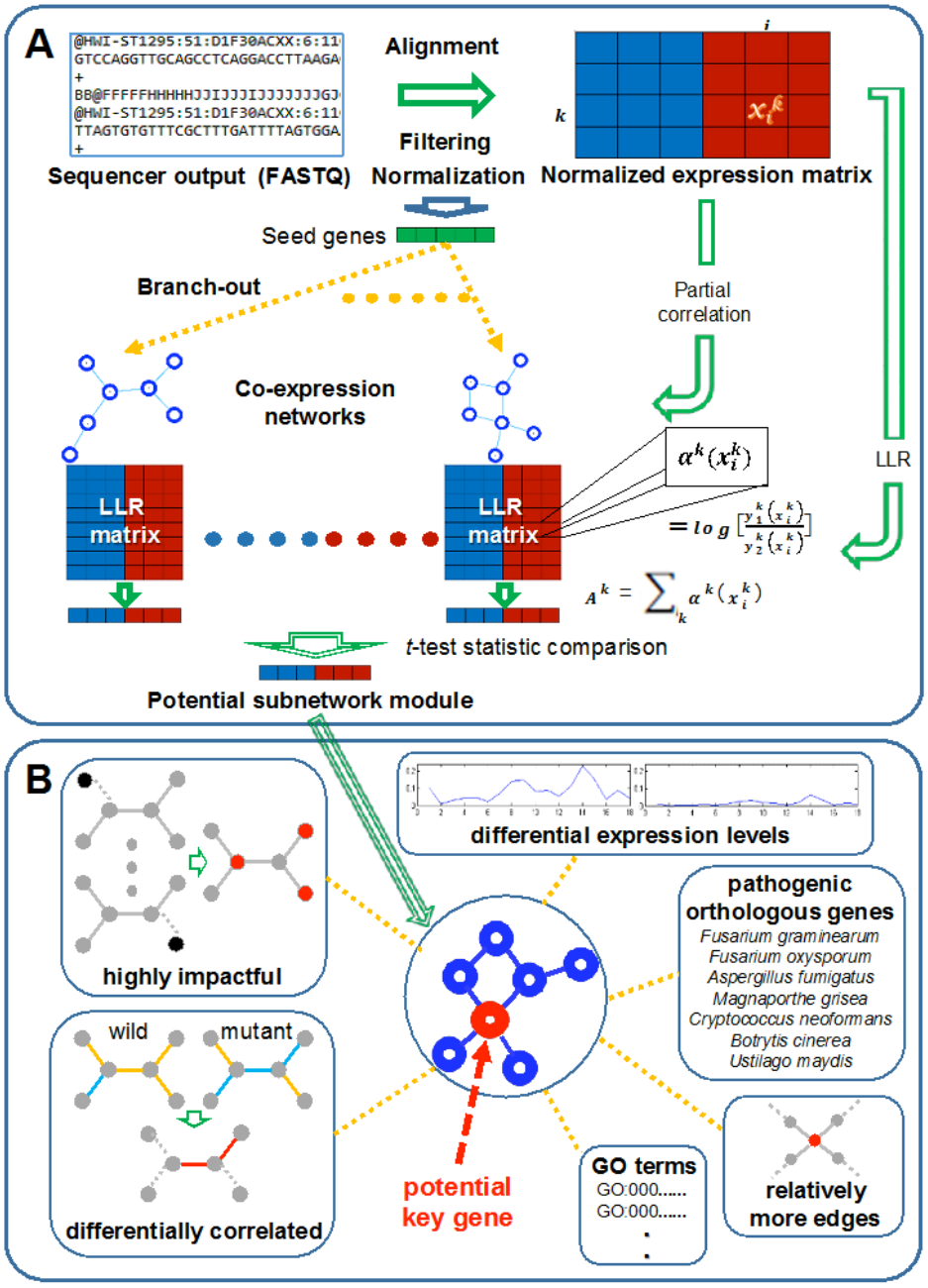
A
@HWI-ST1295:51:D1F30ACXX:6:11
GTCCAGGTTGCAGCCTCAGGACCTTAAGA
+
BB@FFFFFHHHHHJJIJJJIJJJJJJJGJ
@HWI-ST1295:51:D1F30ACXX:6:11
TTAGTGTGTTTCGCTTTGATTTTAGTGGA
+
Sequencer output (FASTQ)
Alignment
Filtering
Normalization
Normalized expression matrix
Seed genes
Branch-out
Co-expression networks
LLR matrix
LLR matrix
Partial correlation
LLR
t-test statistic comparison
Potential subnetwork module
B
highly impactful
differential expression levels
pathogenic orthologous genes
Fusarium graminearum
Fusarium oxysporum
Aspergillus fumigatus
Magnaporthe grisea
Cryptococcus neoformans
Botrytis cinerea
Ustilago maydis
wild
mutant
differentially correlated
potential key gene
GO terms
GO:000.....
GO:000.....
relatively more edges

Computational characterization of three key *F. verticillioides* subnetwork modules

From our network-based comparative analysis, we selected three potential pathogenicity-associated subnetwork modules differentially activated between the wild-type and *fsr1* mutant strains (Figure 3.4). Module A was composed of ten *F. verticillioides* genes, where 80% of these were annotated to a significant GO term cytoplasmic component (GO:0044444) (http://biit.cs.ut.ee/gprofiler/index.cgi) (Reimand et al., 2011). However, it is important to note that majority of these genes have no known function and these GO functions were chosen solely based on predicted protein motifs. Module B was comprised of fifteen genes, where four (FVEG_07930, FVEG_00890, FVEG_11886, and FVEG_00594) were annotated to a significant GO term transport (GO:0006810). The eleven other genes were hypothetical proteins with some knowledge of their functional domains. But this module showed relatively higher percentage of genes with no GO terms and no functional protein domains compared to module A. Lastly, Module C was composed of fourteen genes, where half of these fell under GO term catalytic activity (GO:0003824). Not surprisingly, a significant number of the genes in this subnetwork was also hypothetical proteins with no clear understanding of their functional role. Once we defined these subnetwork modules, we analyzed all member genes *in silico* to predict potential hub genes that may hold a key role in *F. verticillioides* pathogenicity.

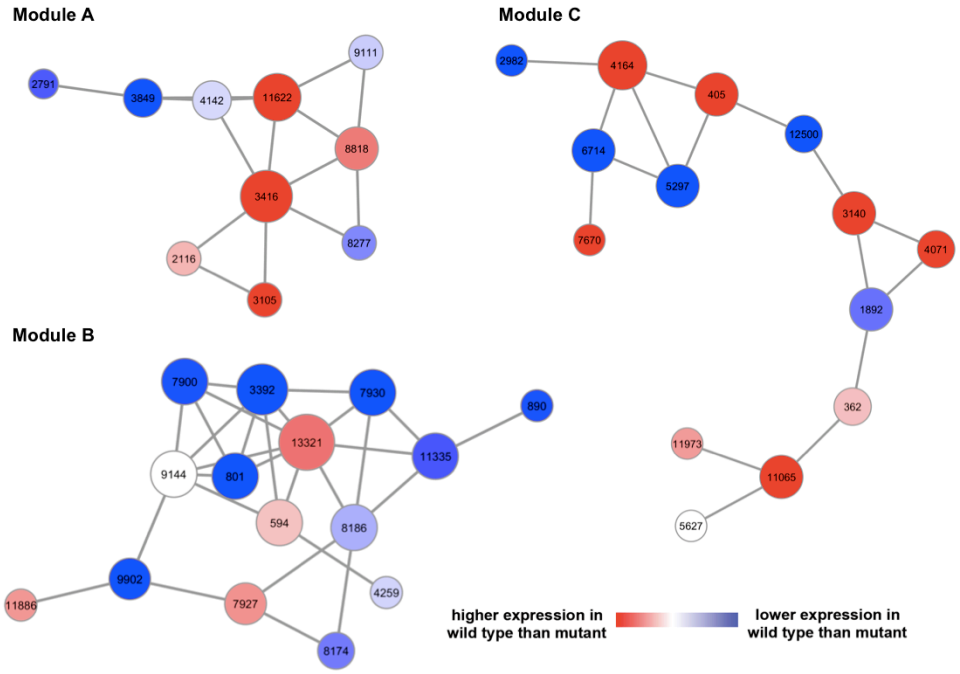

Figure 3.4 Potential subnetwork modules associated with the *F. verticillioides* pathogenicity.
Our network-based comparative analysis identified three potential virulence-associated subnetwork modules differentially activated between the two strains (*F. verticillioides* wild type vs. mutant). Module A is composed of ten *F. verticillioides* genes, where 80% of them were annotated to a significant GO term GO:0044444 "cytoplasmic part". Module B is comprised of fifteen genes, where four of them (FVEG_07930, FVEG_00890, FVEG_11886, and FVEG_00594) were annotated to a significant GO term GO:0006810 "transport". Module C is composed of fourteen genes, where half of them were annotated to a GO term GO:0003824 "catalytic activity".

In module A, we selected FVEG_11622 as a potential pathogenicity-associated hub gene based on following observations: i) FVEG_11622 deteriorated the differential probabilistic activity level of its given module from wild type to mutant by 26% (the mean of other member genes was 16%), ii) correlation coefficients of FVEG_11622

decreased from wild type to mutant by 0.26 and 0.34 for Pearson's and Spearman rank, respectively (the mean of other member genes was 0.14 and 0.19), iii) FVEG_11622 contained four edges to other member genes (the mean of other member genes was 2.8), iv) FVEG_11622 demonstrated significant expression decrease from wild type to mutant (*t*-score of 4.4), and v) orthologous gene of FVEG_11622 in *Botrytis cinerea* (*BC1G*) is recognized as having a role in fungal virulence. The predicted hub gene FVEG_11622, which was tentatively designated as *FvEBP1*, encodes a putative 238-AA hypothetical protein that harbors Emopamil-binding protein (EBP) domain (pfam05241). In mammalian systems, this protein family is known to be associated with endoplasmic reticulum and play a critical role in sterol isomerization and lipoprotein internalization (Seo et al., 2001). An emopamil binding protein BcPIE3 in *Botrytis cinerea* which shares significant structural similarities to mammalian EBPs was shown to be important for virulence (Gioti et al., 2008). *FvEBP1* has four directly edges to FVEG_03416, FVEG_04142, FVEG_08818 and FVEG_09111. FVEG_03416 is an alginate lyase gene, contains alginate lyase domain which is important for fructose and mannose metabolism. FVEG_04142 is a V-type proton ATPase subunit F containing a V-type ATPase, F subunit domain, this gene has hydrogen-exporting ATPase activity which is involved in ATP hydrolysis coupled proton transport biological process. FVEG_09111 is a hypothetical protein, contains a PX-associated domain. The function of this protein is unknown, but its N-terminal is always found to be associated to a PX domain which is involved in targeting of proteins to cell membranes. FVEG_08818 is a hypothetical protein with a methyltransferase domain.

Using the same approach, we identified FVEG_00594 as the potential pathogenicity-associated hub gene in module B based on following observations: i) FVEG_00594 reduced the differential probabilistic activity level of its detected module from wild type to mutant by 24% (the mean of other member genes was 13%); ii) correlation coefficient difference of FVEG_00594 between wild type and mutant was 0.34 and 0.4 for Pearson's and Spearman rank, respectively (the mean of other member genes was 0.24 and 0.2); iii) FVEG_00594 included four edges to other member genes (the mean of other member genes was 3.7); iv) the difference of expression level of FVEG_00594 was higher in wild type although it did not show high significance (*t*-score as 0.8), and v) the ortholog of FVEG_00594 in *F. graminearum* (FG) is recognized as having a role in fungal virulence. FVEG_00594, designated *FvSYN1,* encodes a putative 377-AA protein that harbors two well-recognized domains: syntaxin N-terminus domain (cd00179) and SNARE domain (cd15849). In budding yeast, SNARE protein complex is involved in membrane fusion and protein trafficking for new synthesis and recycling of organelles (Nicholson et al., 1998). SNAREs were originally classified into v-SNAREs and t-SNAREs according to their vesicle or target membrane localization (Sollner et al., 1993). Syntaxins belong to t-SNARE proteins and are shown to play important role in membranes fusion in eukaryotic cells (Gupta & Heath, 2002; Hong, 2005). Syntaxins are known as a family of membrane-associated receptors for intracellular transport vesicles. Syntaxin and SNAREs are also known to anchor these newly synthesized and recycled proteins to cytoplasmic surface (Yuan & Jantti, 2010). SNARE proteins play critical and conserved roles in intracellular membrane fusion in eukaryotic cells (Chen & Scheller,

2001). They were known to mediate membrane fusion during all trafficking steps of the intracellular communication process, including the secretory and endocytic pathways (Hong & Lev, 2014). *FvSYN1* has four directly associated genes in the subnetwork module: FVEG_03392, FVEG_04259, FVEG_09144 and FVEG_13321. Three of these genes (FVEG_03392, FVEG_04259, and FVEG_09144) encode hypothetical proteins with no known functional motif thus making it difficult to predict its role. While FVEG_13321 is a hypothetical protein, it does contain a fungal Zn_2Cys_2 binuclear cluster domain, which is typically found in the family of fungal zinc cluster transcription factors (MacPherson et al., 2006; Schillig & Morschhauser, 2013) .

Analyzing module C was more challenging when compared to the other two subnetwork modules. With our computational prediction, FVEG_03140 was identified as the potential hub gene based on following criteria: i) FVEG_03140 lowered the differential probabilistic activity level of its module from wild type to mutant by 23% (the mean of other member genes was 14%); ii) the difference of correlation coefficient FVEG_03140 between wild type and mutant was 0.3 and 0.23 for Pearson's and Spearman rank, respectively (the mean of other member genes was 0.14 and 0.17); iii) FVEG_03140 had three edges to other member genes (the mean of other member genes was 2.3); iv) FVEG_03140 displayed significant expression alteration from wild type to mutant (*t*-score as 9.9); and v) the orthologous gene of FVEG_03140 in *Magnaporthe grisea* (MGG) is recognized as a pathogenicity gene (Dean et al., 2005). However, FVEG_03140 encodes a hypothetical protein similar to endo-1,4-beta-xylanase, and while cell-wall-degrading enzymes play an important role in host invasion and

colonization (Cho et al., 2015; Jorge et al., 2006; Kubicek et al., 2014) it was difficult for us to accept FVEG_03140 as a potential hub regulatory gene in module C. As an alternative, we selected a neighboring gene FVEG_01892 with the next highest hub-likelihood score, which encodes a cyclophilin-type peptidyl-prolyl isomerase (PPIase), for further investigation.

Functional characterization of predicted hub genes associated with virulence

To test our hypothesis that *FvEBP1* (FVEG_11622), *FvSYN1* (FVEG_00594), and *FvCYP2* (FVEG_01892) are putative hub genes of subnetwork modules A and B, respectively, and that they are important for *F. verticillioides* virulence, we generated gene knockout mutants Δfvebp1, Δfvsyn1 and Δfvcyp2 through homologous recombination following our standard split marker protocol (Sagaram et al., 2007). Hygromycin B phosphotransferase (*HPH*) was used as the selective marker, and homologous recombination outcomes were confirmed by PCR (data not shown) and Southern blots (Figure B-1). We first compared vegetative growth of these mutants on synthetic media (PDA, V8 agar and defined medium agar), and while Δfvsyn1 strain showed reduced colony growth, Δfvebp1 and Δfvcyp2 strains exhibited no defect (Figure 3.5A and Figure B-2). The mutant Δfvsyn1 showed restricted radial vegetative grow while exhibiting more dense and fluffier mycelial growth on solid media when compared to the wild type and the complementation strain FvSYN1C (Figure 3.5B). When cultures were harvested from YEPD broth, we did not observe a significant difference in fungal mass production (Figure 3.5C). For spore production on V8 plates,

Δfvsyn1 produced significantly reduced spores when compared to other strains (Figure 3.5D).

To test virulence, we inoculated B73 maize seedling mesocotyls with spore suspension of wild-type, Δfvebp1, Δfvsyn1, and Δfvcyp2 strains (along with water as a negative control) following the previously described procedure (Christensen et al., 2014). When symptoms were observed after a 2-week incubation, Δfvebp1 and Δfvsyn1 mutants showed significantly decreased levels of rot when compared with the wild-type progenitor (Figure 3.5E) while Δfvcyp2 showed no significant difference (Figure B-2). Mutants Δfvebp1 and Δfvsyn1 showed approximately 70% and 60% reduction in virulence when analyzed by average mesocotyl rot area (Figure 3.5E). In order to test whether the mutant phenotype is due to a targeted gene replacement, we generated complementation strains of Δfvebp1 and Δfvsyn1 by co-transforming each mutant protoplasts with the respective wild-type gene (*FvEBP1* and *FvSYN1* with their native promoter and terminator) along with the geneticin-resistance gene. PCR was performed to confirm reintroduction of wild-type genes in complemented strains. FvSYN1C strain showed complete restoration of virulence on maize seedlings whereas FvEBP1C showed partial (~75%) recovery (Figure 3.5E). These results suggested that *FvEBP1* and *FvSYN1* play an important role in virulence on maize seedling rot, and further convinced us that these two genes serve as the predicted hub gene of their respective subnetwork module.

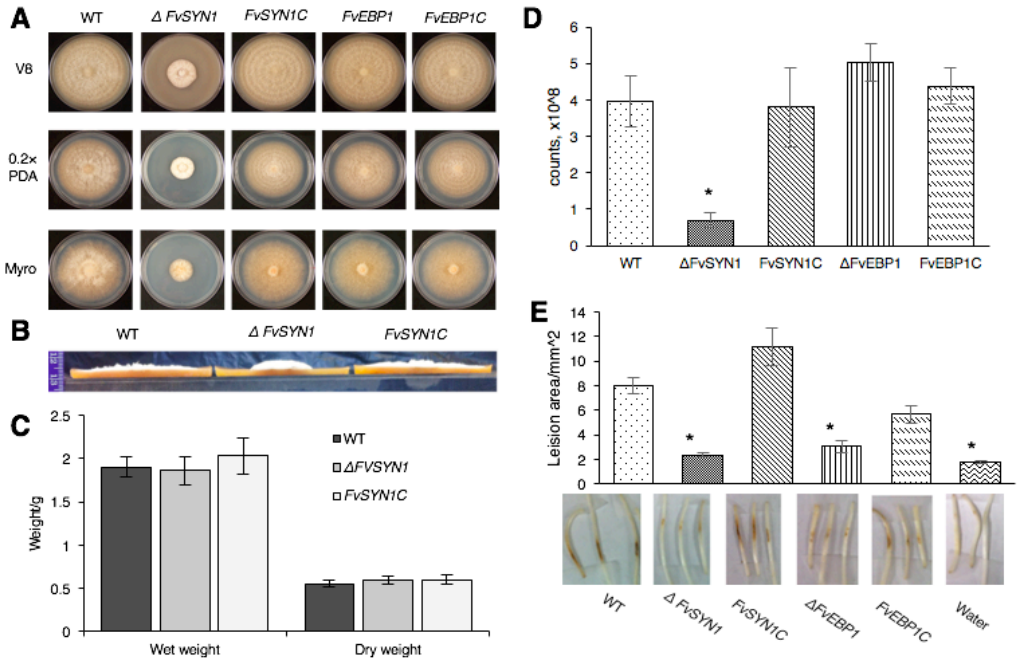

Figure 3.5 Functional characterization of *F. verticillioides FvSYN1* and *FvEBP1*.
(A) Vegetative growth of wild-type (WT), ΔFvsyn1, ΔFvebp1 and their complementation strains (FvSYN1C and FvEBP1C) were examined on V8, 0.2XPDA, and Myro agar plates. Strains were point inoculated with an agar block (0.5 cm in diameter) and incubated for 6 days at 25 °C under 14 h light/10 h dark cycle. (B) Spores (2×10^7) of WT, Δfvsyn1 and Fvsyn1C were inoculated in the center of V8 plates for 6 days at 25 °C under 14 h light/10 h dark cycle. Vegetative growth of WT, ΔFvsyn1 and FvSYN1C on V8 agar plates, strain growth condition was the same as described above. Agar plates were cut into half and pictures were taken from a side view. (C) Fungal mass production of WT, ΔFvsyn1 and FvSYN1C strains was tested in YEPD broth. 100 µl spores (10^8/ml concentration) were inoculated and incubated for 4 days at 25 °C and shaking at 150rpm. Fungal mass production was quantified by weighing wet and dry fungal mass. 3 replications included. (D) Spore production of of WT, ΔFvsyn1, FvSYN1C, ΔFvebp1 and FvEBP1C on V8 agar plates, strain growth condition was the same as described above. Spores were collected from agar plates and counted. (E) One-week-old B73 seedlings were inoculated with 10^8/ml spore suspension of fungal strains on mesocotyls. Lesion areas were quantified by Image J software after 2-week incubation. Asterisk above the column indicates statistically significant difference ($P<0.05$) analyzed by t-Test.

Testing network robustness in gene deletion mutants

A very important feature of these subnetwork modules is having robustness, *i.e.* the ability to respond to and withstand the external as well as internal stimuli while maintaining its normal behavior (Barabasi & Oltvai, 2004). However, it is reasonable to predict that when we eliminate or disable a critical node (*i.e*. hub), a network can be disrupted and shattered into isolated nodes. If a hub gene is eliminated from the subnetwork, we can hypothesize that other member genes, particularly those sharing direct edges, will exhibit disparate expression patterns.

We first tested correlated gene expression patterns in the wild type versus Δfvebp1 mutant. We learned that gene expression levels of FVEG_03416, FVEG_04142, and FVEG_08818 were drastically lowered in Δfvebp1 mutant than those observed in the wild type (Figure 3.6A). Furthermore, FVEG_09111 gene expression level was not detectable in the mutant. Particularly, it is important to note that FVEG_04142 and FVEG_09111 showed higher level of expression in Δfsr1 mutant when compare to wild type. In Δfvebp1, that expression pattern is now reversed. These results show that when *FvEBP1* is no longer present in the subnetwork expression level of these genes are drastically suppressed (Figure 3.6A and B), suggesting *FvEBP1* is critical for proper regulation of these neighboring genes.

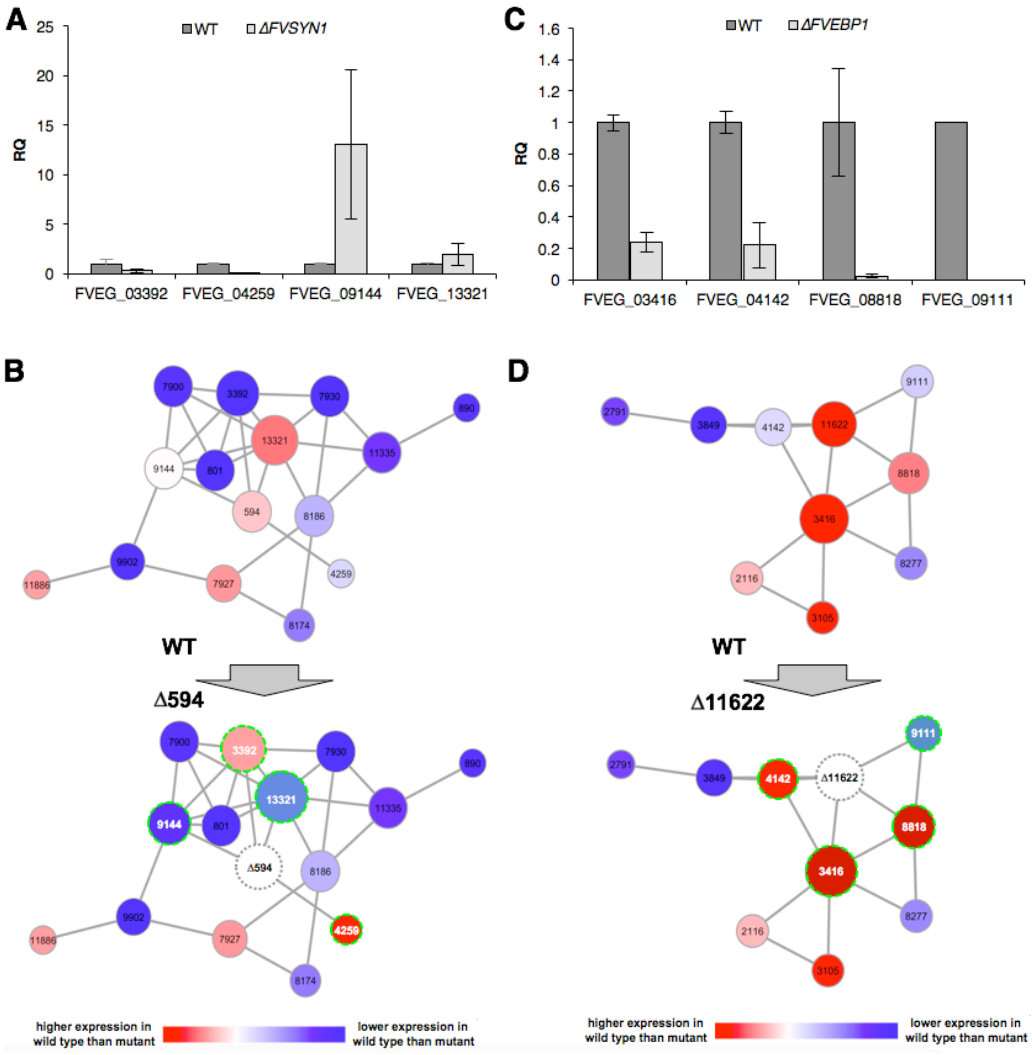

Figure 3.6 Altered expression of select neighboring genes as detected by qPCR.
(A) Relative quantification (RQ) of four neighboring genes (FVEG_3391, FVEG_9144, FVEG_13321, FVEG_4259) to predicted hub SYN1 (FVEG_0594) in wild type (WT) versus ΔFvsyn1. RQ levels of four genes in WT were normalized to 1. (B) Schematic overview of transcriptional changes of four neighboring genes (highlighted) observed in WT versus ΔFvsyn1. (C) Relative quantification (RQ) of four neighboring genes (FVEG_4142, FVEG_8818, FVEG_3416, FVEG_9111) to predicted hub *EBP1* (FVEG_0594) in wild type (WT) versus ΔFvebp1. (D) Schematic overview of transcriptional changes of four neighboring genes (highlighted) observed in WT versus ΔFvebp1.

In Δfvsyn1 strain, we comparatively studied expression pattern of four genes that directly share edges with *FvSYN1*. Three of the four genes tested, FVEG_03392, FVEG_04259 and FVEG_09144 showed significant difference between the wild type and Δfvsyn1 mutant. Significantly, FVEG_03392 and FVEG_04259, which showed lower expression level in the wild type when compared with Δfsr1 mutant, reversed its course and showed higher expression in the wild type when compared with Δfvsyn1 (Figure 3.6C). FVEG_09144, which showed no difference in expression between wild type and Δfsr1, showed significantly higher expression in Δfvsyn1. FVEG_13321, which showed higher expression in wild type compared to Δfsr1, now exhibits statistically similar expression in wild-type and Δfvsyn1 (Figure 3.6C and D). Collectively these data showed that *FvSYN1* and *FvEBP1* are important for regulating the expression of closely correlated genes, further providing evidence that these are important hub genes of their respective subnetworks.

Prospects and challenges in functional subnetwork module analyses of transcriptomes in host-pathogen interactions

In this study, we assembled a streamlined computational network analysis pipeline to investigate the system-level coordinated changes across differentially activated genes rather than simply focusing on individual genes, and to detect subtle processes that are not likely to be revealed by examining a small list of highly significant genes in this host-pathogen interaction. In order to generate meaningful prediction from limited datasets, comprehensive and rigorous investigation was needed. Thus, we mainly

searched for comparable expression patterns probabilistically using a log-likelihood ratio matrix over replicates instead of just considering differential expression for identifying potential subnetwork modules. Also, we analytically investigated the given subnetwork modules with multidirectional analysis considering factors such as probabilistic impact, and differential correlation. Significantly, this comprehensive approach can help identify novel virulence-associated subnetwork modules as well as the key functional "hub" genes in fungal pathogens, such as *F. verticillioides*. This assembly of tool will be instrumental as we continue our effort to harness new and meaningful information from NGS data as we try to better understand complex pathosystems.

Our study mainly focused on analyzing the underlying transcriptional regulation in host-pathogen interactions. However, we do recognize that complex intercellular web of interactions in a living cell, not to mention between a host and its pathogen, are not limited to gene-gene association. Numerous constituents of the cell, *e.g.* DNA, RNA, protein, and metabolites, contribute to the structure and the dynamics of cellular network and ultimately behavior. However, in contrast to DNA and RNA, the resources available for us to generate systems-level proteome and metabolome datasets for network analyses are currently limited. In addition to this challenge, majority of host-pathogen systems have very limited genetic information available. For instance, as you can see from our three predicted models majority of member genes encode hypothetical proteins with unknown, and vaguely predicted, functions. We primarily focused on developing this computational approach with the intent of investigating not-well defined biological

systems with minimal bias toward existing genetic information, *i.e.* allocating higher scores toward known virulence genes in given species.

Furthermore, there is a greater challenge in refining subnetwork model development for host organisms that typically has larger and more complex genomes. Over 95% of our NGS data generated in this study came from maize, suggesting that maize stalk is actively responding to the pathogen invasion and colonization at transcriptional level (Kim et al., 2015b). In our earlier study, we developed a computational analysis pipeline, including the cointegration-correlation-expression approach, to predict potential maize defense-associated genes that show strong differential activation and coordination with known *F. verticillioides* virulence genes (Kim et al., 2015b). Here, we selected three *F. verticillioides* pathogenicity genes identified from our current work (FVEG_11622, FVEG_00594, and FVEG_09767 [*FSR1*]) to predict maize response subnetworks. An illustration of the potential subnetwork module associated with maize defense response against the *F. verticillioides* pathogenicity genes is shown in Figure 3.7. We followed the procedure from narrowing down maize genes using the cointegration-correlation-expression approach to branching out potential defense-associated modules on maize co-expression networks (Kim et al., 2015b). The subnetwork module associated with maize defense system was composed of 28 maize genes, where genes relatively significantly expressed in wild type-infected are indicated in red and genes relatively significantly expressed in mutant type-infected are indicated in blue (Figure 3.7). In this potential maize defense gene subnetwork module, we noticed that five maize genes (GRMZM2G102760_T01, GRMZM5G870932_T01,

GRMZM2G001421_T02, GRMZM2G001696_T01, and GRMZM2G137535_T01) were annotated to a significant GO term defense response/incompatible interaction (GO:0009814), defined as "a response of a plant to a pathogenic agent that prevents the occurrence or spread of disease". However, as seen in *F. verticillioides* subnetwork modules, we recognize that a large percentage of member genes encode hypothetical proteins and that transcriptional coordination does not always result in functional correlation. In addition, unlike *F. verticillioides* genes we characterized in this study, generating null mutants and performing network robustness assays are more strenuous for maize.

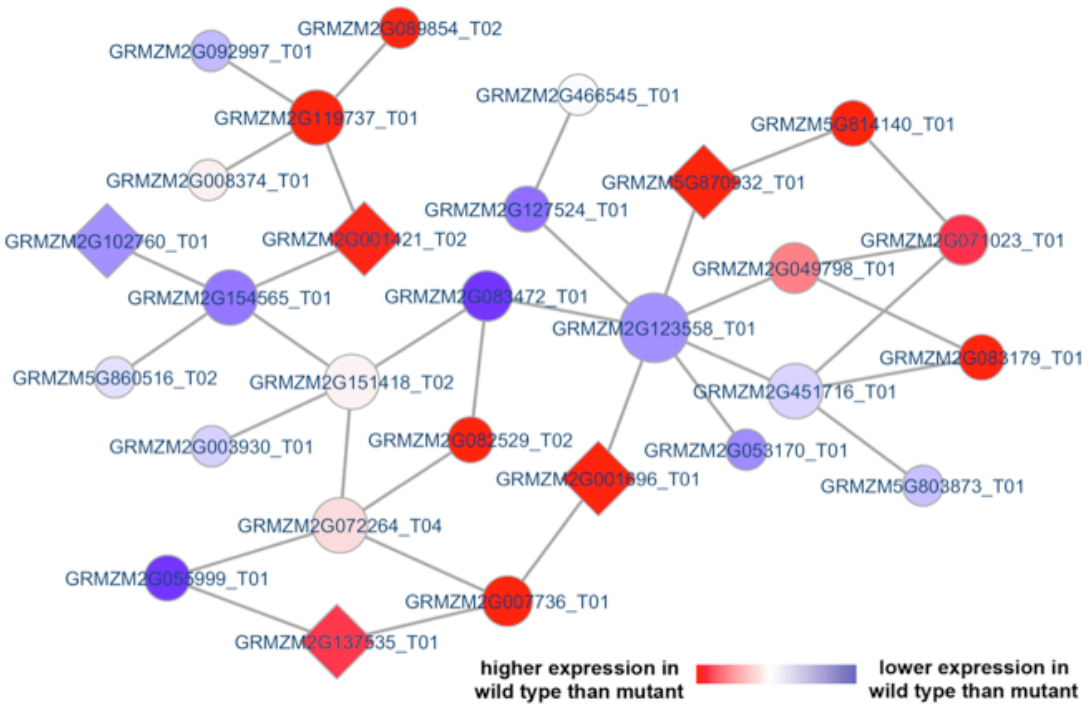

Figure 3.7 Potential subnetwork module associated with maize defense response.
Our network-based comparative analysis of maize genes applied cointegration-correlation-expression strategy to identify a potential maize subnetwork module differentially activated between the two strains (*F. verticillioides* wild type vs. mutant). This predicted maize module is comprised of 28 member genes, and five were annotated to a significant GO term GO:0009814 "defense response, incompatible interaction". These five genes were indicated by diamond-shaped illustration.

While difficulties mentioned above remain as obstacles, our effort demonstrates that the proposed network-based analysis pipeline can improve our understanding of the biological mechanisms that underlie host-pathogen interactions, and that it has the potential to unveil novel genetic subnetwork modules and hub genes critical for virulence in fungal pathogens. We are currently in the process of improving our

computational pipeline with computational network querying that can estimate node correspondence probabilities to find novel functional pathways in biological networks (Qian et al., 2009; Qian & Yoon, 2009; Sahraeian & Yoon, 2011; Su et al., 2010). This gene subnetwork approach can lead to the discovery of new quantifiable cellular subnetworks that can bridge the knowledge gaps in the maize-*F. verticillioides* system and be further applied to other plant-microbe pathosystems.

MATERIAL AND METHODS

Fungal strains, maize line, and RNA sample preparation

F. verticillioides strain 7600 (Ma et al., 2010) and fsr1 mutant (Shim et al., 2006) were cultured at 25°C on V8 juice agar (200 ml of V8 juice, 3 g of $CaCO_3$ and 20 g of agar powder per liter). Maize inbred B73, a progenitor of numerous commercial hybrids with no inherent resistance to stalk rot, was inoculated with *F. verticillioides* wild type and fsr1 mutant spore suspension as described previously (Christensen et al., 2014, Shim et al., 2006). Maize stalk samples were collected 3, 6, and 9 dpi using manual sectioning, and microscopically inspected to identify host tissue damage and/or fungal colonization, particularly in the vascular bundles. For each sample, sectioning was performed on at least three independent stalk samples from each stage of infection, and isolated tissues were pooled for RNA extraction with TRIzol reagent (Invitrogen). For each time point, we collected six pooled samples, thus thirty-six RNA samples in total. Standard QA/QC

procedure for RNA samples was implemented at the Texas A&M AgriLife Research Genomics and Bioinformatics Service (College Station, TX) prior to sequencing.

RNA Sequencing and data preprocessing

RNA sequencing was processed at the Texas A&M AgriLife Research Genomics and Bioinformatics Service using Illumina HiSeq 2000 as described previously (Kim et al., 2015b). We sequenced a total of 36 sample libraries, *i.e.* six libraries per each time point (3 dpi, 6 dpi, and 9 dpi) for wild type and the mutant inoculated maize stalks, but it is worth noting that, in this study, we only used sequencing data for the last two time points (6 dpi and 9 dpi, hence 24 sample libraries in total) to focus on gene regulation mechanism in the latter stages of maize-Fusarium interaction. Next, acquiring read counts of all *F. vrticillioides* genes was completed as described in our earlier reports (Kim et al., 2015a, Kim et al., 2015b) by i) aligning the RNA-seq reads to the reference genome of *F. verticillioides* strain 7,600 obtained from the Broad Institute (http://www.broadinstitute.org) using Bowtie2 (Langmead & Salzberg, 2012) and Samtools (Li et al., 2009), ii) filtering out genes insignificantly expressed over most of the replicates, thereby keeping 9446 genes for downstream analysis, iii) normalizing the read counts of these genes by their corresponding gene length and also based on expression levels of β-tubulin genes (*i.e.* FVEG_04081 and FVEG_05512) to have relative expression quantification across all replicates.

Prediction of *F. verticillioides* subnetwork modules associated with stalk rot

A procedure of identifying candidate functional subnetwork modules follows computational analysis pipeline described earlier (Kim et al., 2017a) with some modifications. From the preprocessed gene expression data, we performed conversion into log likelihood ratio (LLR) matrix, construction of co-expression networks through partial correlation, and selection of the most significantly differentially expressed genes (*i.e.*, top 1%) between the two strains (wild vs. mutant) as seed genes. Based on this preparation, we applied computationally efficient branching out searching from a seed gene until it does not meet minimum discriminative power increase for each subnetwork module. The entire searching process was reiterated for every seed genes and for the five co-expression networks. Note that our approach probabilistically searches for subnetwork modules whose member genes have highly likely associated expression patterns to each other over all the replicates using the log likelihood ratio (LLR) matrix that demonstrates how likely each gene would be wild type or *fsr1* mutant. As a result, our network-based computational analysis approach found candidate subnetwork modules that show harmonious coordination of member genes as well as strong differential activity between the wild type and *fsr1* mutant.

Prediction strategy for hub genes in each subnetwork module

We simultaneously inferred potential *F. verticillioides* pathogenicity-associated hub or key functional genes in each subnetwork module while branching out the modules by performing multidirectional analysis on the detected candidate subnetwork

modules with six different criteria, as depicted in Figure 3B. First, we investigated how each gene is probabilistically impactful in its subnetwork module utilizing the probabilistic inference strategy applied in our previous work (Kim et al., 2015a). We estimated probabilistic differential activity of each gene by comparing discriminative power on the two phenotypes (wild type vs. *fsr1* mutant) between its given module with and without the gene. As described in our previous study (Kim et al., 2015a), we computed discriminative power difference (estimated by *t*-test statistics) between both activity levels (one with the gene and the other without the gene) by supposing $\boldsymbol{\zeta} = \{\boldsymbol{g_1}, \boldsymbol{g_2}, \ldots, \boldsymbol{g_n}\}$, member genes in a subnetwork module, and $\boldsymbol{e} = \{\boldsymbol{e^1}, \boldsymbol{e^2}, \ldots, \boldsymbol{e^n}\}$, expression levels of the given genes. The discriminative power difference $\boldsymbol{D(d)}$ was calculated as follows.

$$\boldsymbol{D(d)} = \left[\sum_{k=1}^{n} \boldsymbol{log}\left(\frac{\boldsymbol{f_1^k(e^k)}}{\boldsymbol{f_2^k(e^k)}}\right)\right]_{\zeta}^{t-test} - \left[\sum_{k=1}^{n} \boldsymbol{log}\left(\frac{\boldsymbol{f_1^k(e^k)}}{\boldsymbol{f_2^k(e^k)}}\right)\right]_{g_d \notin \zeta}^{t-test}$$

where $\boldsymbol{log}\left(\frac{\boldsymbol{f_1^k(e^k)}}{\boldsymbol{f_2^k(e^k)}}\right)$ is the log-likelihood ratio (LLR), and $\boldsymbol{f^k(e)}$ is each conditional probability density functions (*i.e.*, either wild or mutant). We subsequently considered genes whose discriminative power deterioration $\boldsymbol{D(d)}$ relatively larger as candidate key genes. Second, we examined differential correlation of each gene with its connected gene in each module between the wild type versus the mutant using two correlation methods, *i.e.* Pearson's correlation and Spearman rank correlation. We selected genes whose correlation coefficients with its neighboring genes were not only relatively significantly differential between the two different networks, but also higher in the wild-type network as candidate key genes. Third, we calculated number of edges of each gene

to other member genes in each module since it is reasonable to predict that genes with more edges will exhibit more meaningful influence on the module. Fourth, we investigated expression difference of each gene in a given module between the two strains since we predict that altered expression of genes downstream of *FSR1* can follow that of *FSR1*. We selected genes that were significantly differentially expressed between the two conditions and relatively highly expression in in the wild type. Fifth, we listed orthologs of known pathogenicity genes in other well-studied fungal species such as *F. graminearum* (FG), *F. oxysporum* (FO), *Aspergillus fumigatus* (AF), *Botrytis cinerea* (BC1G), *Magnaporthe grisea* (MGG), *Ustilago maydis* (UM), and *Cryptococcus neoformans* (CNAG). We noted genes in a given module shown in the list of pathogenic genes as potential key genes. Lastly, we considered whether each gene in a given module was associated with significant GO term. We applied *p*-values of Benjamini-Hochberg false discovery rate (FDR) method (Benjamini & Hochberg, 1995) to find the most relevant GO term to each gene and its given module based on g:Profiler (http://biit.cs.ut.ee/gprofiler/index.cgi) (Reimand et al., 2011). We chose genes annotated to GO term that is the most significantly associated with the given module as candidate key genes.

After identifying a candidate hub (or key functional) gene in its given subnetwork module, we performed additional fine-tuning procedure for more robust and reliable module prediction. Briefly, once we identified a candidate gene satisfying the abovementioned six criteria through subnetwork module extension process with 10% minimum discriminative power enhance, we performed module adjustment process by

implementing the whole module extension for the given module as well as identifying the same potential gene by escalating the minimum discriminative power enhance by 1%. We repeatedly applied this fine-tuning process until the predicted hub (or key functional) gene did not meet all conditions. This process also stopped when the given subnetwork module grew smaller down to the arbitrary set minimum size of seven genes.

Nucleic acid manipulation, polymerase chain reaction (PCR), and fungal transformation

Standard molecular manipulations, including PCR and Southern hybridization, were performed as described previously (Sagaram et al., 2007). Fungal genomic DNA was extracted using the OminiPrep genomic DNA extraction kit (G Biosciences, Maryland heights, MO, USA). The constructs for transforming *F. verticillioides* were generated with a split-marker approach described earlier (Sagaram et al., 2007). Briefly, DNA fragments of 5' and 3' flanking regions of each gene were PCR amplified from wild-type genomic DNA. Partial Hygromycin B phosphotransferase (*HPH*) gene (*HP*- and -*PH*) fragments were amplified from pBS15 plasmid. 5' and 3' flanking region fragments were then fused with PH- and -HP fragments by single-joint PCR, respectively. The single-joint PCR products were transformed into wild-type fungal protoplast. For complementation, respective wild-type genes driven by its native promoter was co-transformed with a geneticin-resistant gene (*GEN*) into mutant protoplasts. All primers used in this study were listed in Table B-4. *F. verticillioides* protoplast were generated and transformed following standard protocol (Sagaram et al.,

2007) with minor modifications. Murinase (2 mg/ml) was replaced with Driselase (5 mg/ml) (Sigma, St Louis, MO, USA) in the protoplast digestion solution. Transformants were regenerated and selected on regeneration medium containing 100 µg/ml of hygromycin B (Calbiochem, La Jolla, CA, USA) and/or 150 µg/ml G418 sulfate (Cellgro, Manassas, VA, USA) as needed. Respective drug-resistant colonies were screened by PCR and further verified by Southern analysis.

Maize infection assays

Maize seedling rot pathogenicity assay was performed on 2-week old maize inbred lines B73 seedlings as previously described (Christensen et al., 2014) with minor modifications. Briefly, $1x10^8$/ml spore suspensions in YEPD broth along with YEPD control were inoculated on maize B73 mesocotyls. Plant mesocotyls were first slightly wounded by a syringe needle about 3cm above the soil. A 5ul-spore suspension was applied to the wound site. The seedlings were immediately covered with a plastic cover to create a high moisture environment suitable for infection and colonization. The seedlings were collected and analyzed after a 2-week growth period in the dark room. At least three biological and three technical replicates were performed for each fungal strain.

Expression analysis of subnetwork member genes linked to predicted hub genes

Total RNA extractions were conducted by using RNeasy plant mini kit (Qiagen) according to manufacturer's specifications and was quantified by Nanodrop. RNA was converted into cDNA using the Verso cDNA synthesis kit (Thermo Fisher Scientific,

Waltham, MA) following the manufacturer's protocol. qRT-PCR analyses were performed using the SYBR Green Dynamo Color Flash qPCR kit (Thermo Fisher Scientific) on an Applied Biosystems 7500 Real-Time PCR system. The *F. verticillioides* β-tubulin gene (*TUB*-2) was used as the endogenous calibrator. The amplification data analysis was done according to the manufacturer's protocol.

Identification of potential maize defense subnetwork module

We followed our previous analysis strategy (Kim et al., 2015b) to identify potential subnetwork modules associated with maize defense response against *F. verticillioides* virulence genes. We began searching for maize modules possibly responsible for its defense mechanism through cointegration-correlation-expression analysis: i) Cointegration was applied to track an interrelationship of expression levels between maize and *F. verticillioides* over all replicates. We applied the Engle-Granger correlation method to measure single cointegrating relations and the certain *p*-value of the relationship (*i.e.*, *p*-value <= 0.05) was used to determine candidate maize genes corresponding to the identified *F. verticillioides* pathogenicity-associated genes, ii) correlation was utilized to trace patterns of expression levels between maize and *F. verticillioides* over all replicates. We used Pearson's correlation coefficients to estimate their linear relationship and condensed maize genes into candidates whose expression patterns are highly correlated with that of *F. verticillioides* pathogenicity-associated genes (*i.e.*, *p*-value <= 0.005), iii) We considered expression levels of maize genes over replicates and filtered insignificantly expressed maize genes out. (*i.e.*, maize genes

whose mean expression levels were in the bottom 20% or not expressed in at least one replicate). We adjusted *p*-values of the cointegration-correlation-expression approach to have 50% of candidate maize genes predicted from a given *F. verticillioides* pathogenicity-associated gene were also among the candidates inferred from other given *F. verticillioides* gene. Based on the maize genes narrowed down through the cointegration-correlation-expression analysis, we identified subnetwork modules associated with maize defense response using our network-based comparative analysis approach.

CHAPTER IV

A SNARE PROTEIN FVSYN1 IS INVOLVED IN FUNGAL GROWTH AND VIRULENCE IN *FUSARIUM VERTICILIOIDES*

SUMMARY

Fusarium verticillioides (Sacc.) Nirenberg (teleomorph *Gibberella moniliformis* Wineland) is one of the important fungal pathogens that cause maize stalk rots. However, the knowledge of stalk rot virulence mechanism is still very limited. We previously identified the *F. verticillioides FvSYN1* gene, which plays important role in causing maize virulence. FvSyn1 belong to a family of Soluble *N*-ethylmaleimide-sensitive factor attachment protein receptor (SNARE) proteins which play critical role in a variety of developmental processes. In this study, we show that Δfvsyn1 mutant produced rough and hyper-branched hyphae. The FvSyn1::GFP fusion protein was localized in vacuoles, plasma membranes, and septa. Moreover, Δfvsyn1 mutant was sensitive to cell wall stressors. Further characterization of FvSyn1 domains indicated that both N-terminal Syntaxin N-terminus (SynN) domain and C-terminal SNARE domain were important for fungal development and maize seedling rot virulence pathogenicity but dispensable for fumonisin production and sexual mating. Our studies provided that FvSyn1 has key roles in fungal development and virulence in *F. verticillioides*.

INTRODUCTION

Stalk rot is one of the most devastating diseases of maize, which is primarily caused by a series of fungal pathogens. *Fusarium verticillioides, Gibberella zeae*, *Colletotrichum graminicola* and *Macrophomina phaseolina* are the most common stalk rot pathogens that devastate maize-growing regions in the US (Koehler, 1960; Kommendahal & Windels, 1981; White, 1999). Stalk rot pathogens typically overwinters in crop residue by producing thickened hyphae and spores (Leslie et al., 1990). Seed-borne and seed-transmitted fungi usually cause seedling disease (McGe, 1988). Soil-borne and air-borne fungi can penetrate stalks at the base of leaf sheaths and progress to lower internode through natural entry points and wounds created by insects or mechanical damage (Foley, 1962; Kingsland & Wernham, 1962; Koehler, 1960; Sobek & Munkvold, 1999). Environmental stresses, such as low soil moisture, decreased light density by cloudy weather and high plant density, can influence grain fill in maize, and these stresses have been reported to be associated with stalk rots occurrence (Dodd, 1980). The pathogen can also take advantage of and colonize vulnerable stalk tissues at the end of growing season when the developing ear competes with the stalk for nutrients (Dodd, 1980; Smith &White, 1989). Pathogen invasion before physical maturity usually causes reduced grain fill and premature death, resulting in yield reduction. Severe yield loss can result in years with conditions conducive to disease, e.g. high temperature and draught (Dodd, 1980; White, 1999). However, we still have very limited understanding

of the detailed molecular mechanism associated with stalk rots caused by these fungal pathogens.

To better understand the virulence mechanism in stalk rot pathogens, we identified and characterized a striatin-like protein Fsr1 in *F. verticillioides* which plays an important role in pathogenesis (Shim et al., 2006; Yamaura & Shim, 2008). We also revealed that Fsr1 forms a complex with other proteins to regulate stalk rot virulence (Zhang et al., 2017). To further characterize genetic networks downstream of Fsr1, we performed next-generation sequencing (NGS) with maize B73 stalks inoculated with *F. verticillioides* wild type and *fsr1* mutant. We used a computationally efficient branch-out technique, along with an adopted probabilistic pathway activity inference method, to identify functional subnetwork modules likely involved in *F. verticillioides* virulence (Kim et al., 2015a). Through our analyses, we identified one important virulence gene *FvSYN1* from potential virulence-associated subnetwork module identified (Kim et al., 2015b). FvSyn1 is predicted to encode a soluble N-ethylmaleimide-sensitive factor attachment protein receptor (SNARE) with two well-recognized functional domains including a Syntaxin N-terminus (SynN) domain in the N-terminal region and a SNARE domain in the C-terminal region.

SNARE proteins play critical and conserved roles in intracellular membrane fusion in eukaryotic cells (Chen & Scheller, 2001). They are known to mediate membrane fusion during all trafficking steps of the intracellular communication process, including the secretory and endocytic pathways (Hong & Lev, 2014). In eukaryotes, there are many different sets of SNARE proteins found in different cellular

compartments, with each SNARE protein forming a specific SNARE complex involved in different steps in membrane trafficking (Ryu et al., 2016; Scales et al., 2000). Despite the differences in many organisms, all SNARE proteins contain a conserved SNARE domain that consists of approximately 60-70 amino acids with multiple coiled-coil structures forming heptad repeats in the membrane-proximal regions of the SNARE proteins (Chen & Scheller, 2001; Hong & Lev, 2014). Moreover, many SNAREs contain N-terminal regulatory regions (Hong & Lev, 2014). SNAREs were originally classified into v-SNAREs and t-SNAREs according to their vesicle or target membrane localization (Söllner et al., 1993). Later, many SNAREs were found both on vesicles and target membrane, and thus SNAREs were reclassified into Q-SNAREs (glutamine-containing SNAREs) and R-SNAREs (arginine-containing SNAREs) according to the crystal structures of the synaptic SNARE complex (Fasshauer et al., 1998). R-SNAREs act as v-SNAREs and most Q-SNAREs act as t-SNAREs. SNARE proteins are mostly well studied in mammals, and the known mammalian SNAREs have been classified into syntaxin, VAMP (also called synaptobrevin), and SNAP25 families.

FvSyn1 is predicted as a syntaxin protein. Syntaxins belong to t-SNARE proteins and are shown to play an important role in membrane fusion in eukaryotic cells (Gupta & Heath, 2002; Hong, 2005). It has been shown that syntaxins are important for vesicle fusion and development in yeast and filamentous fungi. In *Saccharomyces cerevisiae*, Sso1 and Sso2 syntaxins function redundantly and affect vesicle fusion and sporulation (Nakanishi et al., 2006). The homologs of Sso1 and Sso2 in *Neurospora crassa* are *NSYN1* and *NSYN2*; *NSYN1* was shown to be important for hyphal development,

conidiation and male fertility while *NSYN2* is important for hyphal branching and ascospore development (Gupta et al., 2003). Hong et al. (2010) reported the synthaxin homolog *GzSYN1* and *GzSYN2* in *F. graminearum*, with *GzSYN1* deletion mutant showing reduced hyphal growth rate while *GzSYN2* deletion mutant exhibiting fertility issues. Both genes were shown to be important for fungal virulence in *F. graminearum* (Hong et al., 2010).

Our previous study showed that ΔFvSyn1 mutation severely impaired vegetative growth and maize seedling rot. However, the detailed mechanism by which FvSyn1 regulates virulence was not characterized. To further determine how Fvsyn1 is involved in virulence, we studied ΔFvSyn1 mutant hyphal development and stress response, investigated FvSyn1 localization, and identify the functional roles of two well recognized domains (N-terminal SynN domain and C-terminal SNARE domain) of FvSyn1. Here, we report that FvSyn1 is important for regulating spore germination and hyphal morphology, FvSyn1 is localized in vacuoles, plasma membranes, and septa and plays a role in the response to cell wall stressors. Motif-deletion studies showed that both N-terminal SynN domain and C-terminal SNARE domain of FvSyn1 are required for pathogenicity but dispensable for fumonisin production and sexual mating.

RESULTS

FvSYN1 influences hyphal growth and branching

Our previous study showed that the Δfvsyn1 mutant exhibited reduced vegetative growth while having more dense and fluffier mycelia on solid agar media when compared with the wild type (WT). But there was no significant difference in fungal mass when we compared the mycelia harvested from YEPD broth (Kim et al., 2017). We hypothesized that these outcomes were due to the mutation causing hyphal growth and branching to be altered in the Δfvsyn1 strain. To test this, spores of WT, Δfvsyn1 and the complementation strain (Fvsyn1C) were inoculated into potato dextrose broth (PDB), and we monitored the germination rate under the microscope. After incubating for 9 hours, we learned that *FvSYN1* was germinating slower than wild-type and complementation strains (Figure 4.1). However, while no significant growth rate difference was observed 27 hours after inoculation, hyphae of Δfvsyn1 were more dense and hyper-branched when compared to WT and Fvsyn1C strains (Figure 4.1). The surface of the mutant hyphae was rough while the WT and complementation hyphae was smooth 27 hours after incubation (Figure 4.1). These results suggest that *FvSYN1* plays a role in hyphal development and explain why Δfvsyn1 exhibited slower vegetative growth on solid media while showing no biomass difference in liquid cultures.

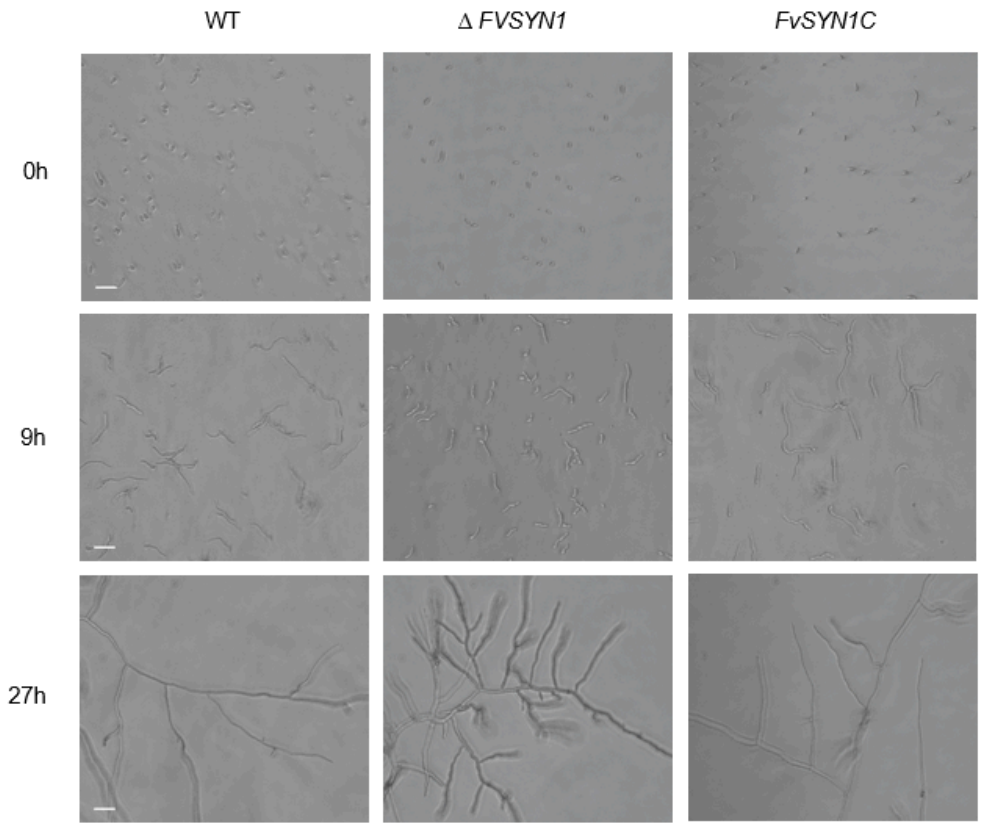

Figure 4.1 Conidial germination of wild-type (WT), *FvSYN1* gene deletion mutant and complementation strain (*FvSYN1C*).
Growth were observed in PDB broth were observed under Optika XDS-2 microscope at different time points. (A-C): Spores of WT, mutant and complementation strains in 96 well plates. (D-F): Spore germination morphology 9 hours after inoculation. (G-I): Hyphae tip area morphology 27 hours after inoculation. Scale bar = 30 μm.

Localization of *FvSYN1* in *F. verticillioides*

In *F. graminearum*, *GzSYN1* was shown to localize to vacuoles, plasma membranes, and septa (Hong et al., 2010). To determine the localization of *FvSYN1* in *F. verticillioides*, we generated a FvSyn1-GFP fusion construct to transform Δfvsyn1

mutant. FvSyn1-GFP strain was inoculated on a PDA plate for 24 hours and the vegetative hyphae were examined. We found that FvSyn1-GFP was localized to plasma membranes, vacuoles and septa of the hyphae, but it exhibited stronger localization to the plasma membrane and vacuoles of the younger part of the hyphae (right part of the image). FM4-64 staining analysis also showed the plasma membrane, vacuolar and septa localization of the FvSyn1-GFP protein (Figure 4.2). This localization study demonstrated that FvSyn1 is localized to vacuoles, plasma membranes, and septa.

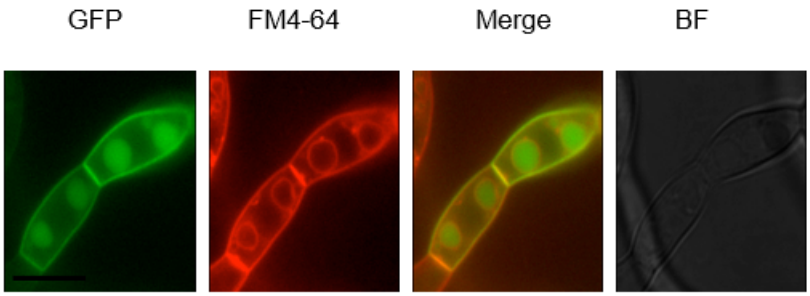

Figure 4.2 Expression and localization of FvSyn1-GFP in *F. verticillioides*.
Vegetative hyphae expressing the FvSyn1-GFP fusion construct were examined. The same field was examined under bright field (BF) and epifluorescence microscopy [green fluorescent protein (GFP) or FM4-64 staining]. Strains were grown for 1 day on PDA before the staining of FM4-64. Scale bar = 5μm.

***FvSYN1* plays an important role in response to various stressors**

As FvSyn1 is mainly localized in vacuole, septa and plasma membrane, indicating possible roles in vacuole and plasma membrane, thus it is reasonable to hypothesize that it may display an altered response to various environmental stresses which is related to vacuole and membrane roles. We tested the response of the mutant to various stressors. Strains were inoculated on 0.2×PDA plates with KCl (1M), NaCl (1M), sorbitol (1M), sodium dodecylsulfate (SDS) (0.01%), congo red (CR) (100μg/ml) and calcofluor white (CFW) (100μg/ml) (Figure 4.3A). As the stressors can inhibit or promote WT growth, we set the growth rates of WT strains on standard PDA plates at 1. The mutant growth rate was greater than WT and Fvsyn1C when grown on plates with SDS, CR and CFW. However, there were no significant differences when grown on plates with KCl, NaCl and sorbitol (Figure 4.3B), although we observed overall growth deficiency on plates amended with KCl and NaCl. SDS, CR and CFW are cell wall stressors. These results indicated that Fvsyn1 mutant grow better than WT and complementation strains in the medium with cell wall stressors, which indicate that the stressors may mediate their effects on cell wall integrity (CWI) through distinct mechanisms, *FvSYN1* may play a role in the CWI maintenance in *F. verticillioides*.

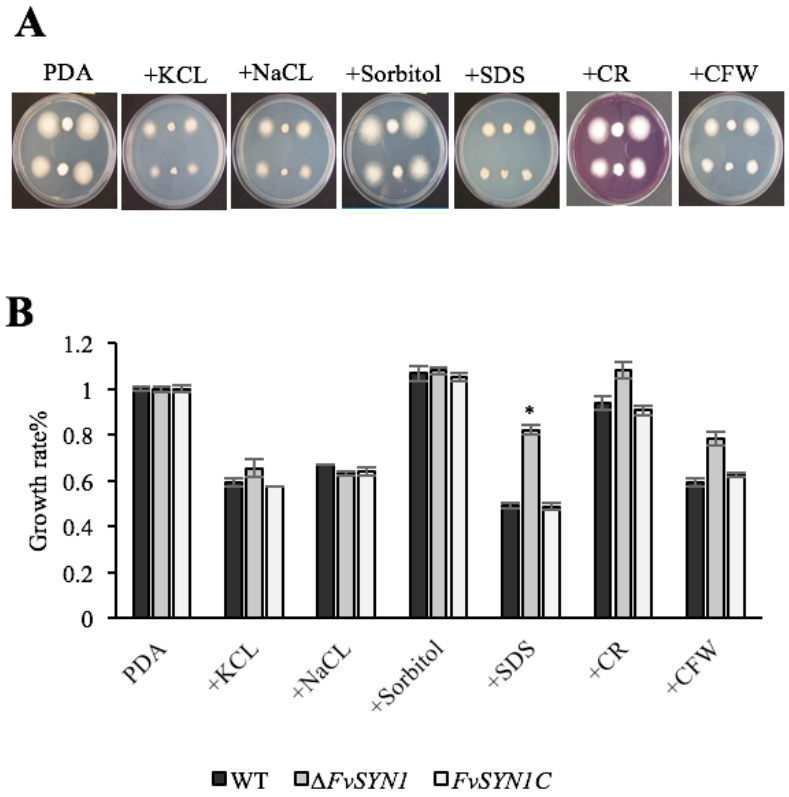

Figure 4.3 Defects of the Δfvsyn1 mutant in response to various stressors.
(A) A 4 µl-10^5 spore suspensions (first row on plates) and 10^4 spore suspensions (second row on plates) of wild type, mutant and complemented strains were cultured on PDA medium supplemented with hyperosmotic, oxidative stressors and cell wall antagonists for 5 days. SDS, sodium dodecylsulfate; CR, Congo red; CFW, Calcofluor white. (B) The growth rates (artificially set to 100% on PDA plates) of the indicated strains under various stress conditions. Error bars represent the standard deviation from three independent experiments and asterisks indicate statistically significant differences ($P < 0.05$) analyzed by t-Test.

SynN domain and SNARE domain of Fvsyn1 are important for vegetative growth

FvSyn1 contains two well-recognized domains, a SynN domain at C-terminus and a SNARE motif at C-terminus. In order to characterize the function of these two

domains, Δ*SynN* (WT gene with a complete deletion of the *FvSYN1* N-terminus with native promoter and terminator) and Δ*SNARE* mutant (WT gene with a complete deletion of the C-terminus with native promoter and terminator) were generated (Figure 4.4A). Complementation strain FvSYN1C (with wild-type *FvSYN1* gene driven by its native promoter transformed into Δfvsyn1) (Kim et al., 2017) was used as a positive control. When we compared the vegetative growth of these mutants on PDA and V8 plates, Δ*SynN* and Δ*SNARE* mutants exhibited a similar growth rate as the Δ*FvSYN1* mutant, but all three mutants showed significantly slower growth rate than the wild-type progenitor and complementation strain (Figure 4.4B). The mutants Δ*SynN* and Δ*FvSYN1* exhibited highly dense and fluffier mycelial growth amongst all strains. Meanwhile Δ*SNARE* mutant mycelial growth was considered in-between these two mutants and WT when grown on PDA plates (Figure 4.4C). When all these strains were inoculated on cracked maize kernels, we did not observe statistical difference in ergosterol production (Figure 4.4D). Previous study also showed that Δ*FvSYN1* mutant, WT and complementation strains produced similar amount of fungal mass when cultures were harvested from YEPD broth (Kim et al., 2017). When we measured conidia production in these strains, we found that Δ*SynN* mutant produced macrospores while all other strains did not produce macrospores, which is a deviation from the typical *F. verticillioides* asexual reproduction method in laboratory conditions (Figure 4.4E). These data demonstrated that both domains, SynN and SNARE, are important for normal growth rate. SNARE domain is more important for colony fluffiness while SynN domain plays an important role for maintaining normal microconidia production.

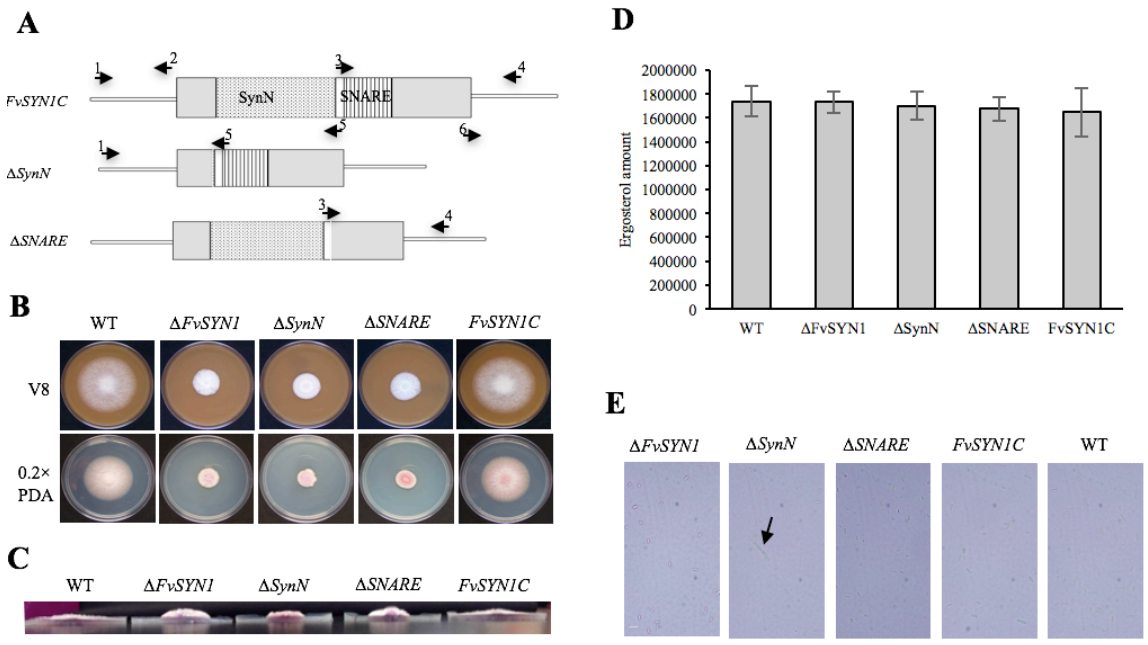

Figure 4.4 SynN domain and SNARE domain of Fvsyn1 are important for vegetative growth.

(A) *FvSYN1* complementation constructs of ΔSynN and ΔSNARE used to test the functional roles of the C-terminus and N-terminus regions. (B)Vegetative growth of WT, *ΔFvSYN1*, *ΔSynN*, *ΔSNARE* and complementation (*FvSYN1C*) strains were examined on V8 and 0.2XPDA agar plates. Strains were point inoculated with a 5µl-10^5 spore suspensions and incubated for 6 days at 25 °C under 14 h light/10 h dark cycle. (C) A 5µl-10^5 spore suspensions of WT, *ΔFvSYN1*, *ΔSynN*, *ΔSNARE* and *FvSYN1C* strains were inoculated and incubated on PDA plates for 6 days at 25 °C under 14 h light/10 h dark cycle. Pictures for colony thickness were taken from a side view. (D) Quantification of ergosterol production in *F. verticillioides* strains. 2×10^6 spores of WT, *ΔFvSYN1*, *ΔSynN*, *ΔSNRE* and *FvSYN1C* strains were inoculated on nonviable autoclaved maize kernels and incubated for 7 days at 25 °C under a 14-h light/10-h dark cycle. Ergosterol production was quantified by high-performance liquid chromatography (HPLC) analysis. All values represent the means of three biological replications with standard errors shown as error bars. (E) WT, *ΔFvSYN1*, *ΔSynN*, *ΔSNARE* and *FvSYN1C* strains were inoculated on V8 plates and spores were collected one week after incubation. Spores were observed under microscope. Scale bar = 20 µm.

SynN domain and SNARE domain of Fvsyn1 are important for virulence

To test virulence, spore suspension of wild-type, Δ*FvSYN1*, Δ*SynN*, Δ*Snare*, *FvSYN1C* strains and water (negative control) were inoculated into silver queen maize seedling mesocotyls as described previously (Christensen et al 2014; Zhang et al., 2017). Seedling rot symptoms were observed 2 weeks after incubation. Δ*FvSYN1,* Δ*SynN* and Δ*SNARE* mutants showed significantly reduced levels of rot when compared with the wild-type progenitor. Δ*FvSYN1*, Δ*SNARE*, Δ*SynN* mutants showed approximately 60%, 50% and 40% reduction in virulence, respectively, when analyzed by average mesocotyl rot area while *FvSYN1C* complementation strain showed complete restoration of virulence in maize seedlings (Figure 4.5). These results suggested that these two domains in *FvSYN1*, independently and collectively, play an important role in *F. verticillioides* virulence.

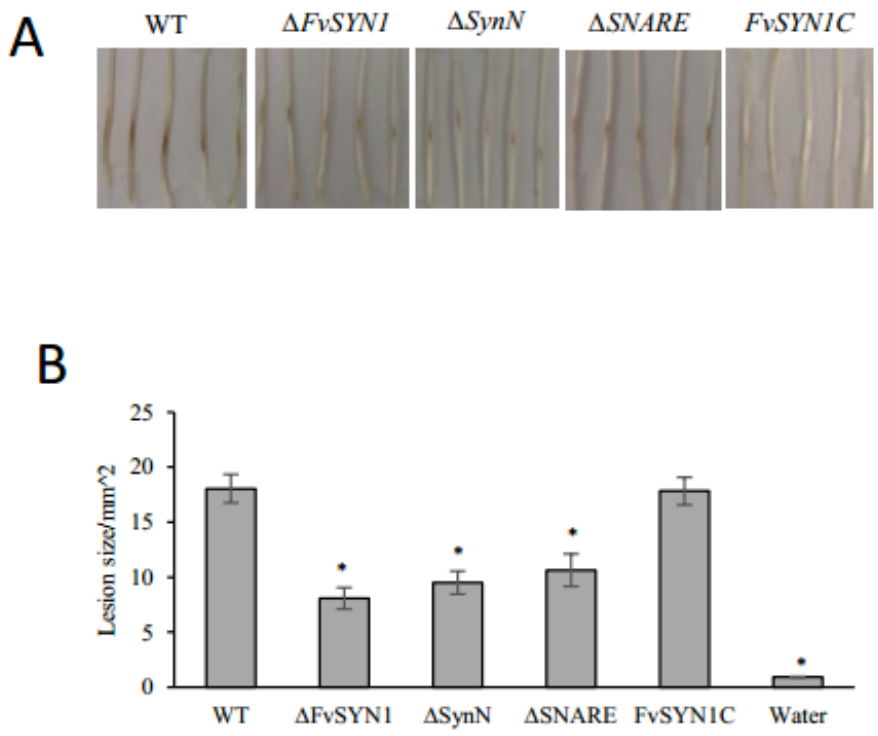

Figure 4.5 SynN domain and SNARE domain of Fvsyn1 are important for virulence. One week old silver queen maize seedlings were inoculated with 10^7/ml spore suspension of fungal strains (WT, *ΔFvSYN1*, *ΔSynN*, *ΔSNARE* and *FvSYN1C* strains) on mesocotyls. Lesion areas were quantified by Image J after 2-week incubation. All values represent the means of three biological replications with standard errors shown as error bars. A sterisk above the column indicates statistically significant difference ($P<0.05$) analyzed by t-Test.

SynN domain and SNARE domain of Fvsyn1 are dispensable for sexual mating and FB1 production

In order to test whether *FvSYN1* gene and its key domains are important for fumonisin production, WT, Δ*FvSYN1* mutant, the complementation strain as well as Δ*SNARE*, Δ*SynN* mutants were inoculated on cracked maize kernels. FB1 levels and fungal biomass were measured after 7 days of incubation. When FB1 production was normalized to fungal growth, *ΔFvSYN1*, *ΔSynN*, *ΔSNARE* and complementation strains produced similar level FB1 with the WT strain (Figure 4.6A). Therefore, we concluded that *FvSYN1* does not play a role in regulating FB1 biosynthesis. To test whether this gene and its domains are important for sexual mating, Δ*FvSYN1*, Δ*SynN,* Δ*SNARE* mutants as well as WT and complementation strain were crossed with the opposite mating type WT strain on carrot agar plates following standard method. After 21 days of incubation under proper light /day, all mating pairs resulted in a similar number of perithecia (Figure 4.6A) with viable ascospores, suggesting that *FvSYN1* is not critical for sexual reproduction in *F. verticillioides*.

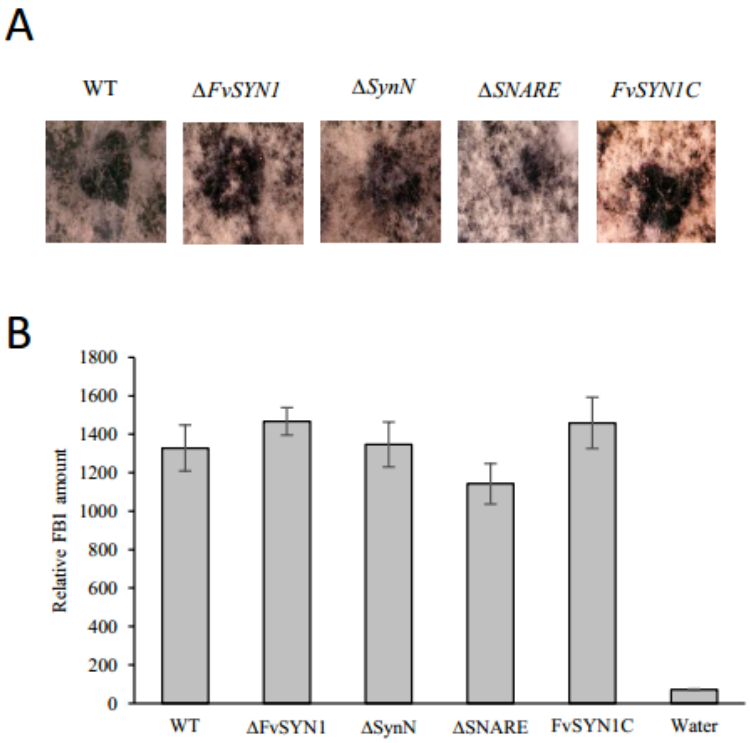

Figure 4.6 SynN domain and SNARE domain of Fvsyn1 are dispensable for sexual mating and FB1 production.

(A) *F. verticillioides* sexual mating assay. Crosses were performed as described previously by Sagaram et al. (2007), carrot agar plates were maintained at 25 °C until perithecia and ascospores were observed and characterized. (B) Quantification of FB1production in *F. verticillioides* strains. 2×10^6 spores of WT, *ΔFvSYN1*, *ΔSynN*, *ΔSNARE* and *FvSYN1C* strains were inoculated on nonviable autoclaved maize kernels and incubated for 7 days at 25 °C under a 14-h light/10-h dark cycle. Ergosterol production was quantified by high-performance liquid chromatography (HPLC) analysis. FB1 biosynthesis was normalized to growth with ergosterol contents. All values represent the means of three biological replications with standard errors shown as error bars.

DISCUSSION

Syntaxin proteins play important roles in membrane fusion and are well conserved in eukaryotes. It has been reported that syntaxin proteins are involved in fungal development and virulence. In *N. crassa* syntaxins *nsyn1* and *nsyn2*, which are homologs of Sso1 and Sso2 in *S. cerevisiae*, were reported to be critical for hyphal development, conidiation and fertility (Gupta et al., 2003). In wheat scab pathogen *F. graminearum* Hong et al. (2010) showed that *GzSYN1* and *GzSYN2* are important for hyphal growth and fungal virulence. In this study, we have shown that FvSyn1 deletion mutant altered morphogenesis and caused reduced virulence on maize seedlings. Although there is about 50% reduction in growth diameter of the Δfvsyn1 mutant when grown on PDA and V8 plates, but there are no fungal mass production differences when grown in liquid broth or in maize cracked kernels. The reduced virulence may be related to the abnormal hyphal morphology observed in the mutants. For example, cell-wall degrading enzyme pectinase in *F. oxysporum* (García-Maceira et al., 2001) and *Botrytis cinerea* (Have et al., 1998) have been shown to have functional roles in fungal virulence and host infection. If the syntaxins in *F. verticillioides* function in the delivery of those kinds of enzymes, defects in the secretory pathway could directly affect the pathogenicity or virulence of the fungus. The abnormal hyphal development observed here suggested that FvSyn1 may mediate membrane fusion to deliver the virulence factors properly for plant infection.

FvSyn1 showed similar localization patterns with its *F. graminearum* and *N. crassa* homologs (Gupta et al., 2003; Hong et al., 2010), namely FvSyn1-GFP mainly localized to the vacuoles, plasma membrane and septa of *F. verticilliiodes*. The localization patterns of FvSyn1 protein suggested that FvSyn1 play important roles at different stages during exocytosis or endocytosis, such as membrane fusion or vacuole assembly and sorting. Previous study showed that SNARE proteins MoVam7 in *M. oryzae* and FgVam7 in *F. graminearum* are involved in endocytosis (Dou et al., 2011; Zhang et al., 2016). In our FM4-64 staining both wild-type cells and mutant cells took up the FM4-64 dye within 1 min of exposure and there was no clear difference among the strains tested, indicating that *FvSYN1* does not directly play a role in endocytosis (Figure C-1). While other important factors may affect the endocytosis in the mutant, the mechanism still remains unclear and awaits future studies. In addition, the vacuole localization also indicated that FvSyn1 is stored in vacuoles. Vacuoles are known to play key roles in cell death, autophagy, storing components associated with secondary metabolism in plants and fungi (Martinoia et al., 2007; Xiang et al., 2013; Xiao et al., 2009). We hypothesize that the mutant is deficient in storing these components in vacuole, resulting in reduced virulence. Moreover, the localization of FvSyn1 on the plasma membrane could explain the abnormal hyphal morphology of the mutant possibly due to the loss of the ability to deliver/transport these components to the plasma membrane through a secretory pathway. Further characterization of a series of secretory proteins regulated by FvSyn1 that are related to stalk rot virulence or other functions will

help us to better understand the regulatory mechanisms of SNARE proteins during host-pathogen interactions.

MoVam7 in *M. oryzae*, and FgVam7 in *F. graminearum* are more sensitive to cell wall stressors, and show a defect in medium with cell wall stressors. In our results, FvSyn1 mutant also showed a difference in susceptibility to cell wall stressors, indicating the possible role in cell wall integrity. However, FvSyn1 mutant grew better in medium amended with cell wall stressors when compared with WT and complementation strains. We propose that the stressors may mediate their effects on CWI through distinct mechanisms in *F. verticillioides*. One possibility is that Δ*fvsyn1 mutant* may lead to cell wall remodeling response, a set of wall maintenance and repair proteins maybe strongly increased on the mutant cell wall. The stressed cell walls have high cell wall enzyme content such as chitin, this phenomenon has been reported in fungi *Candida albicans* (Hellman et al., 2013, Popolo et al., 2001), a small percentage of chitin increase can lead to form a stronger cell wall. Chitin synthases (CHS) gene and chitin degradation (CHT) gene expression are important genes for chitin levels. In addition, the reduced virulence in the Δfvsyn1 mutant may be attributed to its higher level of chitin, which may elicit plant defense mechanisms (Tsutsui et al., 2006; Wan et al., 2004). However, final confirmation of this hypothesis still awaits further future studies.

Both the N-terminal and C-terminal domains of FvSyn1 play important roles in vegetative growth and maize seedling rot in *F. verticillioides*. This is the first time the functions of these two domains were tested in filamentous fungi. C-terminal region is

conserved and contains a SNARE domain. This C-terminal region participates in the formation of the core complex (Kee et al., 1995), which is believed to be directly involved in membrane fusion (Chen & Scheller, 2001; Hanson et al., 1997; Lin & Scheller, 1997; Malsam et al., 2008). It was speculated that *F. verticillioides* Δ*SNARE* mutant has malfunction of membrane fusion which leads to more fluffier and hyper-branched hyphae phenotype in Δ*SNARE* mutant. N-terminal domain is less conserved and variable in all syntaxins when compared. But the N-terminal region is conserved among the t-syntaxins and is likely to have a function that is specific for exocytosis (Fernandez et al., 1998). N-terminal regions of syntaxin was also reported to be required for the disassembly of SNARE complexes (Misura et al., 2000; Nicholson et al., 1998; Parlati et al., 1999). When compared the N-terminal region of yeast syntaxin (Sso1 and Sso2) and neuron-specific isoforms of syntaxin 1A, there is a significant homology among the N-terminal regions. N-terminal domain of Sso1 (Sso1NT) in yeast t-SNARE, was shown to play an important regulatory role for SNARE complex assembly. The Sso1 N-terminal domain inhibits complex formation by interacting with the C-terminal SNARE-binding domain (Fernandez et al., 1998; Nicholson et al., 1998). In our study, Δ*SynN* showed a specific regulation mechanism in macrospore production, while Δ*FvSYN1* and Δ*SNARE* mutants produced only regular microconidia. This indicated the important roles of SynN domain, the interaction of these two domains as well as assembly/ disassembly of SNARE complex in regulating microspore/macrospore production. But further identifications are needed to clarify the mechanisms.

Taken together, our results indicate that the FvSyn1 in *F. verticillioides* performs important roles in hyphal growth, localization, stress response and pathogenicity. Further insight into the virulence mechanism will be provided by the identification and characterization of targets of FvSyn1, interacting complex, and involved secretion pathway during pathogenesis.

MATERIAL AND METHODS

Fungal strains, culture media and nucleic acid manipulation

F. verticillioides strain 7600 (M3125; Fungal Genetics Stock Center, University of Missouri-Kansas City, Kansas City, MO, U.S.A), *F. verticillioides* 7598 (A102; Fungal Genetics Stock Center) and all mutants generated in this study were cultured at 25°C on V8 juice agar (200 ml of V8 juice, 3 g of $CaCO_3$ and 20 g of agar powder per liter) for inoculum preparation and routine maintenance. Colony morphology was visually assayed on V8 agar and potato dextrose agar (PDA; Difco). For stress assay, spores of all strains were cultured on PDA with different concentrations of NaCl, KCl, sorbitol, CFW, SDS and CR, and incubated at 25 °C for 5 days.

Standard molecular manipulations were performed as described previously (Sagaram & Shim, 2007). Strains were grown in YEPD liquid medium (3 g yeast extract, 10 g peptone and 20 g dextrose per liter) at 25 °C and shaking at 150 rpm for genomic DNA extraction. Fungal genomic DNA was extracted using the OminiPrep genomic DNA extraction kit (G Biosciences, Maryland heights, MO, USA).

GFP constructs generation

For *in vivo* localization, we generated GFP strains by introducing FvSyn1::GFP fusion construct under the control of the RP27 promoter into the corresponding mutant protoplast. GFP was amplified from gGFP using the primers sGFP/F and5GAsGFP/Rbs with five glycine–alanine repeat (GA-5) sequences attached at the N-terminus as a linker for GFP tagging at gene N-terminus. Primers RP27-F and RP27-R were used to amplify RP27 promoter form PET11 plasmid. The primers Syn1-GFP-F/R were used to generate *FvSYN1* gene fragment. To generate RP27::GFP::FvSyn1, the RP27::GFP fusion construct was generated first, then fused with *FvSYN1* by joint PCR. All primers used in this study were listed in Table C-1. The construct together with a geneticin-resistance (*GEN*) marker were introduced into the Δfvsyn1 mutant protoplasts following the standard protocol (Sagaram & Shim, 2007).

Cytological Assay

For assessing hyphal growth and morphology, wild-type (WT), Δfvsyn1 mutant and complementation strain (Fvsyn1C) were first inoculated on V8 plated for 7 days, then conidia were collected and inoculated in 96-well plate wells which contains 200 µl PDB broth and incubated at 25 °C. Conidia germination were observed under Optika XDS-2 microscope at 0 hour, 9 hours and 27 hours post inoculation. For macrospore observation, strains were inoculated on v8 plates for one week and spores were collected and observed under Olympus BX60 microscope and images were captured with an INFINITY HD camera.

To visualize GFP strains, GFP strains were grown on PDA media for 1 day at room temperature. An Olympus BX51 microscope (Olympus America, Melville, NY, USA) was used for observation. A detailed description of the features used for imaging from this microscope has been published previously (Upadhyay & Shaw, 2008). To visualize the cell endomembrane, hyphae were treated with 25 μM FM4-64 solution for 20 min before being observed under the microscope. For endocytosis assay, hyphae were treated with FM 4-64 for 1 min before observed under microscope. All GFP images were prepared for publication using ADOBE PHOTOSHOP CS5.1 (Adobe).

Generation of FvSyn1 motif-deletion mutants

To investigate the functional role of FvSyn1 N-terminus and C-terminus regions, we first generated two complementation constructs, one has a complete deletion of the N-terminus domain (Δ*SynN*) with native promoter and terminator, and the other has a complete deletion of the C-terminus (Δ*SNARE*) with native promoter and terminator, that were generated via homologous recombination. Briefly, for Δ*SynN* construct, primers 1 and 2 were used for SynN 5' flanking region generation, and primers 3 and 4 were used for SynN 3' flanking region generation. 5' and 3' flanking region fragments were then fused by single-joint PCR by using primers 1 and 4(Figure 4A). Similarly, Δ*SNARE* construct was generated. Then we introduced each of the constructs together with a geneticin-resistance (*GEN*) marker into the Δfvsyn1 mutant protoplasts. All primers used in this study were listed in Table C-1. *F. verticillioides* protoplast were generated and transformed following standard protocol (Sagaram & Shim, 2007).

Transformants were regenerated and selected on regeneration medium containing 100 μg/ml of hygromycin B (Calbiochem, La Jolla, CA, USA) and 150 μg/ml G418 sulfate (Cellgro, Manassas, VA, USA) as needed. Respective drug-resistant colonies were screened by PCR. Complementation strain with complete wild-type genes driven by its native promoter was also generated (Kim et al., 2017) as a positive control to study motif-deletion mutants.

Maize infection assays

Maize seedling rot pathogenicity assay was performed on 2-week old silver queen (Burpee) maize seedlings as previously described (Christensen et al., 2014; Zhang et al., 2017) with minor modifications. Briefly, $1x10^8$/ml spore suspensions in in 0.1% Tween-20 along with 0.1% Tween-20 (negative control) were inoculated on maize B73 mesocotyls. Plant mesocotyls were first slightly wounded by a syringe needle about 3cm above the soil. A 2μl-spore suspension was applied to the wound site. The seedlings were immediately covered with a plastic cover to create a high moisture environment suitable for infection and colonization. The seedlings were collected and analyzed by Image J software after a 2-week growth period in the dark room. At least three biological and three technical replicates were performed for each fungal strain.

FB_1 and ergosterol analysis

FB1 analysis was performed following the established protocol (Shim & Woloshuk, 1999) with some modifications. $2x10^6$ conidia of the wild type and mutant

fungal strains were inoculated into 2 g cracked corn (corns were placed in small glass vials, rehydrated in 1.5 ml water overnight and autoclaved for use) for 7 days at 25°C. 10 ml of acetonitrile:water (1:1, v/v) was added to the vials and incubated at room temperature 24 hours without agitation for FB1 extraction and 10 ml chloroform:methanol (2:1, v/v) was added to the vials for ergosterol extraction. FB1 extracts were purified by passing through equilibrated SPE C18 columns (Fisher Scientific), washed with water, followed by 15% acetonitrile and then eluted with 70% acetonitrile. Ergosterol extracts were passed through acrodisc 13 mm Nylon 0.45 μm filters (Pall Life Sciences). FB1 and ergosterol HPLC analyses were performed as previously described (Kim et al., 2011; Shim & Woloshuk, 1999). Quantifications of FB1 and ergosterol were done by comparing HPLC peak areas to FB1 and ergosterol standards (Sigma). FB1 levels were then normalized to ergosterol contents in samples by calculating [FB1 ppm / ergosterol ppm] x 100 (Kim et al., 2011).

Sexual cross experiment

F. verticillioides sexual cross was performed as described by Sagaram et al. (2007). All strains were first grown on V8 plates, and then conida of the wild-type strain A102 (MAT1-2 genotype) were collected and spread to carrot agar plates and incubated for 7days at 24 °C. Then conidia of the wildtype M3125 (MAT1-1 genotype) and mutant strains generated in this background were harvested and quantified, same amount of conidia ($5x10^6$ spores) were applied to plates covered with A102 strains. Crosses were maintained at 25 °C until perithecia and ascospores were observed and characterized.

CHAPTER V

CONCLUSIONS AND FUTURE PROSPECTS

Recent studies have demonstrated important cellular and physiological roles of striatin protein in various organisms. Striatin forms a complex with other proteins such as phosphatases, kinases to regulate various cellular process. In this study, I characterized *F. verticillioides FvSTP1*, the homolog of human *STRIP1/2*, one of the key components of STRIPAK complex, to confirm that Fsr1 interacts with FvStp1, and that FvStp1 is also important for virulence. Furthermore, I identified *F. verticillioides* proteins that interact with Fsr1 coiled-coil domain *in vivo* to investigate their role in stalk rot virulence. Three new Fsr1 interacting proteins, FvCyp1, FvScp1, and FvSel1 were discovered through yeast two-hybrid screen of cDNA library generated from *F. verticillioides*-infected maize stalk. Cellular localization of these Fsr1-interacting proteins showed that FvCyp1, FvScp1, and FvSel1 co-localize to endomembrane structures. Moreover, I found that Fsr1 fails to maintain its original localization and was seen inside vacuoles, in FvCyp1, FvScp1 and FvSel1 knockout mutants. The reason for incorrect localization is still not completely understood, and this mechanism remains to be further investigated.

To unravel the genetic network underlying Fsr1-mediated fungal virulence, my research team performed NGS study to capture dynamic changes in gene expression during maize stalk colonization by *F. verticillioides* wild type and *fsr1* mutant. In this study, a computational network-based analysis was successfully performed to identify

pathogenic subnetwork modules downstream of Fsr1. Two hub genes, *FvSYN1* and *FvEBP1*, were identified from the predicted subnetworks for functional characterization, and were shown to be important for maize seedling virulence. Network robustness in gene deletion mutants was tested, deletion of *FvSYN1* and *FvEBP1* altered expression profile of neighboring genes in each subnetwork. Further characterization of *FvSYN1* showed that this gene is important for fungal hyphae development and the two domains are important for regulating pathogenesis. But further identification and characterization FvSyn1 targets, interacting complex, and involved secretion pathway during pathogenesis will provide more us insightful virulence mechanisms.

To conclude, my study showed that protein interactions promote the formation of Fsr1 interacting complex and triggers further downstream signaling associated with stalk rot pathogenesis in *F. verticillioides*. Computational based analysis of NGS data is important to predict functional subnetwork modules and hub genes important for virulence in fungal pathogens. My future research on the gene subnetwork approach is to expand our knowledge to *F. verticillioides*-maize pathosystems and even other plant-microbe interaction systems to bridge the knowledge gaps which will in turn lead to the potential for innovative management strategies.

REFERENCES

Abbas, H., Mirocha, C., Kommedahl, T., Burnes, P., Meronuck, R.*, et al.* (1988) Toxigenicity of Fusarium proliferatum and other Fusarium species isolated from corn ears in Minnesota. *Phytopathology*. 78, 1258-1260.

ApSimon, J. W. (2001) Structure, synthesis, and biosynthesis of fumonisin B1 and related compounds. *Environmental Health Perspectives,* 109, 245.

Arévalo- Rodríguez, M., Cardenas, M. E., Wu, X., Hanes, S. D. and Heitman, J. (2000) Cyclophilin A and Ess1 interact with and regulate silencing by the Sin3–Rpd3 histone deacetylase. *The EMBO Journal,* 19, 3739-3749.

Arévalo-Rodríguez, M. and Heitman, J. (2005) Cyclophilin A is localized to the nucleus and controls meiosis in Saccharomyces cerevisiae. *Eukaryotic Cell,* 4, 17-29.

Arevalo-Rodriguez, M., Wu, X., Hanes, S. D. and Heitman, J. (2004) Prolyl isomerases in yeast. *Frontiers in Bioscience,* 9, 2420-2446.

Baillat, G., Moqrich, A., Castets, F., Baude, A., Bailly, Y.*, et al.* (2001) Molecular cloning and characterization of phocein, a protein found from the Golgi complex to dendritic spines. *Molecular Biology of the Cell,* 12, 663-673.

Ballouz, S., Verleyen, W. and Gillis, J. (2015) Guidance for RNA-seq co-expression network construction and analysis: safety in numbers. *Bioinformatics,* 31, 2123-2130.

Barabasi, A.-L. and Oltvai, Z. N. (2004) Network biology: understanding the cell's functional organization. *Nature Reviews Genetics,* 5, 101-113.

Bartoli, M., Ternaux, J.-P., Forni, C., Portalier, P., Salin, P.*, et al.* (1999) Down-regulation of striatin, a neuronal calmodulin-binding protein, impairs rat locomotor activity. *Journal of Neurobiology,* 40, 234-243.

Beier, A., Teichert, I., Krisp, C., Wolters, D. A. and Kück, U. (2016) Catalytic subunit 1 of protein phosphatase 2A is a subunit of the STRIPAK complex and governs fungal sexual development. *mBio,* 7, e00870-00816.

Benjamini, Y. and Hochberg, Y. (1995) Controlling the false discovery rate: a practical and powerful approach to multiple testing. *Journal of the Royal Statistical Society. Series B (Methodological)*, 289-300.

Benoist, M., Gaillard, S. and Castets, F. (2006) The striatin family: a new signaling platform in dendritic spines. *Journal of Physiology-Paris,* 99, 146-153.

Bernhards, Y. and Pöggeler, S. (2011) The phocein homologue SmMOB3 is essential for vegetative cell fusion and sexual development in the filamentous ascomycete *Sordaria macrospora*. *Current Genetics,* 57, 133-149.

Bild, A. H., Yao, G., Chang, J. T., Wang, Q., Potti, A.*, et al.* (2006) Oncogenic pathway signatures in human cancers as a guide to targeted therapies. *Nature,* 439, 353-357.

Bloemendal, S., Bernhards, Y., Bartho, K., Dettmann, A., Voigt, O.*, et al.* (2012) A homologue of the human STRIPAK complex controls sexual development in fungi. *Molecular Microbiology,* 84, 310-323.

Bluhm, B. and Woloshuk, C. (2005) Amylopectin induces fumonisin B1 production by *Fusarium verticillioides* during colonization of maize kernels. *Molecular Plant-Microbe Interactions,* 18, 1333-1339.

Bluhm, B. and Woloshuk, C. (2006) Fck1, a C-type cyclin-dependent kinase, interacts with Fcc1 to regulate development and secondary metabolism in *Fusarium verticillioides*. *Fungal Genetics and Biology,* 43, 146-154.

Bowman, B. J., Draskovic, M., Freitag, M. and Bowman, E. J. (2009) Structure and distribution of organelles and cellular location of calcium transporters in *Neurospora crassa*. *Eukaryotic Cell,* 8, 1845-1855.

Breitman, M., Zilberberg, A., Caspi, M. and Rosin-Arbesfeld, R. (2008) The armadillo repeat domain of the APC tumor suppressor protein interacts with Striatin family members. *Biochimica et Biophysica Acta (BBA)-Molecular Cell Research,* 1783, 1792-1802.

Brown, D. W., Butchko, R. A., Busman, M. and Proctor, R. H. (2007) The *Fusarium verticillioides* FUM gene cluster encodes a Zn (II) 2Cys6 protein that affects FUM gene expression and fumonisin production. *Eukaryotic Cell,* 6, 1210-1218.

Cantacessi, C., Campbell, B., Visser, A., Geldhof, P., Nolan, M.*, et al.* (2009) A portrait of the "SCP/TAPS" proteins of eukaryotes-developing a framework for fundamental research and biotechnological outcomes. *Biotechnology Advances,* 27, 376-388.

Castets, F., Bartoli, M., Barnier, J., Baillat, G., Salin, P.*, et al.* (1996) A novel calmodulin-binding protein, belonging to the WD-repeat family, is localized in

dendrites of a subset of CNS neurons. *The Journal of Cell Biology,* 134, 1051-1062.

Castets, F., Rakitina, T., Gaillard, S., Moqrich, A., Mattei, M.-G.*, et al.* (2000) Zinedin, SG2NA, and striatin are calmodulin-binding, WD repeat proteins principally expressed in the brain. *Journal of Biological Chemistry,* 275, 19970-19977.

Chalmers, I. W., McArdle, A. J., Coulson, R. M., Wagner, M. A., Schmid, R.*, et al.* (2008) Developmentally regulated expression, alternative splicing and distinct sub-groupings in members of the *Schistosoma mansoni* venom allergen-like (SmVAL) gene family. *BMC Genomics,* 9, 89.

Chen, C., Shi, Z., Zhang, W., Chen, M., He, F.*, et al.* (2014) Striatins contain a noncanonical coiled coil that binds protein phosphatase 2A A subunit to form a 2: 2 heterotetrameric core of striatin-interacting phosphatase and kinase (STRIPAK) complex. *Journal of Biological Chemistry,* 289, 9651-9661.

Chen, H.-W., Marinissen, M. J., Oh, S.-W., Chen, X., Melnick, M.*, et al.* (2002) CKA, a novel multidomain protein, regulates the JUN N-terminal kinase signal transduction pathway in Drosophila. *Molecular and Cellular Biology,* 22, 1792-1803.

Chen, Y. A. and Scheller, R. H. (2001) SNARE-mediated membrane fusion. *Nature Reviews Molecular Cell Biology,* 2, 98-106.

Chiang, H. and Wilcoxson, R. D. (1961) Interactions of the European corn borer and stalk rot in corn. *Journal of Economic Entomology,* 54, 850-852.

Cho, Y., Jang, M., Srivastava, A., Jang, J.-H., Soung, N.-K., *et al.* (2015) A pectate lyase-coding gene abundantly expressed during early stages of infection is required for full virulence in *Alternaria brassicicola*. *PloS One,* 10, e0127140.

Christensen, S. A., Nemchenko, A., Park, Y.-S., Borrego, E., Huang, P.-C., *et al.* (2014) The novel monocot-specific 9-lipoxygenase ZmLOX12 is required to mount an effective jasmonate-mediated defense against *Fusarium verticillioides* in maize. *Molecular Plant-Microbe Interactions,* 27, 1263-1276.

Chuang, H. Y., Lee, E., Liu, Y. T., Lee, D. and Ideker, T. (2007) Network-based classification of breast cancer metastasis. *Molecular Systems Biology,* 3, 140.

Cook, R. (1978) The incidence of stalk rot (Fusarium spp.) on maize hybrids and its effect on yield of maize in Britain. *Annals of Applied Biology,* 88, 23-30.

Davis, R. M., Kegel, F. R., Sills, W. M., Farrai, J. J., Archibald, S. O., *et al.* (1989) Fusarium ear rot of corn. *California Agriculture*, 43, 4-5.

Dean, R. A., Talbot, N. J., Ebbole, D. J., Farman, M. L., Mitchell, T. K., *et al.* (2005) The genome sequence of the rice blast fungus *Magnaporthe grisea*. *Nature,* 434, 980-986.

Dettmann, A., Heilig, Y., Ludwig, S., Schmitt, K., Illgen, J., *et al.* (2013) HAM- 2 and HAM- 3 are central for the assembly of the Neurospora STRIPAK complex at the nuclear envelope and regulate nuclear accumulation of the MAP kinase MAK- 1 in a MAK- 2- dependent manner. *Molecular Microbiology,* 90, 796-812.

Dodd, J. L. (1980) The role of plant stresses in development of corn stalk rots. *Plant Disease,* 64, 533.

Dou, X., Wang, Q., Qi, Z., Song, W., Wang, W.*, et al.* (2011) MoVam7, a conserved SNARE involved in vacuole assembly, is required for growth, endocytosis, ROS accumulation, and pathogenesis of *Magnaporthe oryzae*. *PloS One,* 6, e16439.

Eichhorn, P. J., Creyghton, M. P. and Bernards, R. (2009) Protein phosphatase 2A regulatory subunits and cancer. *Biochimica et Biophysica Acta (BBA)-Reviews on Cancer,* 1795, 1-15.

Fasshauer, D., Sutton, R. B., Brunger, A. T. and Jahn, R. (1998) Conserved structural features of the synaptic fusion complex: SNARE proteins reclassified as Q-and R-SNAREs. *Proceedings of the National Academy of Sciences,* 95, 15781-15786.

Fernandez, I., Ubach, J., Dulubova, I., Zhang, X., Südhof, T. C.*, et al.* (1998) Three-dimensional structure of an evolutionarily conserved N-terminal domain of syntaxin 1A. *Cell,* 94, 841-849.

Flaherty, J. E., Pirttilä, A. M., Bluhm, B. H. and Woloshuk, C. P. (2003) PAC1, a pH-regulatory gene from *Fusarium verticillioides*. *Applied and Environmental Microbiology,* 69, 5222-5227.

Flaherty, J. E. and Woloshuk, C. P. (2004) Regulation of fumonisin biosynthesis in *Fusarium verticillioides* by a zinc binuclear cluster-type gene, ZFR1. *Applied and Environmental Microbiology,* 70, 2653-2659.

Foley, D. (1962) Systemic infection of corn by *Fusarium moniliforme*. *Phytopathology,* 52, 870.

Foreign Agricultural Service (2017). Grain: World Markets and Trade. U. S. Department of Agriculture. Washington DC.

Fox, D. S., Cruz, M. C., Sia, R. A., Ke, H., Cox, G. M.*, et al.* (2001) Calcineurin regulatory subunit is essential for virulence and mediates interactions with FKBP12–FK506 in *Cryptococcus neoformans*. *Molecular Microbiology,* 39, 835-849.

Frey, S., Reschka, E. J. and Pöggeler, S. (2015) Germinal center kinases SmKIN3 and SmKIN24 are associated with the *Sordaria macrospora* striatin-interacting phosphatase and kinase (STRIPAK) complex. *PloS One,* 10, e0139163.

Fu, C., Iyer, P., Herkal, A., Abdullah, J., Stout, A.*, et al.* (2011) Identification and characterization of genes required for cell-to-cell fusion in *Neurospora crassa*. *Eukaryotic Cell,* 10, 1100-1109.

Gaillard, S., Bailly, Y., Benoist, M., Rakitina, T., Kessler, J. P.*, et al.* (2006) Targeting of proteins of the striatin family to dendritic spines: role of the coiled-coil domain. *Traffic,* 7, 74-84.

Gaillard, S., Bartoli, M., Castets, F. and Monneron, A. (2001) Striatin, a calmodulin-dependent scaffolding protein, directly binds caveolin-1. *FEBS Letters,* 508, 49-52.

Galat, A. (2003) Peptidylprolyl cis/trans isomerases (immunophilins): biological diversity-targets-functions. *Current Topics in Medicinal Chemistry,* 3, 1315-1347.

García-Maceira, F. I., Di Pietro, A., Huertas-González, M. D., Ruiz-Roldán, M. C. and Roncero, M. I. G. (2001) Molecular characterization of an

endopolygalacturonase from *Fusarium oxysporum* expressed during early stages of infection. *Applied and Environmental Microbiology,* 67, 2191-2196.

Gardner, R. G., Swarbrick, G. M., Bays, N. W., Cronin, S. R., Wilhovsky, S.*, et al.* (2000) Endoplasmic reticulum degradation requires lumen to cytosol signaling. *The Journal of Cell Biology,* 151, 69-82.

Gatch, E., Hellmich, R. L. and Munkvold, G. P. (2002) A comparison of maize stalk rot occurrence in Bt and non-Bt hybrids. *Plant Disease,* 86, 1149-1155.

Gioti, A., Pradier, J., Fournier, E., Le Pêcheur, P., Giraud, C.*, et al.* (2008) A *Botrytis cinerea* emopamil binding domain protein, required for full virulence, belongs to a eukaryotic superfamily which has expanded in euascomycetes. *Eukaryotic Cell,* 7, 368-378.

Goudreault, M., D'Ambrosio, L. M., Kean, M. J., Mullin, M. J., Larsen, B. G.*, et al.* (2009) A PP2A phosphatase high density interaction network identifies a novel striatin-interacting phosphatase and kinase complex linked to the cerebral cavernous malformation 3 (CCM3) protein. *Molecular & Cellular Proteomics,* 8, 157-171.

Guarro, J. and Gene, J. (1995) Opportunistic fusarial infections in humans. *European Journal of Clinical Microbiology and Infectious Diseases,* 14, 741-754.

Gupta, G. D., Free, S. J., Levina, N. N., Keränen, S. and Heath, I. B. (2003) Two divergent plasma membrane syntaxin-like SNAREs, nsyn1 and nsyn2, contribute to hyphal tip growth and other developmental processes in *Neurospora crassa*. *Fungal Genetics and Biology,* 40, 271-286.

Gupta, G. D. and Heath, I. B. (2002) Predicting the distribution, conservation, and functions of SNAREs and related proteins in fungi. *Fungal Genetics and Biology,* 36, 1-21.

Hanson, P. I., Roth, R., Morisaki, H., Jahn, R. and Heuser, J. E. (1997) Structure and conformational changes in NSF and its membrane receptor complexes visualized by quick-freeze/deep-etch electron microscopy. *Cell,* 90, 523-535.

Hatsugai, N., Kuroyanagi, M., Yamada, K., Meshi, T., Tsuda, S.*, et al.* (2004) A plant vacuolar protease, VPE, mediates virus-induced hypersensitive cell death. *Science,* 305, 855-858.

Have, A. t., Mulder, W., Visser, J. and van Kan, J. A. (1998) The endopolygalacturonase gene Bcpg1 is required for full virulence of *Botrytis cinerea*. *Molecular Plant-Microbe Interactions,* 11, 1009-1016.

He, F., Zhang, Y., Chen, H., Zhang, Z. and Peng, Y.-L. (2008) The prediction of protein-protein interaction networks in rice blast fungus. *BMC Genomics,* 9, 519.

He, Z., Li, L. and Luan, S. (2004) Immunophilins and parvulins. Superfamily of peptidyl prolyl isomerases in Arabidopsis. *Plant physiology,* 134, 1248-1267.

Heilmann, C. J., Sorgo, A. G., Mohammadi, S., Sosinska, G. J., de Koster, C. G.*, et al.* (2013) Surface stress induces a conserved cell wall stress response in the pathogenic fungus *Candida albicans*. *Eukaryotic Cell,* 12, 254-264.

Hero, A. and Rajaratnam, B. (2012) Hub discovery in partial correlation graphs. *IEEE Transactions on Information Theory,* 58, 6064-6078.

Hong, S.-Y., So, J., Lee, J., Min, K., Son, H.*, et al.* (2010) Functional analyses of two syntaxin-like SNARE genes, GzSYN1 and GzSYN2, in the ascomycete *Gibberella zeae*. *Fungal Genetics and Biology,* 47, 364-372.

Hong, W. (2005) SNAREs and traffic. *Biochimica et Biophysica Acta (BBA)-Molecular Cell Research,* 1744, 120-144.

Hong, W. and Lev, S. (2014) Tethering the assembly of SNARE complexes. *Trends in Cell Biology,* 24, 35-43.

Hwang, J. and Pallas, D. C. (2014) STRIPAK complexes: structure, biological function, and involvement in human diseases. *The International Journal of Biochemistry & Cell Biology,* 47, 118-148.

Jorge, I., Navas-Cortes, J. A., Jimenez-Diaz, R. M. and Tena, M. (2006) Cell wall degrading enzymes in fusarium wilt of chickpea: correlation between pectinase and xylanase activities and disease development in plants infected with two pathogenic races of *Fusarium oxysporum* f. sp. *ciceris*. *Botany,* 84, 1395-1404.

Kamauchi, S., Nakatani, H., Nakano, C. and Urade, R. (2005) Gene expression in response to endoplasmic reticulum stress in *Arabidopsis thaliana*. *Febs Journal,* 272, 3461-3476.

Kean, M. J., Ceccarelli, D. F., Goudreault, M., Sanches, M., Tate, S.*, et al.* (2011) Structure-function analysis of core STRIPAK: a signaling complex implicated in Golgi polarization. *Journal of Biological Chemistry,* 286, 25065-25075.

Kee, Y., Lin, R. C., Hsu, S.-C. and Scheller, R. H. (1995) Distinct domains of syntaxin are required for synaptic vesicle fusion complex formation and dissociation. *Neuron,* 14, 991-998.

Kemp, H. A. and Sprague Jr, G. F. (2003) Far3 and five interacting proteins prevent premature recovery from pheromone arrest in the budding yeast *Saccharomyces cerevisiae*. *Molecular and Cellular Biology,* 23, 1750-1763.

Khunlertgit, N. and Yoon, B.-J. (2013) Identification of robust pathway markers for cancer through rank-based pathway activity inference. *Advances in Bioinformatics,* 2013.

Khunlertgit, N. and Yoon, B.-J. (2014) Simultaneous identification of robust synergistic subnetwork markers for effective cancer prognosis. *EURASIP Journal on Bioinformatics and Systems Biology,* 2014, 19.

Kim, H., Smith, J. E., Ridenour, J. B., Woloshuk, C. P. and Bluhm, B. H. (2011) HXK1 regulates carbon catabolism, sporulation, fumonisin B1 production and pathogenesis in *Fusarium verticillioides*. *Microbiology,* 157, 2658-2669.

Kim, H.-K., Cho, E. J., mi Jo, S., Sung, B. R., Lee, S.*, et al.* (2012) A split luciferase complementation assay for studying in vivo protein–protein interactions in filamentous ascomycetes. *Current Genetics,* 58, 179-189.

Kim, M., Zhang, H., Woloshuk, C., Shim, W.-B. and Yoon, B.-J. (2015a) Computational prediction of pathogenic network modules in *Fusarium verticillioides*. *IEEE/ACM Transactions on Computational Biology and Bioinformatics*, DOI: 10.1109/TCBB.2015.2440232.

Kim, M., Zhang, H., Woloshuk, C., Shim, W.-B. and Yoon, B.-J. (2015b) Computational identification of genetic subnetwork modules associated with maize defense response to *Fusarium verticillioides*. *BMC Bioinformatics,* 16, S12.

Kim, M., Zhang, H., Yan H., Yoon, B.-J., Shim, W.-B. (2017) Characterizing co-expression networks underpinning maize stalk rot virulence in *Fusarium verticillioides* through functional subnetwork module analyses. *Molecular Plant Pathology,* In revision.

Kingsland, G. and Wernham, C. (1962) Etiology of stalk rots of corn in Pennsylvania. *Phytopathology,* 52, 519.

Koehler, B. (1960) Corn stalk rots in Illinois. *Bulletin. University of Illinois Agricultural Experiment Station*, 658,90.

Kommedahl, T. and Windels, C. E. (1981) Root-, stalk-, and ear-infecting Fusarium species on corn in the USA. *Fusarium: Diseases, Biology and Taxonomy*, 94-103.

Kriek, N., Kellerman, T. S. and Marasas, W. F. O. (1981) A comparative study of the toxicity of *Fusarium verticillioides* (= *F. moniliforme*) to horses, primates, pigs, sheep and rats. *The Onderstepoort Journal of Veterinary Research*, 48, 129-131.

Kubicek, C. P., Starr, T. L. and Glass, N. L. (2014) Plant cell wall–degrading enzymes and their secretion in plant-pathogenic fungi. *Annual Review of Phytopathology,* 52, 427-451.

Kück, U., Beier, A. M. and Teichert, I. (2016) The composition and function of the striatin-interacting phosphatases and kinases (STRIPAK) complex in fungi. *Fungal Genetics and Biology,* 90, 31-38.

Ledencan, T., Simic, D., Brkic, I., Jambrovic, A. and Zdunic, Z. (2003) Resistance of maize inbreds and their hybrids to Fusarium stalk rot. *Czech Journal of Genetics and Plant Breeding-UZPI (Czech Republic)*.

Lee, E., Chuang, H.-Y., Kim, J.-W., Ideker, T. and Lee, D. (2008) Inferring pathway activity toward precise disease classification. *PLoS Computational Biology,* 4, e1000217.

Leslie, J. F., Pearson, C. A., Nelson, P. E. and Toussoun, T. (1990) Fusarium spp. from corn, sorghum, and soybean fields in the central and eastern United States. *Ecological Studies,* 44, 66.

Leverson, J. D. and Ness, S. A. (1998) Point mutations in v-Myb disrupt a cyclophilin-catalyzed negative regulatory mechanism. *Molecular Cell,* 1, 203-211.

Li, H., Handsaker, B., Wysoker, A., Fennell, T., Ruan, J.*, et al.* (2009) The sequence alignment/map format and SAMtools. *Bioinformatics,* 25, 2078-2079.

Lin, R. C. and Scheller, R. H. (1997) Structural organization of the synaptic exocytosis core complex. *Neuron,* 19, 1087-1094.

Liu, X., Tang, W.-H., Zhao, X.-M. and Chen, L. (2010) A network approach to predict pathogenic genes for *Fusarium graminearum*. *PloS One,* 5, e13021.

Lohoué Petmy, J., Folefack Temfack, M., Kaptue, L., Mbuagbauw, J., Raccurt, C.*, et al.* (2002) Invasive Fusarium infection in aids patients. Report of a case and review of the literature. *Journal de Mycologie Médicale,* 12, 146-148.

Lu, Q., Pallas, D. C., Surks, H. K., Baur, W. E., Mendelsohn, M. E.*, et al.* (2004) Striatin assembles a membrane signaling complex necessary for rapid, nongenomic

activation of endothelial NO synthase by estrogen receptor α. *Proceedings of the National Academy of Sciences of the United States of America,* 101, 17126-17131.

Lysenko, A., Urban, M., Bennett, L., Tsoka, S., Janowska-Sejda, E.*, et al.* (2013) Network-based data integration for selecting candidate virulence associated proteins in the cereal infecting fungus *Fusarium graminearum*. *PloS One,* 8, e67926.

Ma, L.-J., Van Der Does, H. C., Borkovich, K. A., Coleman, J. J., Daboussi, M.-J.*, et al.* (2010) Comparative genomics reveals mobile pathogenicity chromosomes in Fusarium. *Nature,* 464, 367-373.

MacPherson, S., Larochelle, M. and Turcotte, B. (2006) A fungal family of transcriptional regulators: the zinc cluster proteins. *Microbiology and Molecular Biology Reviews,* 70, 583-604.

Malsam, J., Kreye, S. and Sollner, T. (2008) Membrane fusion: SNAREs and regulation. *Cell Molecular Life Science,* 65, 2814-2832.

Martinoia, E., Maeshima, M. and Neuhaus, H. E. (2007) Vacuolar transporters and their essential role in plant metabolism. *Journal of Experimental Botany,* 58, 83-102.

McGee, D. C. (1988) *Maize diseases. A reference source for seed technologists*. APS press.

Misura, K. M., Scheller, R. H. and Weis, W. I. (2000) Three-dimensional structure of the neuronal-Sec1–syntaxin 1a complex. *Nature,* 404, 355-362.

Mittl, P. R. and Schneider-Brachert, W. (2007) Sel1-like repeat proteins in signal transduction. *Cellular Signalling,* 19, 20-31.

Moreno, C. S., Park, S., Nelson, K., Ashby, D., Hubalek, F.*, et al.* (2000) WD40 repeat proteins striatin and S/G2 nuclear autoantigen are members of a novel family of calmodulin-binding proteins that associate with protein phosphatase 2A. *Journal of Biological Chemistry,* 275, 5257-5263.

Munkvold, G. (1996) Corn stalk rot in Iowa. *Iowa State Univ. Ext. Publ. IPM,* 50.

Munkvold, G. P. and Desjardins, A. E. (1997) Fumonisins in maize: can we reduce their occurrence? *Plant Disease,* 81, 556-565.

Nakanishi, H., Morishita, M., Schwartz, C. L., Coluccio, A., Engebrecht, J.*, et al.* (2006) Phospholipase D and the SNARE Sso1p are necessary for vesicle fusion during sporulation in yeast. *Journal of Cell Science,* 119, 1406-1415.

Nicholson, K. L., Munson, M., Miller, R. B., Filip, T. J., Fairman, R.*, et al.* (1998) Regulation of SNARE complex assembly by an N-terminal domain of the t-SNARE Sso1p. *Nature Structural & Molecular Biology,* 5, 793-802.

Nordzieke, S., Zobel, T., Fränzel, B., Wolters, D. A., Kück, U.*, et al.* (2015) A fungal sarcolemmal membrane-associated protein (SLMAP) homolog plays a fundamental role in development and localizes to the nuclear envelope, endoplasmic reticulum, and mitochondria. *Eukaryotic Cell,* 14, 345-358.

Okamoto, T., Schlegel, A., Scherer, P. E. and Lisanti, M. P. (1998) Caveolins, a family of scaffolding proteins for organizing "preassembled signaling complexes" at the plasma membrane. *Journal of Biological Chemistry,* 273, 5419-5422.

Park, D. L. and Troxell, T. C. (2002) US perspective on mycotoxin regulatory issues. In: *Mycotoxins and Food Safety.* Springer, pp. 277-285.

Parlati, F., Weber, T., McNew, J. A., Westermann, B., Söllner, T. H.*, et al.* (1999) Rapid and efficient fusion of phospholipid vesicles by the α-helical core of a SNARE complex in the absence of an N-terminal regulatory domain. *Proceedings of the National Academy of Sciences,* 96, 12565-12570.

Pijnappel, W. P., Schaft, D., Roguev, A., Shevchenko, A., Tekotte, H.*, et al.* (2001) The *S. cerevisiae* SET3 complex includes two histone deacetylases, Hos2 and Hst1, and is a meiotic-specific repressor of the sporulation gene program. *Genes and Development,* 15, 2991-3004.

Pöggeler, S. and Kück, U. (2004) A WD40 repeat protein regulates fungal cell differentiation and can be replaced functionally by the mammalian homologue striatin. *Eukaryotic Cell,* 3, 232-240.

Popolo, L., Gualtieri, T. and Ragni, E. (2001) The yeast cell-wall salvage pathway. *Medical Mycology,* 39, 111-121.

Pracheil, T., Thornton, J. and Liu, Z. (2012) TORC2 signaling is antagonized by protein phosphatase 2A and the Far complex in *Saccharomyces cerevisiae*. *Genetics,* 190, 1325-1339.

Proctor, R. H., Brown, D. W., Plattner, R. D. and Desjardins, A. E. (2003) Co-expression of 15 contiguous genes delineates a fumonisin biosynthetic gene cluster in *Gibberella moniliformis*. *Fungal Genetics and Biology,* 38, 237-249.

Proctor, R. H., Desjardins, A. E., Plattner, R. D. and Hohn, T. M. (1999) A polyketide synthase gene required for biosynthesis of fumonisin mycotoxins in *Gibberella fujikuroi* mating population A. *Fungal Genetics and Biology,* 27, 100-112.

Pyo, Y. J., Kwon, K.-C., Kim, A. and Cho, M. H. (2013) Seedling Lethal1, a pentatricopeptide repeat protein lacking an E/E+ or DYW domain in Arabidopsis, is involved in plastid gene expression and early chloroplast development. *Plant Physiology,* 163, 1844-1858.

Qian, X., Sze, S.-H. and Yoon, B.-J. (2009) Querying pathways in protein interaction networks based on hidden Markov models. *Journal of Computational Biology,* 16, 145-157.

Qian, X. and Yoon, B.-J. (2009) Effective identification of conserved pathways in biological networks using hidden Markov models. *PLoS One,* 4, e8070.

Reimand, J., Arak, T. and Vilo, J. (2011) g: Profiler—a web server for functional interpretation of gene lists (2011 update). *Nucleic Acids Research,* 39, W307-W315.

Rispail, N. and Di Pietro, A. (2009) *Fusarium oxysporum* Ste12 controls invasive growth and virulence downstream of the Fmk1 MAPK cascade. *Molecular Plant-Microbe Interactions,* 22, 830-839.

Roca, M. G., Arlt, J., Jeffree, C. E. and Read, N. D. (2005) Cell biology of conidial anastomosis tubes in *Neurospora crassa*. *Eukaryotic Cell,* 4, 911-919.

Ross, P., Nelson, P., Richard, J., Osweiler, G., Rice, L.*, et al.* (1990) Production of fumonisins by *Fusarium moniliforme* and *Fusarium proliferatum* isolates

associated with equine leukoencephalomalacia and a pulmonary edema syndrome in swine. *Applied and Environmental Microbiology,* 56, 3225-3226.

Ryu, J.-K., Jahn, R. and Yoon, T. Y. (2016) Review: Progresses in understanding N- ethylmaleimide sensitive factor (NSF) mediated disassembly of SNARE complexes. *Biopolymers,* 105, 518-531.

Sagaram, U. S., Kolomiets, M. and Shim, W.-B. (2006) Regulation of fumonisin biosynthesis in *Fusarium verticillioides*-maize system. *The Plant Pathology Journal,* 22, 203-210.

Sagaram, U. S., Shaw, B. D. and Shim, W.-B. (2007) *Fusarium verticillioides* GAP1, a gene encoding a putative glycolipid-anchored surface protein, participates in conidiation and cell wall structure but not virulence. *Microbiology,* 153, 2850-2861.

Sahraeian, S. M. E. and Yoon, B.-J. (2011) Fast network querying algorithm for searching large-scale biological networks. In: *Acoustics, Speech and Signal Processing (ICASSP), 2011 IEEE International Conference on.* IEEE, pp. 6008-6011.

Scales, S. J., Chen, Y. A., Yoo, B. Y., Patel, S. M., Doung, Y.-C.*, et al.* (2000) SNAREs contribute to the specificity of membrane fusion. *Neuron,* 26, 457-464.

Schillig, R. and Morschhäuser, J. (2013) Analysis of a fungus- specific transcription factor family, the *Candida albicans* zinc cluster proteins, by artificial activation. *Molecular Microbiology,* 89, 1003-1017.

Seo, K. W., Kelley, R. I., Okano, S. and Watanabe, T. (2001) Mouse Td^{ho} abnormality results from double point mutations of the emopamil binding protein gene (Ebp). *Mammalian Genome,* 12, 602-605.

Shaoxi, W., Ningro, G. and Guixia, L. (1996) A rare case of *Fusarium verticillioides* facial granuloma successfully treated by itraconazole. *Journal de Mycologie Médicale,* 6, 88-90.

Shim, W.-B., Sagaram, U. S., Choi, Y.-E., So, J., Wilkinson, H. H.*, et al.* (2006) FSR1 is essential for virulence and female fertility in *Fusarium verticillioides* and *F. graminearum*. *Molecular Plant-Microbe Interactions,* 19, 725-733.

Shim, W.-B. and Woloshuk, C. P. (1999) Nitrogen repression of fumonisin B1 biosynthesis in *Gibberella fujikuroi*. *FEMS microbiology letters,* 177, 109-116.

Shim, W.-B. and Woloshuk, C. P. (2001) Regulation of fumonisin B1 biosynthesis and conidiation in *Fusarium verticillioides* by a cyclin-like (C-type) gene, FCC1. *Applied and Environmental Microbiology,* 67, 1607-1612.

Shin, J. H., Kim, J. E., Malapi- Wight, M., Choi, Y. E., Shaw, B. D.*, et al.* (2013) Protein phosphatase 2A regulatory subunits perform distinct functional roles in the maize pathogen *Fusarium verticillioides*. *Molecular Plant Pathology,* 14, 518-529.

Singh, N. S., Shao, N., McLean, J. R., Sevugan, M., Ren, L.*, et al.* (2011) SIN-inhibitory phosphatase complex promotes Cdc11p dephosphorylation and propagates SIN asymmetry in fission yeast. *Current Biology,* 21, 1968-1978.

Smith, D. and White, D. (1989) Diseases of corn. *Diseases of Corn.*, 687-766.

Smith, T. F., Gaitatzes, C., Saxena, K. and Neer, E. J. (1999) The WD repeat: a common architecture for diverse functions. *Trends in Biochemical Sciences,* 24, 181-185.

Sobek, E. and Munkvold, G. (1999) European corn borer (Lepidoptera: Pyralidae) larvae as vectors of *Fusarium moniliforme*, causing kernel rot and symptomless infection of maize kernels. *Journal of Economic Entomology,* 92, 503-509.

Söllner, T., Bennett, M. K., Whiteheart, S. W., Scheller, R. H. and Rothman, J. E. (1993) A protein assembly-disassembly pathway in vitro that may correspond to sequential steps of synaptic vesicle docking, activation, and fusion. *Cell,* 75, 409-418.

Stack, J. P. (1999) Common stalk rot diseases of corn. Cooperative Extension, Institute of Agriculture and Natural Resources, University of Nebraska--Lincoln.

Stockton, R. A., Shenkar, R., Awad, I. A. and Ginsberg, M. H. (2010) Cerebral cavernous malformations proteins inhibit Rho kinase to stabilize vascular integrity. *Journal of Experimental Medicine*, Jem. 20091258.

Su, J., Yoon, B.-J. and Dougherty, E. R. (2009) Accurate and reliable cancer classification based on probabilistic inference of pathway activity. *PloS One,* 4, e8161.

Su, J., Yoon, B.-J. and Dougherty, E. R. (2010) Identification of diagnostic subnetwork markers for cancer in human protein-protein interaction network. *BMC Bioinformatics,* 11, S8.

Subramanian, A., Tamayo, P., Mootha, V. K., Mukherjee, S., Ebert, B. L.*, et al.* (2005) Gene set enrichment analysis: a knowledge-based approach for interpreting

genome-wide expression profiles. *Proceedings of the National Academy of Sciences,* 102, 15545-15550.

Tan, B., Long, X., Nakshatri, H., Nephew, K. P. and Bigsby, R. M. (2008) Striatin-3γ inhibits estrogen receptor activity by recruiting a protein phosphatase. *Journal of Molecular Endocrinology,* 40, 199-210.

The UniProt Consortium (2017) UniProt: the universal protein knowledgebase. *Nucleic Acids Research,* 45, D158-D169

Tian, L., Greenberg, S. A., Kong, S. W., Altschuler, J., Kohane, I. S.*, et al.* (2005) Discovering statistically significant pathways in expression profiling studies. *Proceedings of the National Academy of Sciences of the United States of America,* 102, 13544-13549.

Tsutsui, T., Morita-Yamamuro, C., Asada, Y., Minami, E., Shibuya, N.*, et al.* (2006) Salicylic acid and a chitin elicitor both control expression of the CAD1 gene involved in the plant immunity of Arabidopsis. *Bioscience, Biotechnology, and Biochemistry,* 70, 2042-2048.

Upadhyay, S. and Shaw, B. D. (2008) The role of actin, fimbrin and endocytosis in growth of hyphae in *Aspergillus nidulans*. *Molecular Microbiology,* 68, 690-705.

Viaud, M., Brunet- Simon, A., Brygoo, Y., Pradier, J. M. and Levis, C. (2003) Cyclophilin A and calcineurin functions investigated by gene inactivation, cyclosporin A inhibition and cDNA arrays approaches in the phytopathogenic fungus *Botrytis cinerea*. *Molecular Microbiology,* 50, 1451-1465.

Wan, J., Zhang, S. and Stacey, G. (2004) Activation of a mitogen- activated protein kinase pathway in Arabidopsis by chitin. *Molecular Plant Pathology,* 5, 125-135.

Wang, C. L., Shim, W. B. and Shaw, B. D. (2016) The *Colletotrichum graminicola* striatin orthologue Str1 is necessary for anastomosis and is a virulence factor. *Molecular Plant Pathology*, 17, 931-942.

Wang, C.-L., Shim, W.-B. and Shaw, B. D. (2010) *Aspergillus nidulans* striatin (StrA) mediates sexual development and localizes to the endoplasmic reticulum. *Fungal Genetics and Biology,* 47, 789-799.

Wang, Y., Klijn, J. G., Zhang, Y., Sieuwerts, A. M., Look, M. P.*, et al.* (2005) Gene-expression profiles to predict distant metastasis of lymph-node-negative primary breast cancer. *The Lancet,* 365, 671-679.

White, D. (1999) Fungal stalk rots. *Compendium of corn diseases. 3rd ed. American Phytopathological Society Press, St. Paul, MN*, 38-44.

White, D. G. (1999) Compendium of corn diseases. *Amer Phytopathological Society*.

Wilson, B. and MARONPOT, P. (1971) Causative fungus agent of leucoencephalomalacia in equine animals. *Veterinary Record,* 88, 484-486.

Wilson, T., Ross, P., Owens, D., Rice, L., Green, S.*, et al.* (1992) Experimental reproduction of ELEM. *Mycopathologia,* 117, 115-120.

Woloshuk, C. P. and Shim, W.-B. (2013) Aflatoxins, fumonisins, and trichothecenes: a convergence of knowledge. *FEMS Microbiology Reviews,* 37, 94-109.

Xiang, L., Etxeberria, E. and den Ende, W. (2013) Vacuolar protein sorting mechanisms in plants. *FEBS Journal,* 280, 979-993.

Xiang, Q., Rasmussen, C. and Glass, N. L. (2002) The ham-2 locus, encoding a putative transmembrane protein, is required for hyphal fusion in *Neurospora crassa*. *Genetics,* 160, 169-180.

Xiao, H., Chen, D., Fang, Z., Xu, J., Sun, X.*, et al.* (2009) Lysosome biogenesis mediated by vps-18 affects apoptotic cell degradation in *Caenorhabditis elegans*. *Molecular Biology of the Cell,* 20, 21-32.

Yamamura, Y. and Shim, W.-B. (2008) The coiled-coil protein-binding motif in *Fusarium verticillioides* Fsr1 is essential for maize stalk rot virulence. *Microbiology,* 154, 1637-1645.

Yang, D., Zhang, C. and Wang, Y. (2002) Review of maize stalk rot in China. *Journal of Maize Science,* 10, 88-90.

Yuan, Q. and Jäntti, J. (2010) Functional analysis of phosphorylation on *Saccharomyces cerevisiae* syntaxin 1 homologues Sso1p and Sso2p. *PloS One,* 5, e13323.

Zhang, H., Li, B., Fang, Q., Li, Y., Zheng, X.*, et al.* (2016) SNARE protein FgVam7 controls growth, asexual and sexual development, and plant infection in *Fusarium graminearum*. *Molecular Plant Pathology,* 17, 108-119.

Zhang, H.-D., Cui, Y.-L., Huang, C., Yin, Q.-Q., Qin, X.-M.*, et al.* (2015) PPR protein PDM1/SEL1 is involved in RNA editing and splicing of plastid genes in Arabidopsis thaliana. *Photosynthesis Research,* 126, 311-321.

Zhang, H., Mukherjee, M., Kim, J.-E., Yu, W. and Shim, W. B. (2017) Fsr1, a striatin homolog, forms an endomembrane-bound signaling complex that regulates

virulence in maize pathogen *Fusarium verticillioides*. *Molecular Plant Pathology,* DOI: 10.1111/mpp.12562.

Zhao, X.-M., Zhang, X.-W., Tang, W.-H. and Chen, L. (2009) FPPI: *Fusarium graminearum* protein− protein interaction database. *Journal of Proteome Research,* 8, 4714-4721.

Zheng, W., Chen, J., Liu, W., Zheng, S., Zhou, J.*, et al.* (2007) A Rho3 homolog is essential for appressorium development and pathogenicity of *Magnaporthe grisea. Eukaryotic Cell,* 6, 2240-2250.

Zheng, X., Xu, C., Di Lorenzo, A., Kleaveland, B., Zou, Z.*, et al.* (2010) CCM3 signaling through sterile 20–like kinases plays an essential role during zebrafish cardiovascular development and cerebral cavernous malformations. *The Journal of Clinical Investigation,* 120, 2795-2804.

APPENDIX A

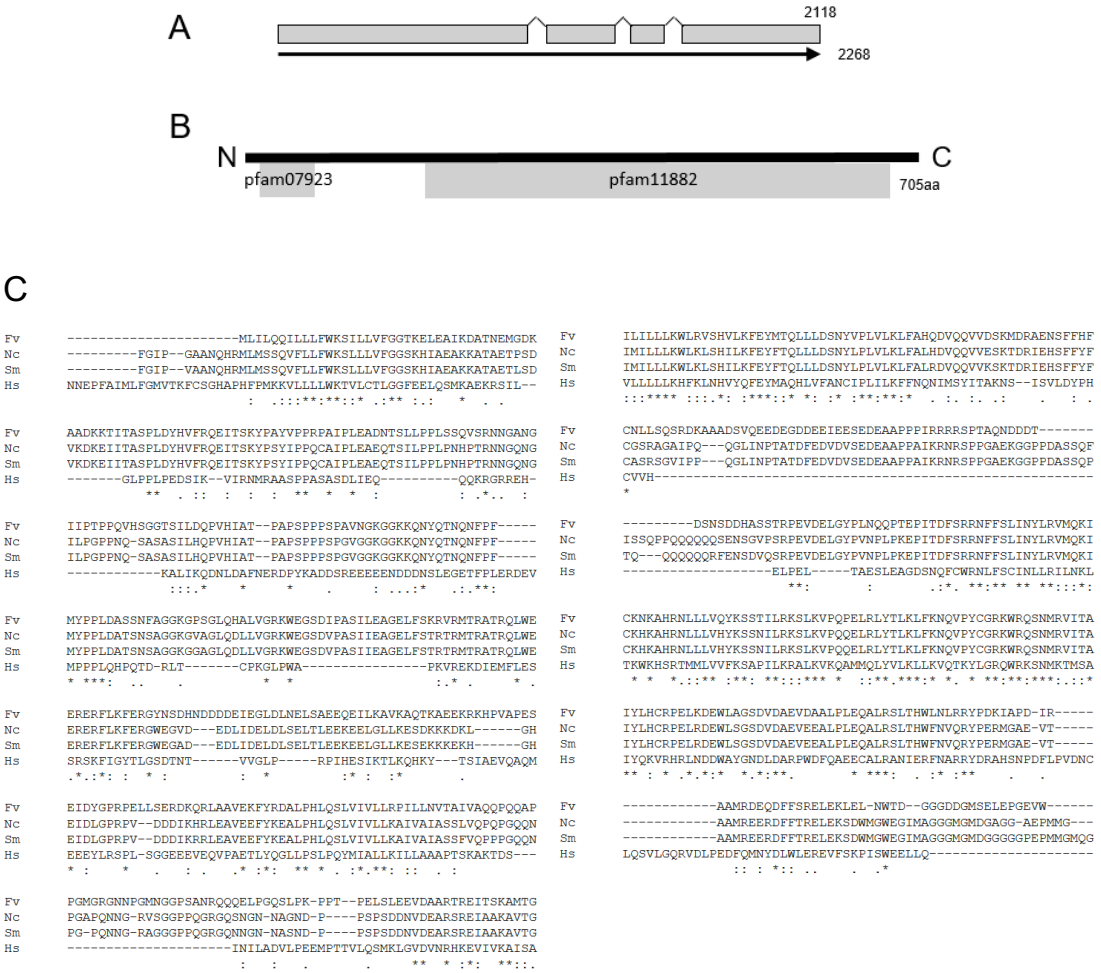

Figure A-1 (A) Schematic depiction of *FvSTP1* locus with exons (gray box) and introns (line) that results in 2,118-bp transcript from 2,268 genomic DNA. (B) The 705-aa predicted protein harbors two putative functional domains (shown in light gray box): a N1221-like domain (pfam07923) and a conserved domain of unknown function (pfam 11882), in predicted protein. The N1221-like domain featured in this family are similar to a hypothetical protein product of ORF N1221 in the CPT1-SPC98 intergenic region of the yeast genome (P53917). This encodes an acidic polypeptide with several possible transmembrane regions. DFU3402 domain (pfam 11882) is functionally uncharacterized, but found in eukaryotes and is associated with PF07923. This predicted domain is typically between 350 to 473 amino acids in length. (B) Amino acid alignment of four fungal FvStp1 homologs by using CLUSTAL O (1.2.2) multiple sequence alignment. Sm (*S. macrospora*, accession no. AJ627567 [NCBI]), Nc (*N. crassa*, accession no. CAC28842 [NCBI]), Hs (*H. sapiens*, accession no. AAH19064 [NCBI]).

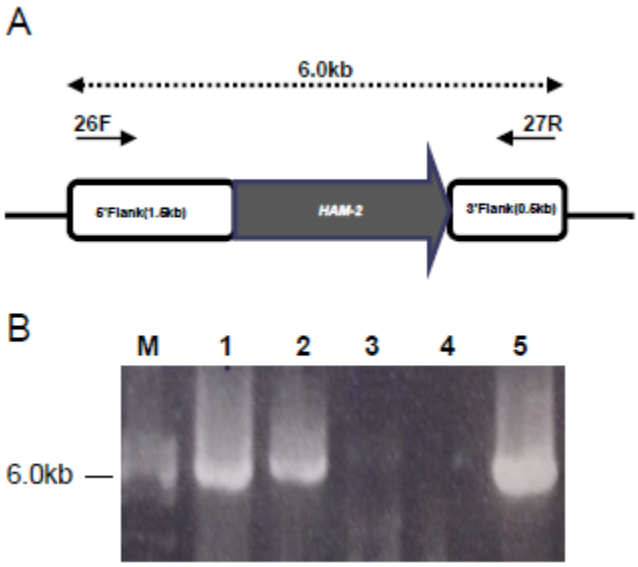

Figure A-2 (A) The fragment of *FvSTP1* homolog in *Neurospora crassa* was generated by PCR with primers 26F and 27R. The fragment was co-transformed along with geneticin- resistant cassette into D*FvSTP1* mutant protoplast. Geneticin-resistant colonies were selected for PCR screening to verify complementation. (B) PCR screening was performed by using 26F and 27R primers: 1: *FvSTP1-NC1*; 2, *FvSTP1-NC2*; 3, WT control; 4, Blank control; 5, *N. crassa* gDNA positive control.

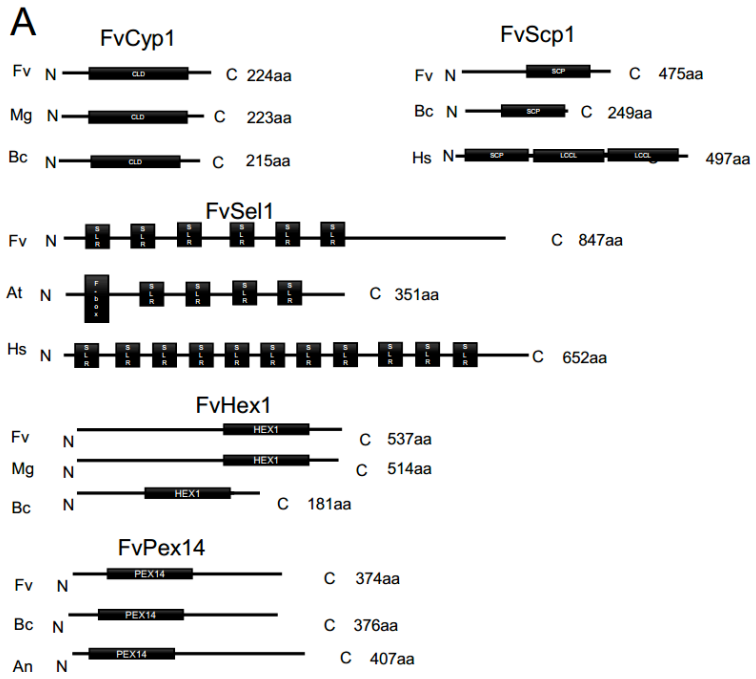

Figure A-3 Comparison of conserved domains in *F. verticillioides* (Fv), *Magnaporthe grisea* (Mg), *Botrytis cinerea* (Bc), *Homo sapiens* (Hs), *Arabidodpsis thaliana* (At) and *Aspergillus nidulans* (An). (A) Schematic representation of protein orthologues shows the location and alignment of conserved domains. Physical map of FvCyp1, FvScp1, FvSel1, FvHex1 and FvPex14 and their homologs showing putative domains (black box): cyclophilin-like domain (CLD) (PF04126), spermcoating protein (SCP)-like extracellular protein domain (PF00188), Sel1-like repeat (SLR) (PF08238), Hex1(cd04469) and a Pex14_N (pfam04695). (B) Amino acid alignment of four fungal FvStp1 homologs by using CLUSTAL O (1.2.2) multiple sequence alignment.

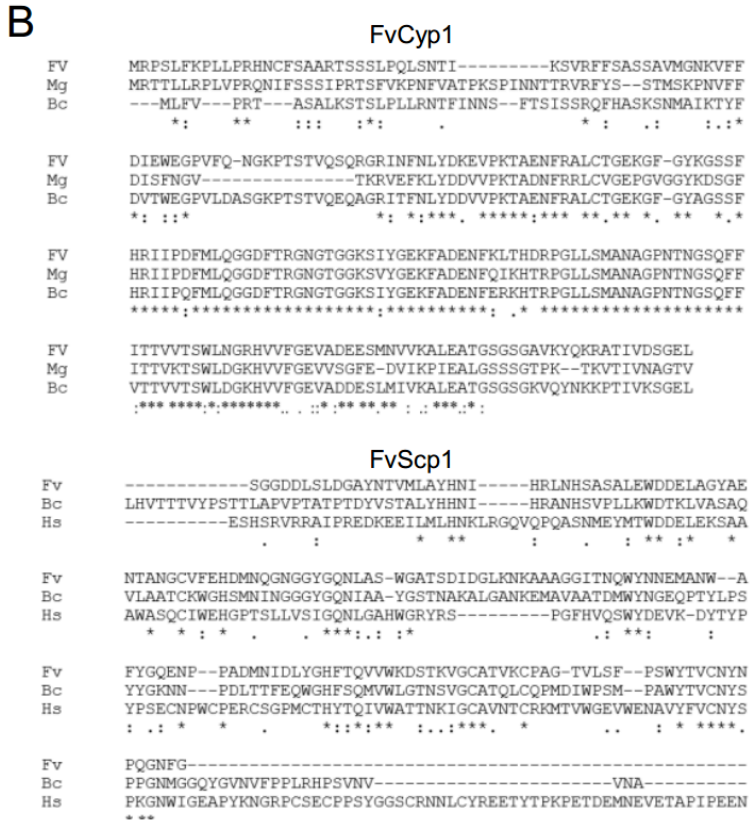

Figure A-3 Continued.

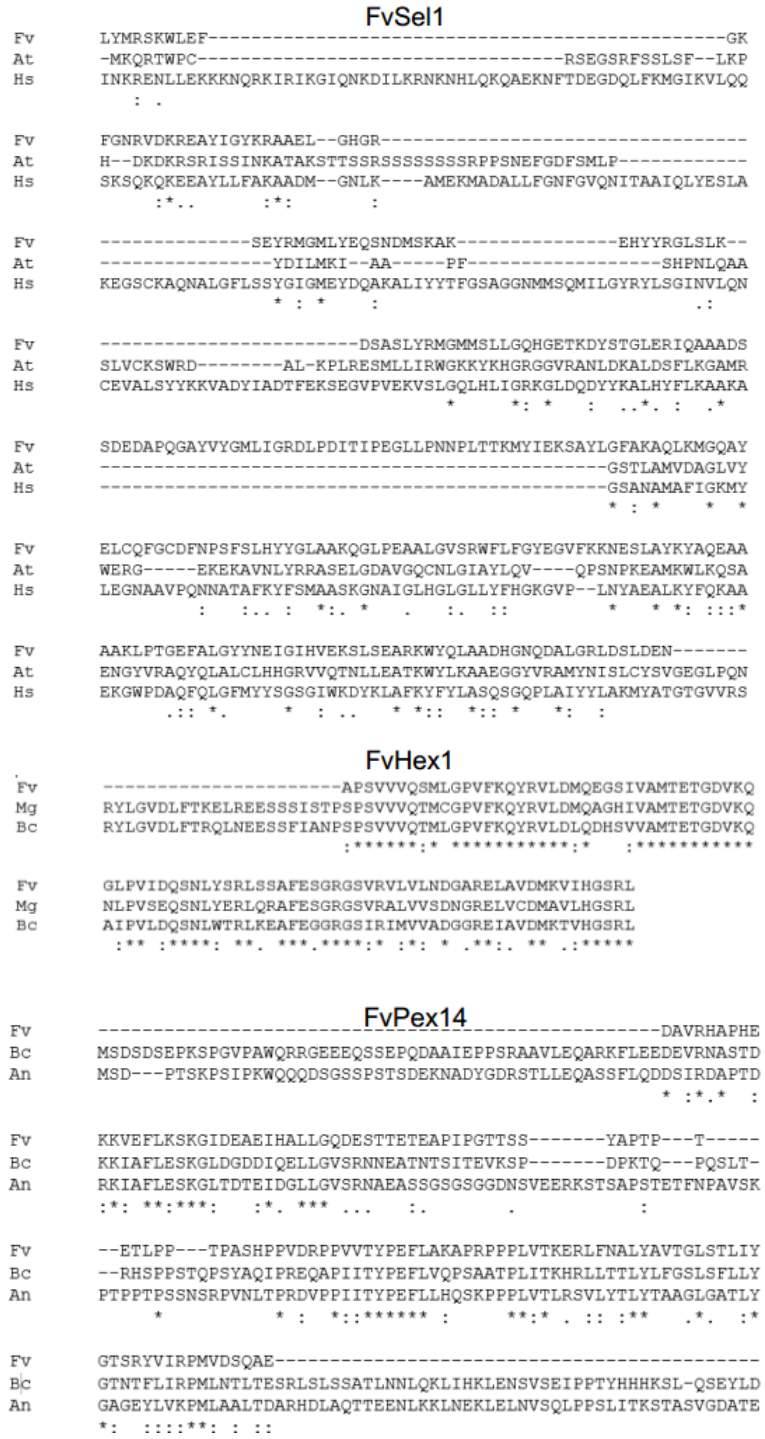

Figure A-3 Continued.

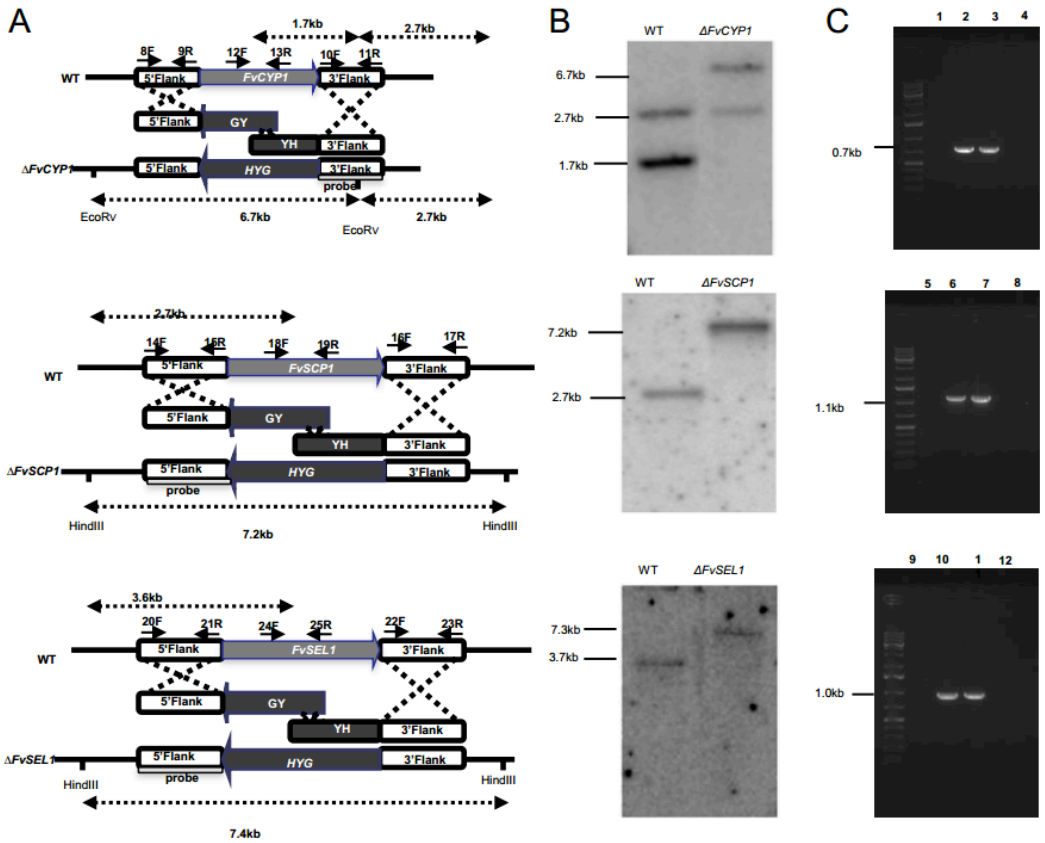

Figure A-4 (A) The targeted gene disruption was achieved by homologous recombination with following our standard split marker strategy. Disruption constructs were generated by single Joint-PCR, and Hygromycin phosphotransferase (HYG) was used as the selective marker. (B) The gene deletion was confirmed by Southern analysis. Anticipated band sizes before and after recombination are indicated on the left. (C) Complementation strains PCR screening was done by using the same set of primers to screen mutant strains: 1: ΔFvCYP1; 2, FvCYP1C; 3, WT positive control; 4, Blank control; 5: ΔFvSCP1; 6, FvSCP1C; 7, WT positive control; 8, Blank control; 9: ΔFvSEL1; 10, FvCSEL1C; 11, WT positive control; 12, Blank control. PCR screenings were performed at least three times with same results.

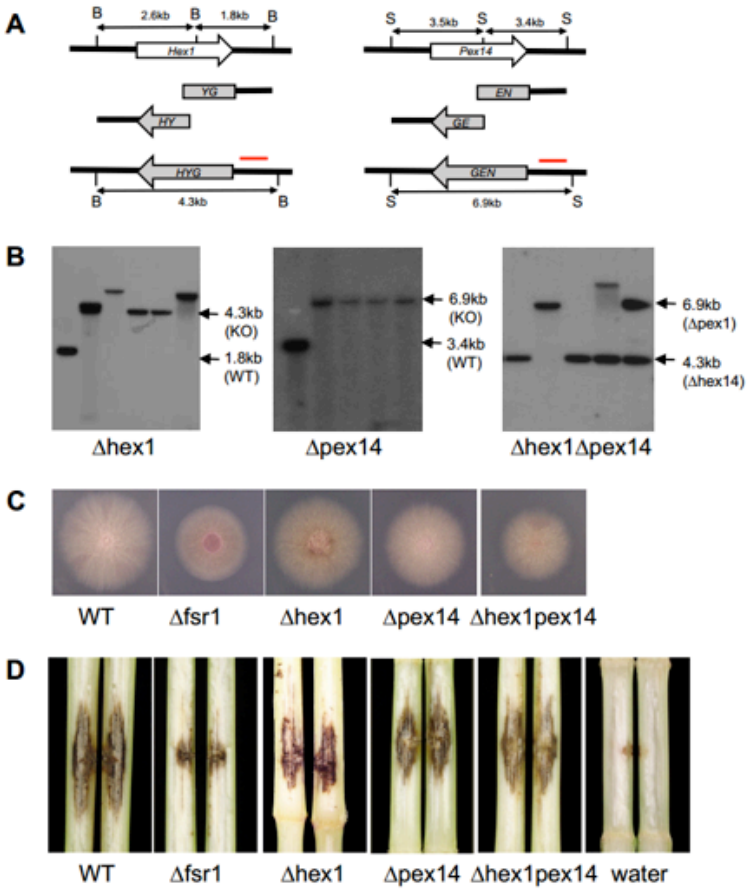

Figure A-5 (A) Schematic overview of gene disruption strategy using split-marker approach. Hygromycin marker (*HYG*) and geneticin marker (*GEN*) were used for *HEX1* and *PEX14* replacement, respectively. *Bgl*II (B) and *Sal*I (S) restriction enzymes were used for genomic DNA digestion when preparing Southern blot. Red bars indicate the probe DNA fragments used in each Southern blot. (B) Southern blot results confirming the replacement of target genes in Dhex1, Dpex14, and the double mutant. (C) Vegetative growth of WT, Dfsr1, Dhex1, Dpex14, and Dhex1Dpex14 strains were examined on 0.2X potato dextrose agar. Strains were point inoculated with an agar block (0.5 cm in diameter) and incubated for 6 days at 25 °C under 14 h light/10 h dark cycle. (D) Eight-week-old B73 maize stalks were inoculated with 10^4 spores of fungal strains at the internodal region and incubated in a growth chamber for 10 days at 25C. Subsequently, maize stalks were split longitudinally to observe the extent of the rot. Four independent biological repetitions were performed.

Table A-1 Y2H screening results.

Table A-1.1 Fsr1 N-terminal as bait.

Fv Locus	Gene name (domain)
FVEG_00233.3	Hypothetical protein
FVEG_00403.3	putative cyclophilin peptidyl-prolyl cis-trans isomerase
FVEG_00510.3	Hypothetical protein
FVEG_00562.3	40S ribosomal protein S6-B
FVEG_01143.3	putative alpha keto acid dehydrogenase
FVEG_01304.3	cystathionine gamma-lyase
FVEG_01449.3	conserved hypothetical protein (TF)
FVEG_01920.3	conserved hypothetical protein (Hex1)
FVEG_02319.3	putative mitochondrial carrier protein
FVEG_02948.3	C-1-tetrahydrofolate synthase
FVEG_03125.3	putative glyoxalase
FVEG_04097.3	SCP like extracellular protein
FVEG_05696.3	conserved hypothetical protein
FVEG_06063.3	conserved hypothetical protein
FVEG_07050.3	Heat shock protein HSP98
FVEG_07289.3	Eukaryotic translation initiation factor 5A-2
FVEG_07318.3	putative cystathionine beta-lyase
FVEG_07509.3	conserved hypothetical protein
FVEG_08088.3	putative transcription initiation factor
FVEG_08459.3	putative phospholipase B homolog
FVEG_08486.3	conserved hypothetical protein
FVEG_08639.3	conserved hypothetical protein
FVEG_08746.3	putative phospholipase B homolog
FVEG_08950.3	hypothetical protein
FVEG_09495.3	O-acetylhomoserine
FVEG_09511.3	putative glutamate synthase
FVEG_09578.3	putative choline sulfatase
FVEG_10001.3	conserved hypothetical protein
FVEG_10119.3	putative Antigen1 precursor (no domains)
FVEG_10127.3	conserved hypothetical protein
FVEG_10358.3	putative pyruvate dehydrogenase complex
FVEG_10441.3	putative short-chain dehydrogenase
FVEG_10833.3	hypothetical protein
FVEG_11066.3	putative glutamyl-tRNA synthetase
FVEG_11334.3	peroxisomal membrane anchor protein
FVEG_11642.3	putative 2-oxoglutarate dehydrogenase
FVEG_12134.3	Conserved hypothetical Sel1 repeat protein

Table A-1.1 Continued

Fv Locus	Gene name (domain)
FVEG_12379.3	conserved hypothetical protein
FVEG_12379.3	conserved hypothetical protein
FVEG_12398.3	putative mannose-binding lectin
FVEG_12529.3	O-acetylhomoserine
FVEG_12531.3	putative FMN-dependent dehydrogease
FVEG_12848.3	conserved hypothetical protein
FVEG_12878.3	putative carboxypeptidase Y
FVEG_13501.3	conserved hypothetical protein
FVEG_13647.3	conserved hypothetical protein
No Fus homolog	hypothetical protein
No Fus. homolog	Unknown protein
No Fv homolog	hypothetical protein
No Fv homolog	putative NADH dehydrogenase
No Fv homolog	Mitochondia protein of unknown function
No Fv homolog	No known homolog
No Fv homolog	No known homolog
No Fv homolog	putative mitochondia protein

Table A-1.2 Fsr1 N-terminal without coiled coil as bait.

Fv Locus	Gene name (domain)
FVEG_00510.3	Hypothetical protein
FVEG_00562.3	40S ribosomal protein S6-B
FVEG_01143.3	putative alpha keto acid dehydrogenase
FVEG_01304.3	cystathionine gamma-lyase
FVEG_01920.3	conserved hypothetical protein (Hex1)
FVEG_02297.3	2-dehydropantoate 2-reductase
FVEG_04927.3	Glyceraldehyde 3-phosphate dehydrogenase
FVEG_07050.3	Heat shock protein HSP98
FVEG_07509.3	conserved hypothetical protein
FVEG_08088.3	putative transcription initiation factor
FVEG_09511.3	putative glutamate synthase
FVEG_09578.3	putative choline sulfatase
FVEG_10833.3	hypothetical protein
FVEG_11334.3	peroxisomal membrane anchor protein
FVEG_12379.3	conserved hypothetical protein
FVEG_12752.3	predicted protein

Table A-1.2 Continued

Fv Locus	**Gene name (domain)**
FVEG_12878.3	putative carboxypeptidase Y
No Fv homolog	No known homolog
No Fv homolog	No known homolog
No Fv homolog	No known homolog
No Fv homolog	No known homolog
No Fv homolog	No known homolog
No Fv homolog	No known homolog
No Fv homolog	No known homolog
No Fv homolog	No known homolog
No Fv homolog	No known homolog
No Fv homolog	No known homolog
No Fv homolog	No known homolog
No Fv homolog	No known homolog
No Fv homolog	No known homolog
No Fv homolog	No known homolog
No Fv homolog	No known homolog
No Fv homolog	No known homolog
No Fv homolog	No known homolog

Table A-2 Additional Description of putative Fsr1-interacting protein.

Fv Locus	**Gene Name**	**Key pfam motif**	**Proposed function**
FVEG_00403	*FvCYP1*	cyclophilin-like domain (CLD) (PF04126)	Act as a virulence determinant during plant infection in *Magnaporthe grisea* and *Botrytis cinerea* (Viaud *et al.*, 2003); act as modulators of protein function in eukaryotes such as budding yeast cyclophilin Cpr1 (Arevalo-Rodriguez & Heitman, 2005)
FVEG_04097	*FvSCP1*	sperm-coating protein (SCP)-like extracellular protein (PF00188)	Act as a Ca^{2+}-chelator in various signaling processes (Cantacessi *et al.*, 2009)
FVEG_12134	*FvSEL1*	Sel1-like repeat (SLR) (PF08238)	Involved in signal transduction pathways, involved in the ER-associated protein degradation under cellular stress (Kamauchi *et al.*, 2005) (Gardner *et al.*, 2000)
FVEG_01920	*FvHEX1*	Hex1 (cd04469)	Physiology and functioning of the Woronin body (Curach *et al.*, 2004), asexual production and pathogenicity in *F. graminearum* (Son *et al.*, 2013)
FVEG_11334	*FvPEX14*	Pex14_N (pfam04695)	Sustain the formation of fruiting bodies and the maturation and germination of sexual spores (Peraza-Reyes & Berteaux-Lecellier, 2013). Important for lipid metabolism (Wanders *et al.*, 2010) and are implicated in the homeostasis of reactive oxygen species (Fransen *et al.*, 2012).

Table A-3 *F. verticillioides* strains used in this study.

Strain	Source
F. verticillioides 7600	FGSC
Δfsr1	Shim et al., 2006
ΔFvstp1	This study
ΔFvcyp1	This study
ΔFvscp1	This study
ΔFvsel1	This study
Fvstp1c	This study
Fvstp1nc	This study
Fvcyp1c	This study
Fvscp1c	This study
Fvsel1c	This study
Fvcyp1-gfp	This study
Fvscp1-gfp	This study
Fvsel1-gfp	This study
Fsr1-gfp	This study
Fvcyp1-Fsr1-gfp	This study
Fvscp1-Fsr1-gfp	This study
Fvscp1-Fsr1-gfp	This study

Table A-4 Primers used in this study. The underlined sequences were for fusion purpose. The recognition site of the restriction enzyme is shaded in select primer sequences.

Primer Name	**5'-3' sequence**
FsrExon1for	CATCTCTCCCAAACCGACTC
FsrExon1revt	CACTGGCATATCCTCCAAGGTAGATCTAAGCTTCTCTTGTATCTTTGC
FsrExon2fort	GCAAAGATACAAGAGAAGCTTAGATCTACCTTGGAGGATATGCCAGTG
FsrExon2rev	CTTCGTGGCCAGAAATGATAG
FNcos	GCCGCCATGGGCCCTA ATGCT
FBrev	CAGCCATGGGATCCGTCCACC
T7seq	TAATACGACTCACTATAGGGC
jRv	CTCCCGAGCCTGAAGCTGAGCCGTCGAGTTCCTATCGCGCTCATG
iFw	CATGAGCGCGATAGGAACTCGACGGCTCAGCTTCAGGCTCGGGAG
3'BDseq	TTTTCGTTTTAAAACCTAAGAGTC
5'BDnfor	CATCATGGAGGAGCAGAAG
3'BDnrev	CATAAATCATAAGAAATTCGCCCGG
5'LD Amplimer	CTATTCGATGATGAAGATACCCCACCAAACCC
3'LD Amplimer	GTGAACTTGCGGGGTTTTTCAGTATCTACGAT
FCC1n LUC-F	AAGCTCGAGTAGTCGACATGTCAGCCAATTATTGGCAC
FCC1nLUC-R	CGTACGAGATCTGGTCGACCTTATCTAAGCCTCTTGCCTT
FCK1cLUC-F	CGTCCCGGGGCGGTACCCCTCTCCGTCCTCACATCG
FCK1cLUC-R	TTGGATCCCCGGGTACCCTATTCCTTCTGCCTCTTGGC
STR1nLUC-F	AAGCTCGAGTAGTCGACATGGGCCCTAATGCTGGCAA
STR1nLUC-R	CGTACGAGATCTGGTCGACTCGTGCAAACACCTTGACCAC
STR2cLUC-F	CGTCCCGGGGCGGTACCCTCATTCTTCAACAGATACTTCTAC
STR2cLUC-R	TTGGATCCCCGGGTACC TTACCAGACCTCACCCGG
STR3cLUC-F	CGTCCCGGGGCGGTACC AGACCCTCCCTCTTCAAGCC
STR3cLUC-R	TTGGATCCCCGGGTACCTTACAGCTCACCAGAGTCGACA
STR4cLUC-F	CGTCCCGGGGCGGTACCCCTTTTGTCACCGTCTGTAGTG
STR4cLUC-R	TTGGATCCCCGGGTACCTTAGACAGTAACGCGCTTCTCG
STR5cLUC-F	CGTCCCGGGGCGGTACCGCCAGCTATCAGCAATATGC
STR5cLUC-R	TTGGATCCCCGGGTACCTTACATGAGGATCTGTCAATGGT
1F	CGTTACCAATTCCCAAGGCTG

Table A-4 Continued

Primer Name	**5'-3' sequence**
2R	TAGATGCCGACCGGGAACGTTTGGGGCATGGCATTTTG
3F	CCACTAGCTCCAGCCAAGGCCTCCACTGTTACACAAAGG
4R	CAGCTGCACTGGCTATCTAG
5F	AAGAGCGCGAGCGATTTC
6R	GAAATCGCTCGCGCTCTT
7F	GGCAAAAGCAAAAGGACAGAA
8F	TCTACCACAGAGAGCTCTGG
9R	TAGATGCCGACCGGGAACCTCATTTTGAGGAAGCTGGAGG
10F	CCACTAGCTCCAGCCAAGGACAAAGGGATGGGATTTGGGA
11R	AGAAGCGACTGAACATGCACG
12F	TACTCAACTGAGAACAGCCA
13R	CACAGAGATGGACTTACCCT
14F	CCGCTCTCAACTCCGATAGTAG
15R	TAGATGCCGACCGGGAACAAAGGCATGGCTCTGCTTC
16F	CCACTAGCTCCAGCCAAGGGCACGCTTCTACATCGATC
17R	TGCCTCGCAAGTATCTCTACC
18F	GGCTTCTTTTGTACTCCCTG
19R	AGCACTCCGTCAATAAACAC
20F	AATTCGAGAAGCAGGCGAG
21R	TAGATGCCGACCGGGAACGCCAAGCTGTGCATATTGCT
22F	CCACTAGCTCCAGCCAAGGGACTAAACCAAGTGGGACATG
23R	TTGCACTTCCACATGCTGC
24F	GGCTTCTTTTGTACTCCCTG
25R	AGCACTCCGTCAATAAACAC
26F	GGAGAAGACCCAGAAGAAGG
27R	CGGGAGCAGAACTCACTACA
HYG-F	CTTGGCTGGAGCTAGTGGAGGTCAA
HY-R	GTATTGACCGATTCCTTGCGGTCCGAA
YG-F	GATGTAGGAGGGCGTGGATATGTCCT
HYG-R	GTTCCCGGTCGGCATCTACTCTAT
GFP-R2	GGCACCGGCTCCAGCGCCTGCACCAGCTCCCTTGTACAGCTCGTCCATGC

Table A-4 Continued

Primer Name	**5'-3' sequence**
RP27-F	TCT TCG CTA TTA CGC CAG C
RP27-R	TTT GAA GAT TGG GTT CCT ACG
CYP-F	GGA GCT GGT GCA GGC GCT GGA GCC GGT GCC ATG AGA CCC TCC CTC TTC AAG
CYP-R	TTA CAG CTC ACC AGA GTC GAC A
SCP-F	AGG AAC CCA ATC TTC AAA ATG CCT TTT GTC ACC GTC TG
SCP-R	GGCACCGGCTCCAGCGCCTGCACCAGCTCCGAC AGT AAC GCG CTT CTC G
SEL-F	AGG AAC CCA ATC TTC AAA ATG GCT CCC CCA CAG TTA G
SEL-R	GGCACCGGCTCCAGCGCCTGCACCAGCTCCCAT GAG GAT CTG TCA ATG GTG TT
FSR1-F	AGG AAC CCA ATC TTC AAA ATG GGC CCT AAT GCT GGC AA
FSR1-R	GCTTGGCGGACCATGGTATTGT
GFP-SF	ACA TGA AGC AGC ACG ACT TC
GFP-SR	GAA GTC GTG CTG CTT CAT GT

APPENDIX B

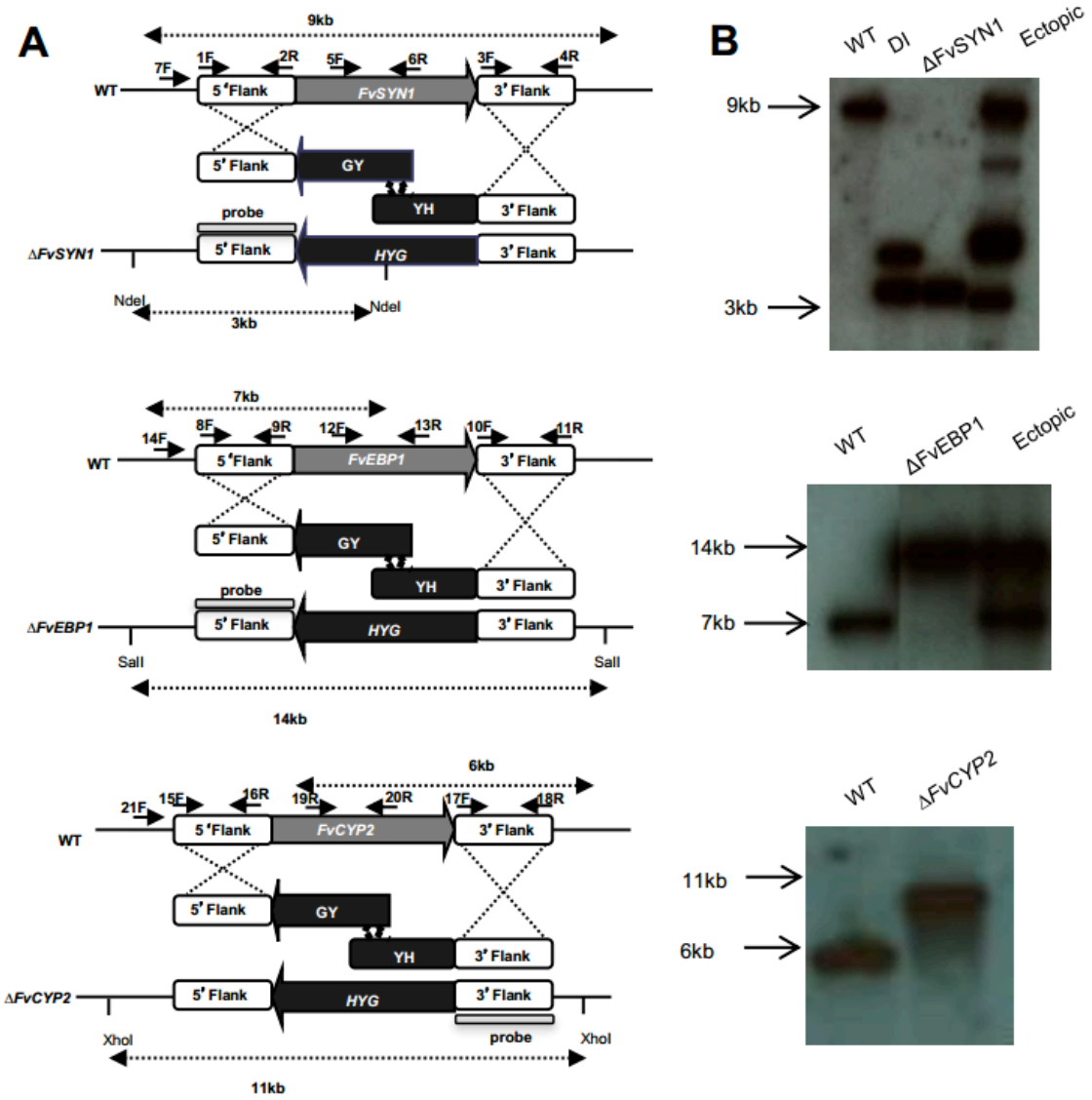

Figure B-1 Gene knockout strategies. (A) The targeted gene disruption for *FvSYN1*, *FvEBP1*, and *FvCYP2* was achieved by homologous recombination with following our standard split marker strategy (Sagaram *et al.* 2007; Zhang *et al.* 2017). Primers used in these experiments are listed in Table S4. Disruption constructs were generated by single Joint-PCR, and Hygromycin phosphotransferase (*HYG*) was used as the selective marker. Probe used for Southern analysis is shown in gray bar. (B) The gene deletion was confirmed by Southern analysis. Anticipated band sizes before and after recombination are indicated on the left.

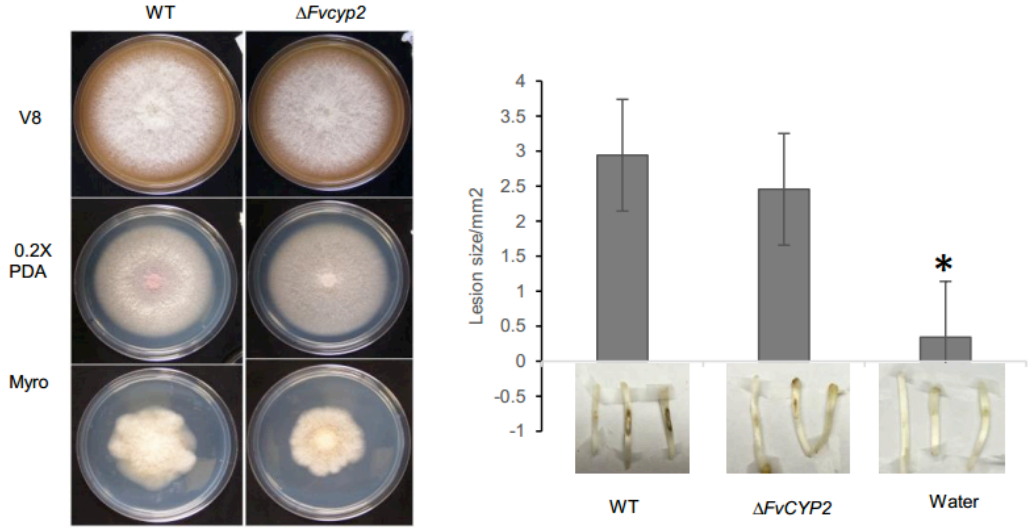

Figure B-2 FvCyp2 phenotype. (A) Vegetative growth of WT and DFvcyp2 was examined on V8, 0.2X potato dextrose agar (PDA) and Myro agar plates. Strains were point inoculated with an agar block (0.5 cm in diameter) and incubated for 6 days at 25 °C under 14 h light/10 h dark cycle. (B) Germinating B73 seedlings were inoculated with 10^8 /ml spore suspension of fungal strains on mesocotyls. Lesion areas were quantified by Image J after 2-week incubation. Asterisk above the column indicates statistically significant difference ($P<0.05$) analyzed by t-Test.

Table B-1 Primers used in this study. The underlined sequences were for fusion purpose.

Primer Name	5'-3' sequence
1F	ACC AGG ATT ATT GGA GAG CAG G
2R	TAG ATG CCG ACC GGG AAC TGA GCT GGA GCT CTG CTT TG
3F	CCA CTA GCT CCA GCC AAG ACG ATG AGA GAA TGG TTC GGA G
4R	TTC AAT CCT TGC AGC TGG TG
5F	CAT ACT GAC ATG GCT TGA GG
6R	CTT CGC TTC TTG TTG TCG TT
7R	ACG CAA TTC ACG ACC GCC TAG
8F	TAG AGA GCT ATG GAC AAG CTG G
9R	TAG ATG CCG ACC GGG AAC GTC AGT ATC TGC TGT GCA AGA G
10F	CCA CTA GCT CCA GCC AAG AGG ACA GGT GAC AGA CAA GTT G
11R	TAA TGG CAG CAA CAC TCA CG
12F	ACG CTG TTC GAT GTG TTT CGC
13R	ACC AAG ACT GGC GAA GAA GAG C
14F	ATC GTG GAA ACG CCA GAC TG
15F	GAA TGT CAG GGT CCT TGA GC
16R	TAG ATG CCG ACC GGG AAC CCA GCT TTA GTC TAC CAG CAT G
17F	CCA CTA GCT CCA GCC AAG ATA GAA AGT ATT CGC GGA GTG GA
18R	TTC CCC TCA GCT ACT TGC A
19F	TCT ATG GAT GGA TGG GTT CGC
20R	TCC TCT ACA ATG CGA GCC TTG
21F	GAA TGT CAG GGT CCT TGA GC

APPENDIX C

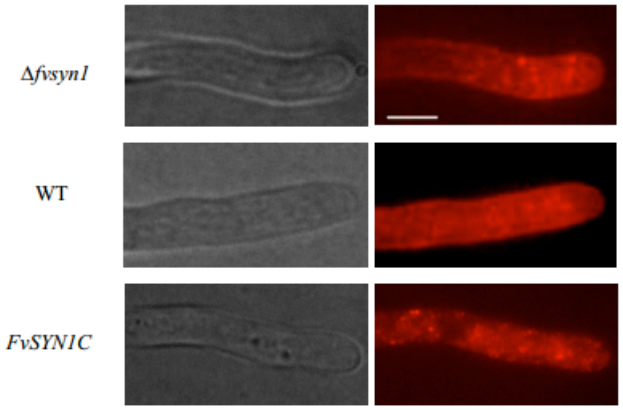

Figure C-1 The Δ*FvSYN1* mutant was not defective in endocytosis. FM4-64 staining assay. Strains were grown for 1 day on PDA before the addition of FM4-64. Photographs were taken after 1min staining. Scale bar = 5μm.

Table C-1 Primers used in this study. The underlined sequences were for fusion purpose.

Primer Name	**5'-3' sequence**
1	ACC AGG ATT ATT GGA GAG CAG G
2	TGA GCT GGA GCT CTG CTT TG
3	A AGC AGA GCT CCA GCT CA CCA GCT CGA CTC GCT TTC C
4	TTC AAT CCT TGC AGC TGG TG
5	GGA AAG CGA GTC GAG CTG G
6	CA GCT CGA CTC GCT TTC C TACCTCAGCTACCGCGGAAC
Syn1-GFP-F	GGA GCT GGT GCA GGC GCT GGA GCC GGT GCC ATG AGT GTT AGT TTG CGC CTC C
Syn1-GFP-R	TTC AAT CCT TGC AGC TGG TG
sGFP/F	AGG AAC CCA ATC TTC AAA ATGGTGAGCAAGGGCGAG
5GAsGFP/Rbs	GGCACCGGCTCCAGCGCCTGCACCAGCTCCCTTGTACAGCTCGTCC ATGC
rp27-f	ACT ATA GGG CGA ATT GGG TAC TC
RP27-R	TTT GAA GAT TGG GTT CCT ACG